THE CONTROL OF ATTACK BY MOLTEN ZINC AND ZINC-CONTAINING ALLOYS ON SOLID METALS

by

G.D.S. PRICE, B.A.

Selwyn College, Cambridge.

A dissertation submitted for the degree of Doctor of Philosophy in the University of Cambridge.

September 1971.

GEOFFREY DAVID SMYTH PRICE

PREFACE

This dissertation is based on work carried out in the Department of Metallurgy, University of Cambridge, between October 1968 and September 1971 under the supervision of Mr. J.A. Charles, B.Sc., M.A. Except where acknowledgment and reference to other investigations is made, the work described is original. This dissertation has not been submitted for a degree at any other University.

Geoffrey Price

G.D.S. Price

September 1971

This dissertation is the result of my own individual work and no part has been carried out in collaboration with anyone else.

Geoffrey Price

Acknowledgments

I am most indebted to my supervisor, Mr. J.A. Charles, for his continued guidance, encouragement and support. I am also very grateful to Professor R. W. Honeycombe for the provision of laboratory facilities.

My thanks are due to friends and colleagues for frequent helpful discussions and advice, and to the Assistant Staff of the Department for ready help and guidance.

The work was made possible by a generous grant from the Imperial Smelting Corporation Ltd., for which I am most grateful. I am also grateful to various other firms and organisations for their help, specifically to B.I.S.R.A. for the supply of steels used in this investigation, Tube Investments Ltd., for carrying out some analyses, The Calorizing Corporation, Metallisation Ltd., and Metco Ltd., for the provision of samples, and to the Zinc Development Association for information services.

Introduction

The phenomena of the attack of molten zinc on steel and other metals is of particular interest to galvanisers and zinc smelters, both of whom have to handle molten zinc. Galvanisers are interested in the short term attack on the steel to be galvanised and also in the long term attack on the galvanising bath itself; zinc smelters are aware of the possible catastrophic attack rates at rather higher temperatures than the galvanisers use, and have tried to avoid such attack by the use of non metals such as refractories wherever feasible. Such substitution is not always possible however, and it is then necessary to seek ways of minimising the rate of attack. This has been attempted by alloying or surface coating, particularly with refratory oxides or cements, and enamelling. No method has yet proved entirely satisfactory in service.

This work has been undertaken to investigate the attack phenomena with particular reference to possible ways of controlling it. To this end it has been necessary to identify the most aggressive conditions likely to be found in practice, and then determine the effectiveness of possible protection systems under these conditions. Thus the effect of steel composition has been considered, the effect of temperature, relative motion between zinc and steel, the permeability of porous refractory coatings and several other factors.

Not much attention has been given to the effect of elements dissolved in the zinc on the grounds that intentional alloying would probably be impossible if the desire was to produce pure zinc in a smelter. However the effect of aluminium in the zinc has been looked at because of its importance in modern galvanising practice due to its short term inhibiting effect on the iron-zinc reaction.

This led to an investigation of the effect of aluminium in the iron, and to the protection offered by oxide layers on iron-aluminium alloys, and some encouraging results were obtained.

CONTENTS

			Page No.
Chapter 1.		Previous work	
	1:1	Early work	1
	1:2	The Fundamental Reaction	2
	1:2:1	Reactions in the Lower Parabolic Range	
	1:2:2	Reactions in the Linear Range	11
	1:3	The effect of applied pressure	14
	1:4	The effect of surface roughness	14
	1:5	The effect of alloying elements in the iron	15
	1:6	The effect of alloying elements in the molten zinc	19
Chapter 2.		Initial Investigations	
	2:1	Evaluation of attack	25
	2:2	Effect of surface inclination	29
	2:3	Effect of specimen curvature	31
	2:4	Effect of some other factors	32
Chapter 3.		Dissolution of a rotating disc.	
	3:1	Reasons for the work	33
	3:2	Previous work	34
	3:3	This work.	
	3:3:1	Experimental Method	41
	3:3:2	Results	51

Chapter 3 (continued)

3:4 Conclusions.

3:4:1 The proposed model of the system 52

3:4:2 Mathematical relationships 55

3:4:3 Measurements from erosion spirals 57

3:4:4 Reconciliation with other work 57

Chapter 4. Effect of Aluminium in Zinc

4:1 Background 60

4:2 Experimental Methods 61

4:2:1 One hour runs 62

4:2:2 Longer runs 63

4:2:3 Sources of error 64

4:3 Results 65

4:4 Conclusions. 68

Chapter 5. Effect of Aluminium in Iron.

5:1 Introduction 73

5:2 Properties of Iron-Aluminium layers 73

5:3 Methods of coating iron with aluminium 75

5:4 Aluminium coatings: Methods used and results 78

5:4:1 Hot Dipping 78

5:4:2 Calorized coatings 81

5:4:3 Sprayed coatings of aluminium 88

5:5 Attack on Iron-Aluminium alloys 91

5:6 Attempts to reduce the oxide layer 93

5:7 Diffusion of zinc vapour through porous membranes 94

Chapter 5 (Continued)

5:8	Discussion of results	96
5:9	Investigation of some other coatings	99
5:10	Conclusions	100

Chapter 6. Effect of Carbon in Steel

6:1	Previous work	103
6:2	Initial Observations	105
6:3	Investigation into the effect of carbon in steels	110
6:3:1	Effect of transformation temperature	113
6:3:2	Investigations of electrolytic effects	116
6:4	Conclusions	119

Chapter 7. Some miscellaneous results.

7:1	Twisting of thin specimens	121
7:2	Effect of an applied electrical potential	123
7:3	Effect of gases in the molten zinc	125
7:4	Effect of inclusions	126
7:5	Selective dissolution of alloy layers	127
7:6	Dilatometry	128
7:7	Effect of crystal structure	128

Chapter 8. Conclusions and suggestions for further work 130

Appendix 1. Calculations of effusion rate for zinc vapour 132

Appendix 2. Details of surface treatments applied to discs of armco iron 134

References. 136

CHAPTER 1

PREVIOUS WORK

1:1 Early Work

The reactions between iron and zinc are difficult to assess because of the ease with which they can be disturbed and radically changed, and because of the large number of important variables. Many of the early workers in this field did not appreciate some of the important factors and their published work is thus incomplete by modern standards; in many cases the results cannot be compared with other works because of the difference in important but unrecognised variables.

One of the first of the more systematic papers was by Daniels (1). He was among the first to realise that the evaluation of the rate of attack must be by means of weight loss per unit area rather than by the change in dimensions, i.e. the diameter of the specimen. He used a stripping solution consisting of 6% sulphuric acid in water with 2% arsenic trioxide to inhibit the attack on the steel. Using this to remove the adherent zinc and intermetallic alloy layers from the steel he was able to show that the attack on the low carbon steel he used was parabolic with time between 440°C and 495°C, with $L=n_1\sqrt{t}$, where L=weight loss in grams per sq. metre in "t" minutes,

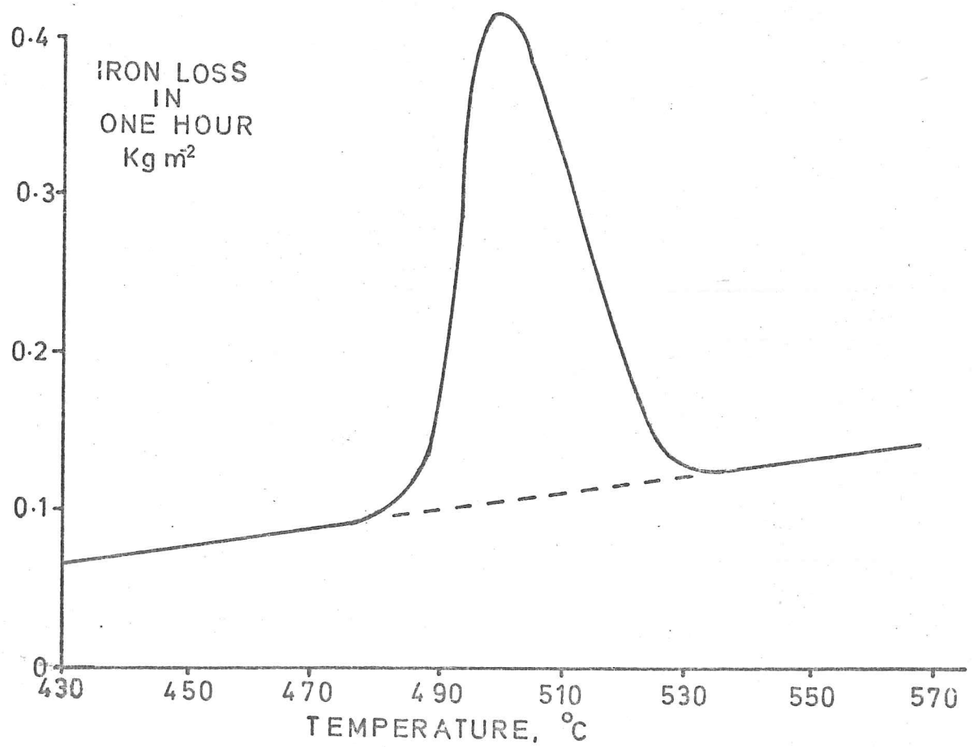

FIG.1 FROM REFERENCE (4)

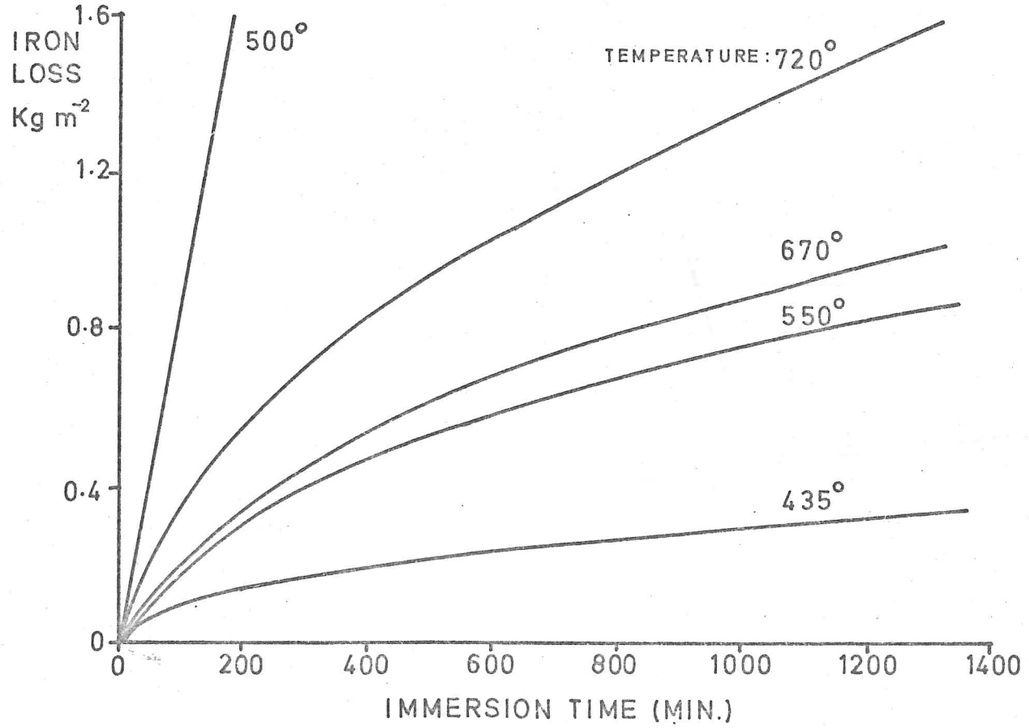

FIG.2 FROM REFERENCE (9)

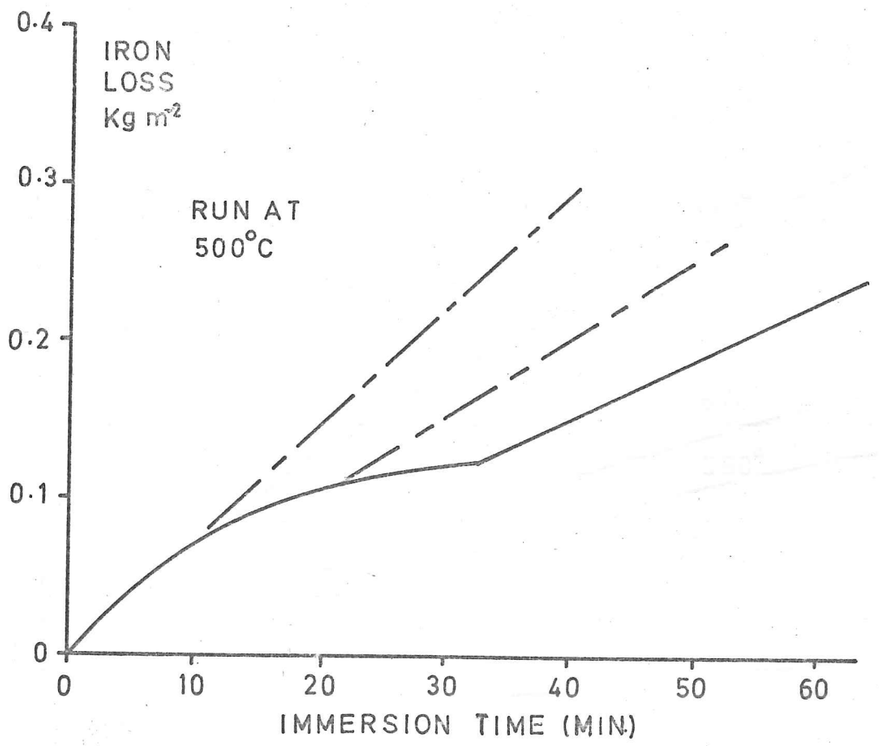

FIG. 3 FROM REFERENCE (4)

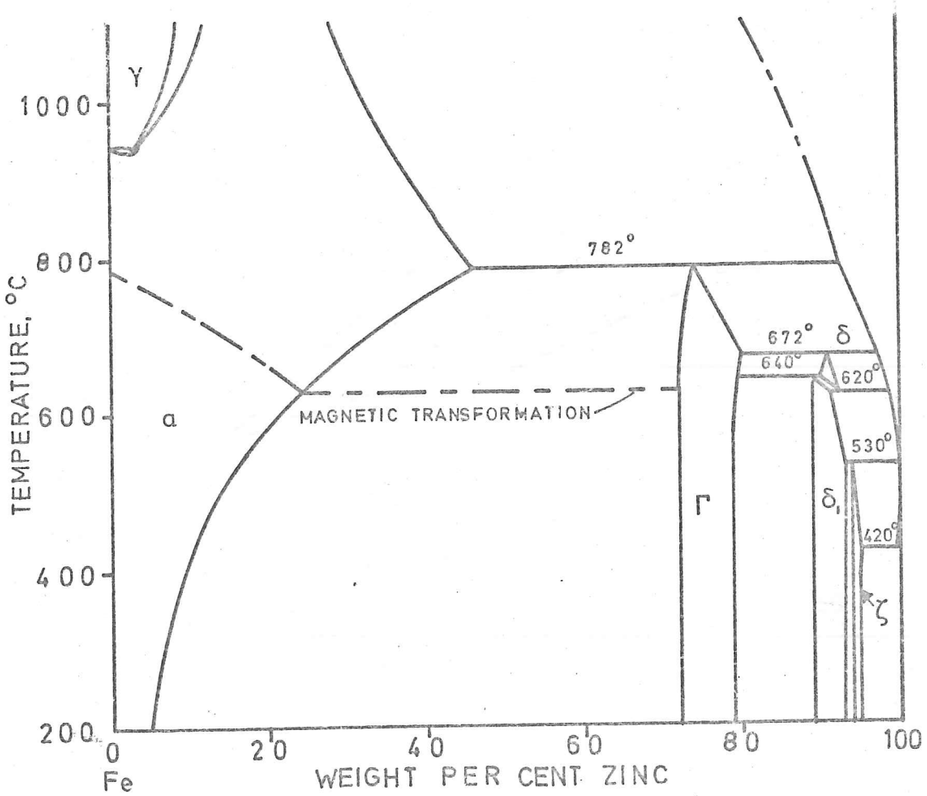

FIG. 4 FROM REFERENCE (5)

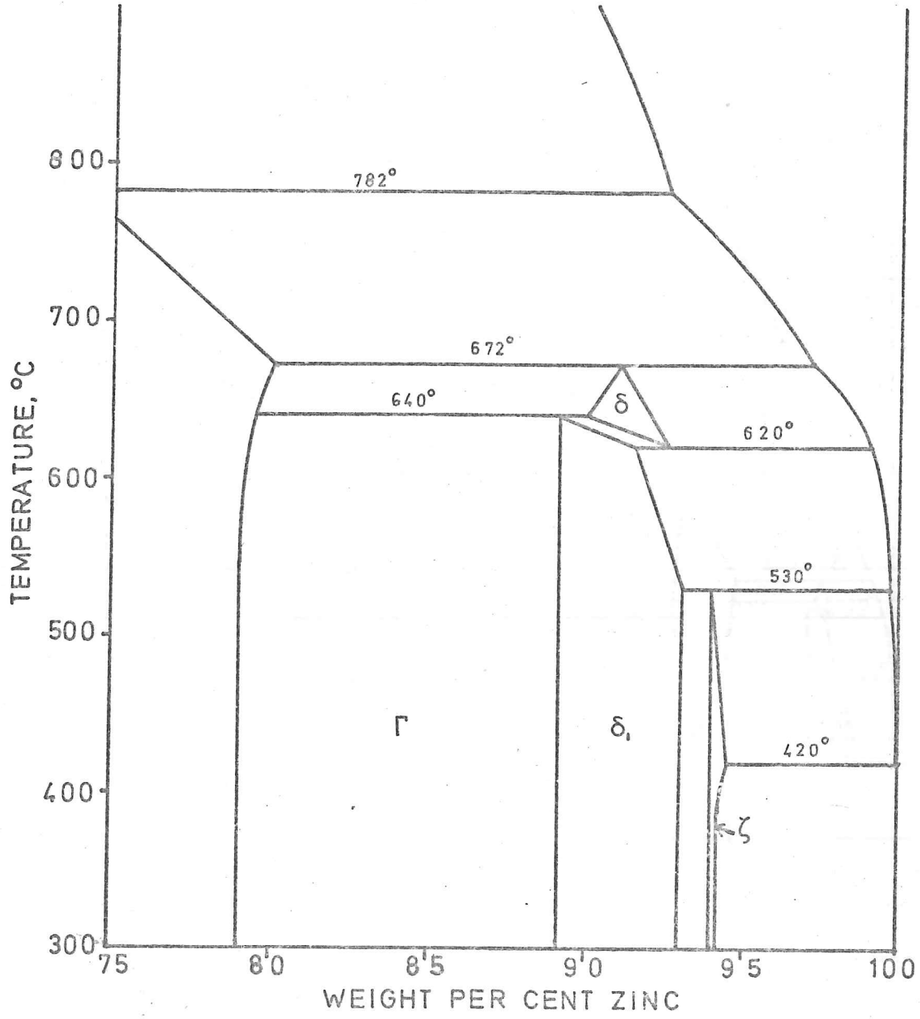

FIG.5 FROM REFERENCE (5)

and n_1 a constant. Around 500° C the attack was linear, $L=n_2 t$, reverting to parabolic above 530° C although he erroneously interpreted his results as being linear in this region. These three regions are now known as the Lower Parabolic Range, (420°-490° C), Linear Range (490°-510°) and Upper Parabolic Range, (530° C upwards); see Figs. 1 and 2. The transition from Lower Parabolic to Linear is quite sudden, but that from Linear to Upper Parabolic is gradual. Detailed investigations regarding the attack in the Linear range have shown it to start off as parabolic, becoming linear after some short time. (Fig. 3)

Since Daniels work efforts have been directed in three main directions; towards a fundamental understanding of the basic reactions between iron and zinc; to an appreciation of the effects of alloying elements in the iron; and the effects of alloying elements in the zinc. These latter two overlap to some degree, but there are many differences.

1:2 The Fundamental Reaction

1:2:1 Reactions in the Lower Parabolic Range.

If given quantities of pure iron and zinc are brought together at a certain temperature, the eventual equilibrium components will be given by the phase diagram. (Figs. 4 and 5) In practice the galvanising reaction may involve impure materials, a large excess of zinc, fluctuating temperatures and rapid quenching

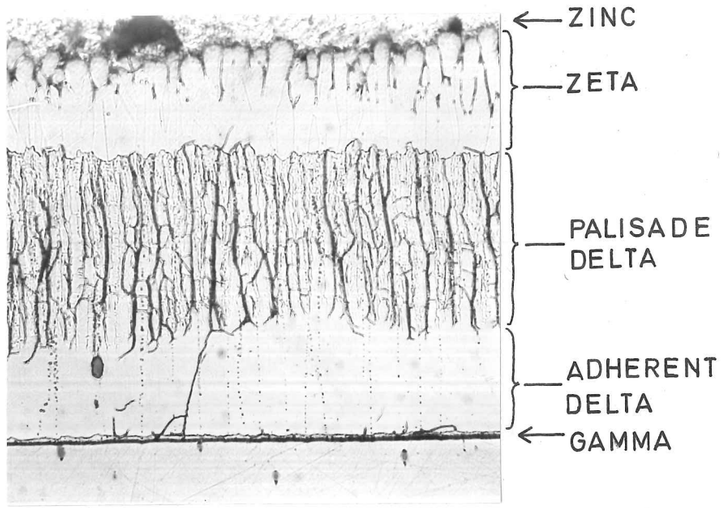

Fig. 6 Alloy layers on armco iron after 6 hours at 450°C. Picral etch, x 170.

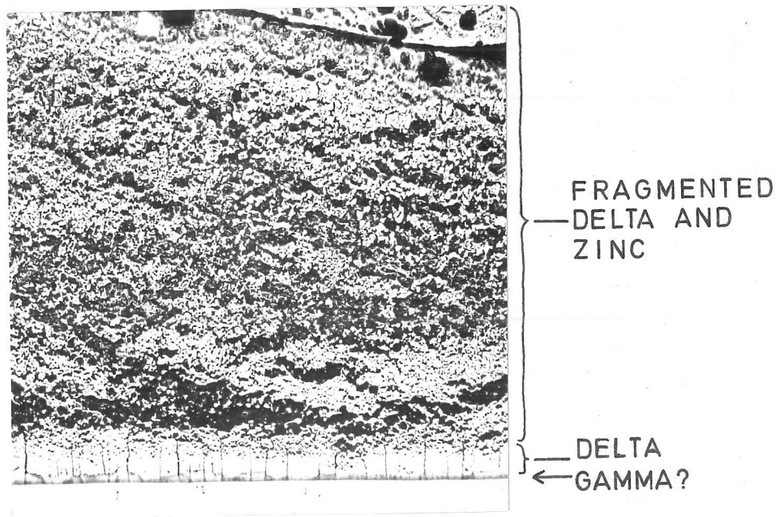

Fig. 7 Alloy layers on armco iron after 1 hour at 500°C. Picral etch, x 75.

of the reaction before final equilibrium is reached. In such circumstances the equilibrium phase diagram is not necessarily applicable, but it seems that in many cases a dynamic equilibrium is set up for which the phase diagram can be used.

Because of the local nature of the equilibrium there must be a diffusion gradient between the iron and the zinc, so that the composition varies across the alloy layers. Application of the phase rule to this situation shows that one phase regions on the phase diagram can be present as layers of intermetallic alloy, whereas two phase regions become interfaces between such layers. Thus the alloy layers produced at a given temperature should consist of all the one phase regions on an isotherm at that temperature (Fig. 6). Although all the layers predicted by the above considerations are not always observed (Fig. 7), it is difficult to be absolutely certain of their absence since it needs only a very thin layer to satisfy the thermodynamic requirements. It may also be difficult to reveal the layers metallographically, particularly if adjacent to the iron, because of electrochemical and hardness effects in this region. This may be the reason why some workers do not detect the presence of a gamma layer at 500°C (2), whereas other find a very thin layer (3,4). The gamma phase (~72-79 wt. % zinc) is cubic, the delta phase (~87-93% zinc) is hexagonal, while the zeta phase (~94% zinc) is monoclinic. (2).

The gamma phase has previously been denoted $FeZn_3$ (77.9 wt.% Zn), Fe_3Zn_{10} (79.6 wt.%) or Fe_5Zn_{21} (83.1 wt.%), while the $delta_1$ phase has been designated as $FeZn_7$ (89.2 wt.%) or $FeZn_{10}$ (92.1 wt.%).

The relative thickness of the intermetallic phases in the alloy layer is governed not by the thermodynamics but by the rate of diffusion through the various layers, the rate of transference across phase boundaries, and the ease of nucleation and growth of these phases. There is also the possibility that the outermost layer, that in contact with the molten zinc, may suffer attrition because of movement of the zinc or another solid, or may dissolve into unsaturated zinc. This can occur even in a bath containing an excess of iron in the molten zinc (i.e. containing free zeta phase) if there are thermal gradients within the bath, so that the zinc cools, becomes supersaturated with respect to iron and seperates out zeta phase, and then warms up, becomes unsaturated, and dissolves more iron from the intermetallic layer.

It has proved to be very difficult to obtain massive particles of the various intermetallic phases in a pure state and without porosity, cracks and segregation (6). There is thus no reliable data as to the diffusion rates of important elements, and in any case such data would be of doubtful practical use without further information on the rate of reaction at phase boundaries, the effect of short circuiting paths such as cracks and grain boundaries, and the

structural sensitivity of the diffusion rate. Nevertheless, by ignoring possible barriers at phase boundaries, and assuming essentially volume diffusion, application of Fick's laws shows that the overall thickness of the alloy layer should vary parabolically with time, and in the Lower Parabolic region this is broadly what is observed.

Such work as has been done on this aspect has been to plot the thickness of the various layers against time at a given temperature. Thus at 450°C the zeta phase is believed to be the first to form, and initially grows very rapidly, occupying most of the total alloy layer in conventional galvanised coatings, but at longer times the rate of growth slows down, and after immersion of about 1 hour the $delta_1$ layer is thicker. This may explain why various published values of the exponent "n" from the simple power law of the form thickness = constant x $(time)^n$ vary so much, from 0.16 to 0.5 for zeta, 0.5 to 0.58 for $delta_1$ and 0.1 to 0.5 for gamma (2).

If Fick's laws were applicable then it can be shown that the displacement of a particular phase boundary with respect to a fixed marker should have "n"=$\frac{1}{2}$. with the constant of proportionality dependent on the magnitude of the diffusion in the two adjacent phases i.e. on the diffusion coefficient and concentration gradient in the adjacent phases (4).

Since the growth of a particular layer involves the movement of two boundaries, its thickness will depend on the rate of diffusion in each of the adjoining phases as well as in itself, and in a similar manner the diffusion in the adjoining layers is controlled partly by their thickness, which in turn depends on the diffusion in yet other layers. It can thus be seen that the situation is very complex even before taking into account reactions at phase boundaries and other factors. It is nevertheless clear that no particular layer can be uniquely "rate controlling". If one layer, say the gamma phase, is a barrier to diffusion then the other layers will tend towards a thickness which produces a similar diffusion rate. An argument along these lines might explain the rapid growth of delta, subsequent to the formation of the gamma phase in the early stages of galvanising.

Use of inert molybdenum wires spot welded to armco iron before galvanising showed that the main diffusion process was that of zinc moving inward, eventually lifting the markers away from the iron surface. Any diffusion of the iron in the intermetallic layers was at a much lower rate (7). This is what would be expected from knowledge of the relative melting points of iron and zinc, but the experiment has been criticized on the grounds that the markers were too large relative to the size of the layers being

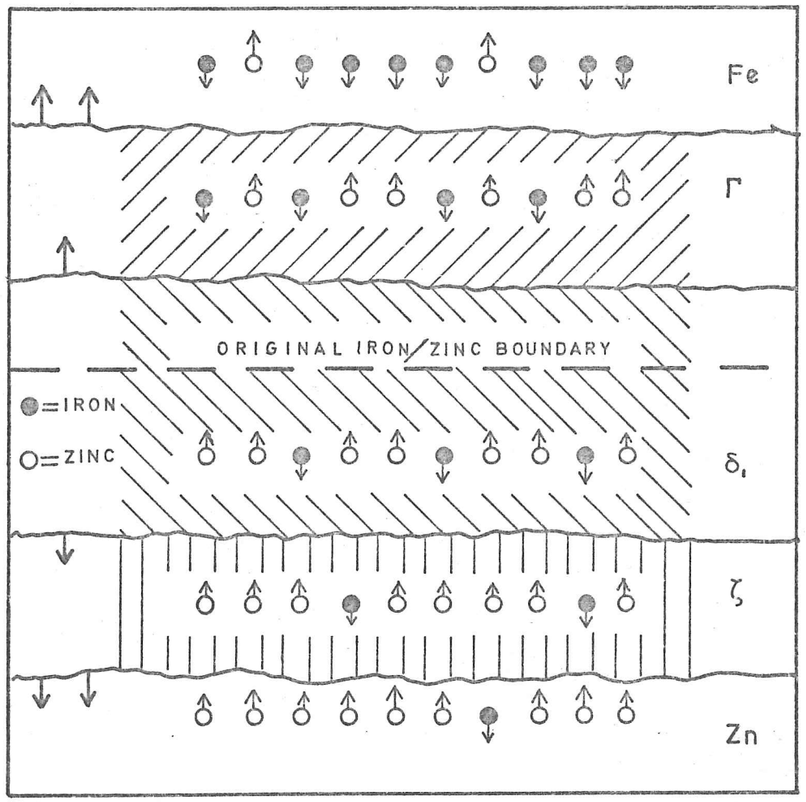

FIG.8 DIFFUSION OF IRON AND ZINC THROUGH THE ALLOY LAYERS (DIAGRAMATIC)

FROM REFERENCE (3)

investigated, and the experiment therefore lacked sensitivity (3).

Assuming the zinc to be diffusing faster than the iron it is possible to construct a model as in Fig. 8 with iron and zinc atoms moving in opposite directions across the phase boundaries. The inward diffusion of the zinc will tend to move the phase boundaries towards the current iron-intermetallic boundary, while diffusion of the iron will have an opposite effect. The iron-gamma and gamma-delta$_1$ boundaries will be displaced towards the iron, and the delta$_1$-zeta and zeta-zinc boundaries towards the zinc. Since the loss of iron obeys a parabolic law the iron-gamma boundary must move in accordance with that law relative to the original interface. Similarly the roughly parabolic law for the growth of the coating must mean that the zeta-zinc boundary must move in a similar way relative to the current iron-gamma interface. The other two boundaries must then move at a similar rate or they would eventually disappear.

The apparent adherence to parabolic laws at 450° C thus suggests that the overall process is one of simple volume diffusion, with no problems at phase boundaries. Electron-probe microanalysis traces for iron taken across the intermetallic phases show slow increases across the zeta and delta$_1$ regions, with a slight step at the interface (3,8) thus suggesting similar diffusion rates in the two phases with a slight barrier at the

interface. The concentration gradient across the gamma layer has been found to be very steep (9). This is one of the reasons why this layer has been suggested as the overall "valve" controlling the rate of attack (2).

Micro-examination of the structure produced at 450°C reveals that the delta$_1$ phase can be subdivided into 2 regions: the adherent or coherent delta, and the palisade or columnar delta. The former appears even and continuous whereas the palisade delta shows many flaws running normal to the iron surface (Fig. 6). These flaws have been thought of as cracks (10), grain boundaries (2), crystallographic planes (2) or merely etched grooves (10, 13). Bablik (11) has shown that the density of such flaws depends very much on the rate of cooling of the alloy when withdrawn from the bath, slow cooling producing fewer flaws.

These flaws have been widely accepted as cracks, acting as "short-circuiting" paths comparable to the gaps between the zeta crystals and thus making diffusion relatively easy up to the palisade-coherent boundary. Indeed the concentration gradient has been found to change across the palisade-coherent boundary (7). Nevertheless no evidence has been produced to show that these cracks are present at the galvanising temperature, and not just formed on cooling. Indeed it has been shown that the alloy layer as a whole is under considerable compression while being formed. A thin piece of steel sheet, if

protected from attack on one side, is found to rapidly curl up with the alloy layer on the outside (2). A piece of thin annealed steel shim has been observed to twist through some 90° in 10 minutes. It is not surprising that such compressive forces are produced; the alloy layers grow epitaxially from the iron base with iron atoms being replaced by the more bulky zinc. The greatest change in density is likely to occur between the α iron and the gamma phase, the difference in zinc content being some 64 wt.%. It is often found that a metallographic section has a crack running along this boundary, and slow cooling and careful sectioning are needed to prevent this, but because such cracks are not inevitable it is clear that they form on cooling or subsequent mechanical distortion and are probably not present at the galvanising temperature. Because of its relatively wide composition range and small thickness over which this transition takes place, it is likely that the gamma layer produces the largest stresses. The zeta layer, having an unconstrained interface with the molten zinc, grows in a much freer manner, and the stresses here are probably minimal.

There is however insufficient evidence to describe the behaviour on cooling. Doubtless the layers contract to different extents. Using the published data (12) and assuming a linear law with respect to composition, one can show that the gamma layer might contract at twice the rate of the iron base. The zeta layer will

also contract more than the $delta_1$ layer, and bearing in mind the original compression in the gamma layer it is possible that the gamma layer ends up with some slight degree of compression, the zeta layer also in compression and the $delta_1$ in slight tension. The "cracks" then observed in the delta palisade region might be existing grain boundaries which have opened up under the tensile stress. Such an argument would suggest that when formed there was no difference between the coherent and palisade delta, both parts containing distinct columnar grains. Any difference in diffusion gradients observed with the electron microprobe might be explained by a slight step produced on polishing at the palisade-coherent boundary, or perhaps by infiltration of molten zinc on cooling, with subsequent reaction with the delta.

This question of the difference between palisade and coherent delta is inadequately explained, and requires further investigation, perhaps by hot-stage microscopy.

In summary then, it can be said that the attack in the Lower Parabolic Range is parabolic with time, giving reason to believe that the rate is controlled by diffusion through a layer of increasing thickness. It is not clear whether the whole alloy layer forms this barrier, or perhaps only one section of it.

1:2:2 Reactions in the Linear Range

In the Linear Range the system is quite different and the explanations more complex. The attack rate is initially roughly parabolic, proportional to $(\text{time})^{0.6}$ (3), and only becomes linear after some 10-20 mins. When the curve of iron loss is plotted against time, the linear portion extrapolates back to near the origin (Fig. 3). During the initial parabolic period alloy structure is dense and coherent, becoming fragmented in the linear region. Up to about 495°C the alloy layers in the linear range consist of a thin, compact delta_1 layer covered by a zeta layer which becomes increasingly columnar and discontinuous (3). By 500°C such zeta crystals that are observed are small and isolated, seeming to originate and grow freely within the zinc melt. (2). Above 500°C no zeta crystals can be found, and up to 515°C the coating consists of a thin dense delta_1 layer covered by mixed delta_1 fragments and zinc (Fig 7). Some investigations have detected the presence of a thin gamma layer in this region (3,4,13) but this is always found to be very thin. The thickness of the compact delta_1 layer is found to remain constant with time (4) whereas the mixed delta_1 and zinc becomes very thick and may slough off into the bulk zinc. This mixture has a consistency similar to that of soft clay.

Two explanations have been generally advanced for the enhanced attack in the linear region; one of these

can be rapidly dismissed. Metallography of a galvanised section is not particularly easy. Over polishing can rapidly result in a difference in level between the iron and the intermetallic, and the electrochemical difference between the iron and the zinc alloys makes etching somewhat difficult (14). This effect is particularly concentrated at the interface, making it difficult to etch the iron right up to the intermetallic, and also tending to cause over-etching of the alloy near the interface. Thus a thin gamma layer in this region is not always detected and its absence is hailed as the reason for the rapid attack (15,16). The fact that it can be detected suggests that it is generally present even if not observed.

The more acceptable explanation is based on the absence of any continuous layer of zeta. Once this fails to completely cover the $delta_1$, then the $delta_1$ is in contact with zinc, an unstable situation, and the $delta_1$ is attacked and broken up by the zinc. The thickness of the $delta_1$ is thus reduced and diffusion through to the iron becomes easier until a dynamic equilibrium is set up where the thickness of the compact delta is such as to allow diffusion at a rate equal to that at which it is being destroyed by the zinc. The $delta_1$ thickness and the attack rate are thus linear with time. The initial short parabolic behaviour presumably relates to the initial growth of $delta_1$ to a stable thickness.

Horstmann's (17) explanation for the lack of a zeta layer at 500° C, contrary to the prediction of the phase diagram, has been to show that the $delta_1$ + melt → zeta reaction proceeds slowly above 475° C, and between 500° and 530° C the zeta is not nucleated on the $delta_1$ but precipitates directly from the melt, and thus cannot form a protective layer over the $delta_1$.

The full explanation may be somewhat more complicated than this. It has been shown (13) that the alloy layers formed in the Lower Parabolic Region are unstable in the Linear Region, and the outer zeta layer is suffering severe attack after one hour, and the structure changes to that characteristic of the higher temperature within three hours. This seems to suggest that the zeta layer is positively unstable at the higher temperature, rather than just difficult to nucleate as suggested by Horstmann. Two explanations are possible to reconcile these facts. The zeta formed at the lower temperature is unstable at the higher because it contains more zinc. Its composition must therefore alter, and during this period it may become cracked or fissured. Alternatively such fissures might have been produced by thermal stresses when the temperature was increased. If the fissures extend through the zeta layer to the $delta_1$, allowing zinc to contact the $delta_1$ and if Horstmann's hypothesis is correct so that the fissures are not blocked by the production of zeta, then the $delta_1$ layer will be continually attacked and the zeta layer eventually broken off.

1:3 The effect of applied pressure.

Several workers (15,18,19,20) have looked at the effect of an applied pressure on the reaction rate. They report that given pressurs of up to $5x10^5 Kgm^{-2}$, but generally around $5x10^3 Kgm^{-2}$ it is possible to reduce the rate of attack in the Lower Parabolic Range, and at higher temperatures to change the attack law from linear to parabolic. These results were believed to be due to the closure of cracks and fissures, and the consolidations of the dissolving $delta_1$ in the Linear Range.

These results must be looked at very critically. The method used was to form some alloy layer on the specimen and then apply pressure by means of a rod and a piston covering the specimen. This is bound to some degree to restrict the contact between the molten zinc and the alloy, and it may well be that the reactions are slowed because they are effectively starved of zinc. Unfortunately there is no obvious way of avoiding this; isostatic pressure would close up any cracks, but at the same time would be forcing molten zinc into them.

1:4 The effect of surface roughness

The effect of roughness of the steel surface is probably also due to "starvation" of zinc in concave regions. Roughened specimens are found to be attacked more than smooth ones (11). It is reported that this is not due to any work-hardening effect (4), but rather to the surface contours produced. Convex regions

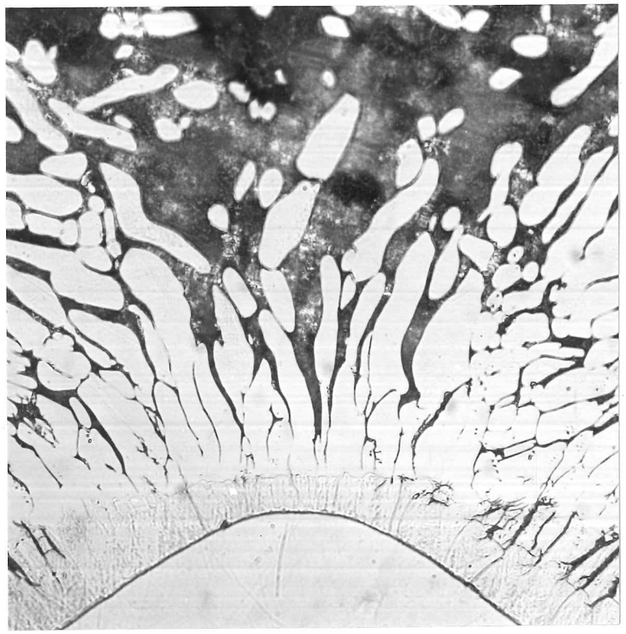

Fig. 9 Alloy structure on a corner; armco iron after 1 hour at 450° C. Picral etch, x 250.

such as corners show a well known fan like microstructure (Fig. 9), and similar structures are observed on roughened surfaces. The zeta grows normal to the $delta_1$ surface and cannot form a continuous compact layer. The gaps between the zeta crystals allow zinc to penetrate closer to the $delta_1$, causing the $delta_1$ to be attacked faster and be thinner. In concave regions however, the zeta very effectively covers the $delta_1$, and the $delta_1$ layer may be very thick. The overall result is of greater attack on the convex regions and less on the concave, tending eventually to produce a smooth surface. Polishing may also increase the attack in the short term (11) and produce a thicker zeta layer (21). This may be due to the work hardening in the surface layers.

1:5 <u>The effect of alloying elements in the iron</u>

If a third element is introduced into the system, either to the iron or the zinc, then the simple binary model breaks down. A ternary phase diagram is required to attempt to determine which phases should be present, and it seems that the prediction of this is difficult (4). Duplex layers, i.e. two phases growing side by side are thermodynamically possible, and have been observed in practice (22).

In fact, with the additions commonly added to produce a low alloy steel, there is no evidence of any ternary behaviour, and the phases present strongly resemble those produced by pure iron and zinc. They

may differ slightly in thickness and compactness.

A most thorough and systematic evaluation of the effects of steel composition has been carried out by Horstmann (16). A range of iron alloys were immersed for between 1 and 5 hours in pure zinc at temperatures between 430°-550° C. These were essentially binary alloys, but contained small amounts of other elements. The attack was evaluated in terms of iron loss, and the results can be split into two sections.

It was found that the presence of a third element altered the transition temperatures between the Lower Parabolic-Linear and Linear-Upper Parabolic regions. Carbon up to 2% had little effect, but between 0.9 and 1.6% silicon the range of linear attack extends down to the zinc melting point. Thick alloy layers and rapid attack are thus produced at very low temperatures. By 4.9% silicon however, the linear range has disappeared. Any steel containing more than about 0.3% silicon can be considered particularly reactive.

In contrast, between 3 - 5% manganese causes the linear region to disappear, but by 8% it has reappeared and covered the whole range from 420°-550° C. Other elements investigated did not produce such notable effects.

Horstmann (23) also determined values of "a" in the equation:

$$a = \frac{m^2}{t}$$

where m = iron loss in time t, and, taking

$$a = a_0 \times e^{-u/RT}$$

was able to find values of a_0 and U. For pure iron a_0 = 0.178 Kgm^{-2} mm^{-1}, and U = 14.2 Kcal $mole^{-1}$. Each level of alloying element produces a new value for a_0 and U, and for a given element these were proportional to concentration of impurity in weight %. Further, by plotting the variation of ($\sqrt{1/a_0}$/concentration) vs. atomic number a periodic variation was observed similar to that for other atomic properties. No explanation was offered for this, but if this function of ($\sqrt{(1/a_0)}$/concentration) is re-plotted vs. atomic radius a reasonable straight line correlation appears, although the point for aluminium is rather far out. Such a plot would appear to have more significance than that vs. atomic number, but the atomic radius can vary considerably with coordination number etc., and care is needed if a truely significant result is to be obtained. Horstmann also showed that the plot of ΔU/concn. against maximum solubility at the galvanising temperature on a log scale, was linear. He further proposed that the constants for each component in a particular practical alloy could be added to give an overall effect.

A criticism of this work, brought up in the discussion of this paper (16) was that iron loss was evaluated in terms of the thickness of the alloy layers produced, and that this required a knowledge of their densities and degree of porosity.

However, at least the broad outlines of this work have been confirmed (3,24,25,26,27). It seems that the marked effect of silicon is to make the nucleation of zeta more difficult, hence exposing delta to attack by zinc over a wide temperature range. No evidence is offered to explain the opposite effect of manganese. The other elements investigated appear to alter the reaction rates by altering the morphology of the alloy layers or the reactions at phase boundaries rather than by alteration of the diffusion rate in the bulk alloys (4); the attack rate is thus generally increased. It is realised that it is unlikely to be possible to produce a normal alloyed steel resistant to molten zinc (28).

Certain other metals are resistant (29), and heavy alloying of iron with silicon, boron, chromium, manganese, tungsten or molybdenum can produce a resistant alloy, perhaps because of very strong covalent bonding; such alloys are generally hard, brittle and unworkable. It has been pointed out (27) that the concentration of certain elements may become enriched in time at the surface of the steel if these elements are surface active and reduce surface energy, and might thus protect the steel without much influencing bulk properties. Similar effects might occur within the molten zinc. The degree of enrichment cannot be very high however, and the rate of replenishment low, and this phenomenon cannot be of great significance in practice.

1:6 The effect of alloying elements in the molten zinc.

The effect of an alloying element in the zinc is potentially even more complex than one in the iron, and there is no common theory to link up the various results observed. There are perhaps three classifications into which all results would fall. In some few cases there is essentially no effect. Lead comes into this category (11). Zinc will dissolve some 1.1% lead at 450° and any excess will tend to form a layer at the bottom of the bath. Pure lead does not react with iron, but in a galvanising bath the lead is saturated with zinc, which therefore is as active as pure zinc. Nevertheless the lead itself, whether free or in solution seems to take no part in the reaction, and may be observed as globules scattered through the zinc layer (8).

Other elements may modify the alloy structure and the rate constant to some degree. This is probably caused by modification to the structure of the intermetallics in a manner similar to that of alloying elements in the iron. Most elements commonly added in small amounts will come in this category. The British Standard for commercial galvanising zinc gives maximum impurity levels as 1.35% lead, 0.15% cadmium, 0.04% iron and 0.02% tin. Regardless of the initial iron content the bath will eventually become saturated, containing some 0.03% iron at 450°C, the excess forming a dross (zeta phase) which settles to the bottom of the bath. There is no evidence that the rate of attack

differs between this purity of 98.5% zinc and 99.995% zinc (30).

The third category would be for elements which cause a marked change in the alloy formation, with new phases existing for some or all the time. This will be the result with many elements if present in concentrations beyond those normally encountered, and also for certain very active elements, like aluminium, at quite low levels.

In practice the molten zinc may contain several elements deliberately added to produce various effects, and the individual effect of each may be enhanced by the action of others. Furthermore the steel will contain an assortment of elements producing further effects. The system then passes beyond the possibility of theoretical assessment, and even the practical results are very fickle and difficult to reproduce reliably.

The effect of iron in the bath is slight but distinct. Unsaturated baths show a rather smoother zeta layer than those saturated (31), due to the lack of equilibrium between the zeta and the melt. The term "iron saturation" is loosely used to describe a bath in which the zinc can dissolve no more iron, but a better term is "dross-saturation", (22). If a third element is added to the melt then the dross may not be zeta phase, and the maximum iron content of the liquid zinc will depend on the concentration of the third element. Thus pure zinc will contain some 0.03% iron if saturated with

respect to the dross (zeta) at 450°, 0.0025% iron in zinc + 0.2% aluminium, and 0.0004% iron in zinc + 4% aluminium (32).

Aluminium as an alloying element causes drastic changes, and causes an unpredictability of behaviour, even on adjacent areas, which has led to many disagreements as to the mechanisms involved. Only very low levels. ~0.01% are needed to modify the physical characteristics of the bath and cut down surface oxidation of the zinc, but at this level there is little effect on the galvanising reaction. Higher concentrations react with the flux blanket on the surface of a galvanising bath, causing defects in the coating, but modern practice in continuous baths uses no flux and concentrations of up to about 0.3% aluminium are commonly used.

At this and higher levels the action of aluminium is initially to produce an alloy layer on the iron which has been identified as Fe_2Al_5 (31). This layer grows very slowly and is generally very thin, but may form thicker nodules at certain points on the iron. While it is present the rate of attack on the steel is negligible, and this period is known as the incubation or inhibition period. This period is variously quoted as lasting between 20 secs. (33) and greater than 120 minutes (22)., and during it the attack is parabolic (33).

The length of the inhibition period has been shown

to be increased by high aluminium content of the bath, low iron content and low temperature, agitation and silicon in the steel, and decreased by roughness of the steel surface (4). With so many factors it is not surprising that the values for the inhibition period vary so widely. Continuous strip galvanising lines of the Sendzimir type generally work under conditions such that the immersion time is less than the incubation time, resulting in a coating with high ductility because of the virtual absence of any alloy layer.

The end of the inhibition period occurs when the zinc bath starts to react with the Fe_2Al_5 alloy, probably forming some ternary phase. The possible reactions are many and complex (22,34). This new reaction is probably due to a local depletion of aluminium, and is therefore favoured by a high iron content and static conditions. It may be that from the very first there are two competing reactions, the formation of Fe_2Al_5 and its transformation to a ternary, and that the former is just very much faster in the early stages. The transformation would then start to be noticed when the initial rapid formation of Fe_2Al_5 had slowed down. With longer times the particles of ternary grow and coalesce, eventually forming loosely adherent layers that slough off into the bath, and at this stage localised growth of the iron-zinc phases starts, producing mainly $delta_1$. The attack rate in this period is more rapid than in pure zinc baths, and

may be linear with time. It is possible that this rate later diminishes (35).

The presence of other elements may modify the behaviour of aluminium in the earlier stages of this reaction. Because of the possible nucleation of phases such as $FeAl_3$ or Fe_2Al_5 within the bath, the iron and aluminium contents vary inversly, so that a bath high in iron will be low in aluminium, and the inhibition period shortened. Silicon increases the inhibition period; this has been shown to be due to its removal of iron from the bath as ferrosilicon (4). Most other additions seem to have little effect or else react with the aluminium and thus remove it as a relatively insoluble dross.

Most other elements which might be present in or added to the zinc bath have little effect. Some, i.e. copper and aluminium, lower the viscosity of the zinc, so producing thinner pure zinc layers over the zeta crystals when withdrawn. Others alter the corrosion resistance of the galvanised article when in service (22). Silver has been found to increase the growth rate of the alloy layers, and chromium, manganese, nickel, titanium and vanadium to reduce it. The effects vary with concentration and time. Investigation of alloyed galvanised coatings (8) showed that a high concentration of manganese was found in the zeta phase, about twice that in the bulk zinc. Nickel, titanium, vanadium and chromium were found to be concentrated at the outer surface of the zeta phase, with levels up to 20 times higher than the bath concentrations. These

regions were thought to be ternary compounds, and were associated with a thin zeta layer. These compounds were felt to act as both diffusion and mechanical barriers, so reducing the overall attack rate. Vanadium was the most effective element in reducing attack. It was also thought that such reactive metals might also initially react with the iron base to form protective alloys similar to those produced by aluminium. Care must then be taken to separate the short and long-term effects.

CHAPTER 2

INITIAL INVESTIGATION

2:1 Evaluation of Attack

It is quite clear that quantitative results for the attack rate of molten zinc on steel must be by means of weight loss. Measurement of the thickness of the total coating or intermetallic layers gives information which may be of interest, particularly if the aqueous corrosion resistance of the article is of importance, but because of the possibility of the sloughing off of some or all of the alloy layers while in the zinc, such thicknesses may bear no relation to the amount of iron removed. This will be especially true under conditions of agitation, where the outer alloy layers are being continually eroded.

Methods involving measurement of specimen size before attack, and then again on a cross-section afterwards are open to many sources of error. The likely change of size is in many cases very small and being the difference of two larger measurements cannot be determined very accurately. The measurement is a "spot" one, and should be taken each time at the same point; several measurements must be taken to obtain a useful average figure. Thus several cross sections should be examined and it is difficult to arrange that the section prepared is in exactly the right plane relative to the dimension to be measured. Thus the

section across a cylindrical rod might be elliptical instead of circular, and corrections must be made to allow for this.

Direct measurement of the rate of growth of alloy layers using some form of probe and a clock gauge (18) must involve some restraint on the natural formation of the intermetallics, either by the application of pressure or by restriction of the movement of zinc in the region of the probe. This might be very important in regions where the alloy layer is naturally loose and broken up.

The method used in this work is similar to that of Bernick and Sievert (36). The specimen is weighed before testing to 0.1 mg., and its surface area measured as accurately as possible. (generally to 0.05 cm^2* or better). After attack in the zinc the adherent zinc and iron-zinc alloy layers are stripped off in 50% HCl soln., and the specimen removed when the initial rapid effervesence ceases, and no Fe/Zn alloy is visible. The specimen is then reweighed and the loss per unit area calculated.

Other workers have used an acid soln. containing an inhibitor, often arsenious oxide. It was found that the rate of attack of such a solution on zinc is markedly reduced, so that the stripping process takes much longer, and the steel is exposed to the acid for a greater period while the last of the intermetallic is being removed. Observation would seem to suggest that there is little effective cathodic protection by the zinc

* 0.25 - 1.0% of total area.

under such circumstances and despite the inhibitor there is some attack on the steel. The overall result is that the time taken for dissolution is much longer, and the overall accuracy of the procedure is not improved. This was confirmed by electroplating zinc onto weighed steel sheet, and then stripping it with HCl 1:1 with water, and diluted acid with 1% antimony pentachloride, 10^{-3}N thiourea or 0.2% arsenic trioxide added. The most effective stripping agent was the diluted HCl, which produced an overall weight loss of $5x10^{-4}$ Kg m^{-2} during stripping, and subsequently attack on the steel base at the rate of $8x10^{-5}$ Kg m^{-2} min^{-1}, the stripping process lasting some 5 mins. Thus for specimens showing a weight loss of $50x10^{-3}$ Kg m^{-2} would be liable to an error of perhaps 10^{-3} Kg m^{-2} from the stripping process, giving an overall error of around 5% in the measurement of wt. loss per unit area.

At this time, before any major tests were carried out, it was felt advisable to investigate the possible effect of certain parameters which might be involved later. Thus some measurements were made on the weight loss from surfaces facing upward and downwards, surfaces with positive and negative radii of curvature, surfaces of varying roughness, and on the position within the zinc bath of the specimen.

For the first two of these, and for many subsequent tests it was necessary to limit the attack by the zinc to a defined region only, i.e. protect most of the specimen but expose one face. The ideal protective medium should be easy to apply, bond well to the steel, be unaffected by the elevated temperature and the

molten zinc for the period of the test, and subsequently be easily removed without in any way affecting the steel substrate. Such an ideal combination of factors is difficult to obtain, and several possible materials, such as milk-of-lime wash, failed completely on at least one factor. The most satisfactory compromise was achieved by a proprietry compound known as "White Gun-Gum". This is a viscous paste consisting mainly of powdered asbestos and sodium silicate soln. If diluted a little it could be readily painted onto the steel surface to be protected. Slow drying gave a hard coating which gave off some water vapour on heating to 500° C, producing a more porous layer which nevertheless was not readily penetrated by molten zinc. On subsequent cooling and acid stripping of the zinc from the exposed surfaces the Gun Gum was soft enough to be removed by scraping with a wooden spatula, leaving the steel underneath virtually unaffected.

This material was however imperfect in two respects. It was eroded by flowing zinc and over a period of some days it was penetrated by the zinc. Thus certain portions of the apparatus protected by this "Gun Gum", such as the magnets used in the rotating disc experiments, had to be removed periodically and recoated. Attempts were made to reduce this penetration and increase the erosion resistance by means of a layer of asbestos paper between 2 coats of "Gun-Gum". This was only moderately successful.

Another problem that was met with at this stage was that even clean steel is not necessarily immediately wetted on immersion in molten zinc. Slow submersion can allow the oxide layer to thicken, and it takes a certain time for this layer to be removed by the zinc and attack to begin. Thus it is quite possible to immerse a specimen for several minutes and on removal to find no appreciable attack. Over a period of 1 hour most oxide films are removed and attack begins, but it was found that the measured weight loss could be quite variable unless a flux was used. At first it was thought undesirable to use a flux, on the grounds that this would be adding another variable to the system, and that the effect of Cl^- in the bath was an unknown factor, but it soon became clear that useful results could not be achieved without the use of some flux. A thin coating of a proprietary resin based flux (containing some chloride) was therefore used throughout. This seems to have had no deleterious effects.

2:2 Effect of surface inclination

It was felt that under conditions where the iron-zinc alloy layer was sloughing off there might be a difference in the attack rate on an upward facing surface on to which the alloy particles might settle as compared with a downward facing surface from which the particles would fall away. To try to detect any such difference discs about 3 mm. thick were cut from En 1a bar stock (1" dia.) (Analysis 0.07 - 0.15% C, 0.8 - 1.2% Mn, 0.2 - 0.3% S, 0.07% P max, 0.10% Si max.). These were

ground on 180 grade emery paper all over, measured, weighed and treated under 5 different headings:

1. Attack on all faces - flat faces horizontal
2. Protected with Gun Gum on all but one face; this face directed upwards
3. As 2 but directed downwards

These 3 were attacked by molten zinc in a small crucible in a Muffle furnace for 1 hr. at 450°C.

4. and 5: As 2 and 3 but at 500°C for 1 hr.

The results are displayed in Table 1. It is clear that there is little difference between groups (2) and (3), but these both differ to some degree from (1). From this it may be concluded that any difference there may be in attack rate between upward and downward facing surfaces is too small to be reliably detected by this method, and that either there is a systematic source of error involved in using "Gun Gum" on specimens, or else that the attack rate on the curved surfaces of the specimens is detectably different to that on flat surfaces. In view of the results which follow, and the relatively small area of curved surface on these specimens ($\sim \frac{1}{5}$ of total) it is felt that the difference between groups (1) and (2) or (3) is due to the slight uncertainty in measurement of areas of attacked surface which follows from the painting of "Gun Gum" by hand up to the edges of such a surface. It should be noted that no decarburization or other effects were noticed at the edges of these specimens.

TABLE 1

(A) One hour in molten zinc at 450° C

weight loss/area (Kg m^{-2})x10^3

Group 1 (All surfaces)	Group 2 (Facing Upward)	Group 3 (Facing Downwards)
71	75	76
70	76	72
71	73	73
72	72	74
72	71	73
76	72	
71		
73		
72		
69		
70		
Mean = 71.5	Mean 73.2	Mean 73.6
σ = 1.9	σ = 1.9	σ = 1.5

Students "t" correlation

1:2 - 1.7 1:3 - 2.2 2:3 - 0.4

(B). One hour in molten zinc at 500° C

Group 4 (Facing Upwards)	Group 5 (Facing Downwards)
446	371
390	393
419	407
407	405
396	
371	
Mean = 405	Mean = 394
σ = 26	σ = 17

students "t" correlation 4:5 0.7

2:3 Effect of surface curvature

To determine the effect of the radius of curvature of the attacked surface on attack rate lengths of flat steel bar 10 mm wide and about 3 mm thick, of unknown composition, (probably En1a) were bent around formers of various radii . Specimens were cut from these and annealed under hydrogen to produce strain free equi-axed grains in each case. The area of the curved surface to be attacked was measured as accurately as possible using simple geometric principles and the edges and other face of the specimen blanked off with "Gun Gum". The inner and outer radius of curvature of the specimens differed because of the specimens thickness, and were measured separately. The one type of specimen obviously possess surfaces of positive and negative curvature. Thus there are two sets of results of weight loss per unit area (L) against radius of curvature (R) as displayed in Table 2. Bearing in mind the uncertainty in the individual values there is no evidence for any variation of attack rate down to the smallest radii of curvature used. Because of the distorted, fan-type, intermetallic micro-structure observed at the corners of specimens (Fig. 9) it is felt that the attack rate is likely to alter at some small radius, but the above results suggest that any such effect is likely to be unimportant on specimens of the size used later. Any specimen with sharp edges or corners between faces would be liable to such an increased attack rate at these edges, resulting in the progressive rounding-off

TABLE 2

Specimens tested in molten zinc at 450°C for one hour.

(a) Curvature positive

Radius of curvature (R) mm	Wt. loss (Kg m^{-2})x10^3 (L)
9 ± 1	103
9	101
13	107
17	118
17	97
33 ± 1	108
62	105
62	97
105	98
105	101
	Mean = 104
	σ = 6

(b) Curvature negative

6.5 ± 2	98
6.5	100
17	103
21	100
24	92
33	108
60	105
60	107
104	104
104	99
	Mean = 103
	σ = 5

(c) Flat surface, i.e. R = ∞

Mean of 11 measurements 103

σ = 5

of such edges, but the area of the "edge" on which the attack is much altered is likely to be small. It can also be concluded that it is possible to use the curved surfaces of cylindrical or disc specimens without appreciable inaccuracy provided that the radius of curvature of such specimens is not too small.

2:4 Effect of some other factors

By a series of tests for 24 hours in molten zinc at 450°C it was determined that no difference in the attack rate could be detected between specimens polished on 3 micron diamond paste or roughened with a bastard file, bearing in mind the degree of error involved in the measurements. Similarly no difference was detected between specimens hung near the top or bottom of the bath, or between specimens in the middle of the bath or buried in the iron-zinc alloy at the bottom of the bath. This latter fact is presumably because the alloy is very accicular in structure, and not much denser than the molten zinc; it is thus heavily infiltrated with molten zinc whose activity is thus effectively unity.

Metallographic examination at x50 showed no observable difference between a specimen air cooled after removal from the zinc, and one quenched into iced brine.

CHAPTER 3

DISSOLUTION OF A ROTATING DISC

3:1 Reasons for the work

In many cases where molten zinc is used there is a relative velocity between the zinc and a solid, and if the solid is metallic it is often found to suffer rapid attack. Thus in a modern continuous zinc smelting plant molten zinc, or a lead zinc alloy containing around 2% Pb, at temperatures up to 600°C, flows down water cooled launders, and is pumped from one level to another by centrifugal pumps. In continuous galvanising plants there is generally some handling gear in the form of chains and pulleys which move through the molten zinc. The flow in such cases can be specified by some form of Reynolds Number, and this can vary between zero and perhaps 3×10^5. It is not surprising that this can give rise to enhanced attack on metallic surfaces, and centrifugal pumps are often made of ceramics to avoid catastrophic attack.

It was decided to investigate this phenomenon so as to collect data which would define conditions under which attack might be considered to be enhanced, and to define a "worst case" which a protective system might be expected to resist. Because of the problems involved in passing molten zinc at a known temperature at velocity over a static specimen it was decided that

it was the specimen which should be moved relative to the zinc. It seems that very little reliable work has been done on this system in the past, although attention has been paid to the simpler systems where no alloy is formed.

3:2 Previous work

Several workers have studied the dissolution of cylindrical specimens when rotated in molten metals, particularly where the reaction is not complicated by the formation of solid alloy layers. Thus Ward and Taylor (37) rotated cylinders of copper in molten bismuth or lead for 1-40 mins, 0-200 r.p.m., at temperatures from 360° C to 460° C. The apparatus was run under vacuum, and the lead or bismuth charge was of relatively small mass. The whole of this charge was analysed after a run, and it was possible to determine the solution rate constant K. It was found that even very mild agitation (16 mm sec^{-1}, = 60 r.p.m.) increased the solution rate markedly, by a factor of 2 or 3. It was concluded that in the systems studied the effective rate of solution was controlled by the rate of transfer, by convection and turbulence, of solute atoms from a saturated layer adjacent to the solid/liquid interface, into the bulk of the liquid metal.

In a similar work Stevenson and Wulff (38) rotated cylinders of copper, nickel and three copper-nickel alloys in molten lead at 527° C and 727° C under hydrogen.

The cylinders were capped with inert molybdenum, and were rotated to give peripheral velocities from 8.6 to 126 cm. per sec. Samples of the bath could be taken by withdrawing the specimen for a short time. Again it was found that quite low speeds caused a marked increase in the solution rate. It was felt that for most velocities transport within the liquid was the controlling factor, rather than the transfer from solid to liquid. Intergranular attack was noticed at high velocities.

The results of such work using rotated cylinders, although indicating the general trend of increasing attack with increasing speed, are difficult to apply to systems with different geometry because the Reynolds number is not well defined. Some workers (39) have suggested that the characteristic dimension for the Reynolds number should be the diameter of the cylinder, others the gap between the cylinder and the sides of the bath. The appropriate dimension may well depend on the relative sizes of the cylinder and the bath, or the rotational velocities, and obviously such a situation is theoretically somewhat unsatisfactory.

A system which is now better understood is that of the rotating disc, for which the equations for the flow system have been solved by Levich (40). The solutions apply to the convective diffusion to a perfectly smooth horizontal disc of infinite radius rotating at a constant angular velocity about an axis

perpendicular to the plane, in an infinite liquid under conditions of laminar flow.

It has been found that a practicable system can approximate to these conditions without great error, and such systems are now widely used for the study of reaction kinetics, particularly of electrode kinetics. The practical requirements are that (1) the radius of the disc is very large compared with the momentum boundary layer thickness δ_o which can be given approximately as $\delta_o \simeq 3.6\ (\nu/\omega)^{\frac{1}{2}}$ if laminar, where ν = the kinematic viscosity, η/ρ , and ω = the angular velocity; (2) all other surfaces within or bounding the liquid are at a distance large compared with the radius of the disc; (3) surface irregularities on the disc are small compared with the momentum boundary layer thickness; and (4) the rotation rate for the disc is such that the critical Reynolds number for the onset of turbulence (Re_c) is not exceeded. $Re = r^2\omega/\nu$ where r = radius of the particular point on the discs surface being considered. It is unfortunate that the Reynolds number varies with radius across the disc, but it must be noted that the thickness of the momentum boundary layer is constant at a given velocity, and this is of considerable advantage in many kinetic problems.

Gregory and Riddiford (41) carefully checked Levich's result using a zinc disc dissolving in potassium iodide solution. It was found that for discs 53 mm diameter, rotating at 146 r.p.m. the diameter of the vessel did not matter if greater than about 110 mm

and the height of the disc above the bottom of the vessel if greater than 5 mm. Similar sorts of result have been obtained by other workers (42).

A physical picture of the fluid flow to a rotating disc is as follows. As the disc rotates liquid in an adjacent thin layer acquires the rotational motion of the disc, and from the centrifugal force also develops a radial velocity away from the centre of the disc. This flow pattern in which liquid moves horizontally outward from the centre of the disc, requires an upward axial flow to replenish the liquid at the surface. As a resultant of the two velocities, rotational and radial, a particle within the fluid would trace out a form of spiral over the disc's surface (Fig. 15) If the flow is laminar the momentum boundary layer has a thickness constant in time and space. If however the flow is turbulent then eddy currents are formed and disturb the boundary layer. These eddy currents cause greater erosion than laminar flow, and may thus create channels for themselves, thus becoming stationary relative to the surface of the disc.

This phenomenon provides a method of determining the Reynolds number at which turbulence occurs. In some very careful and rigorous work Gregory, Stewart and Walker (43) rotated perspex discs of 1 foot or 2 foot diameter within a large, still room. The discs were very smooth and flat, and were rotated at stable speeds with minimal wobble. The surface of the discs was coated with china clay, and under conditions of turbulent

flow this was disturbed by the eddy currents and thrown off. By noting the radius at which this disturbance first occurred the Reynolds number could be obtained. It was found that laminar flow could be maintained up to $Re<2x10^5$; in the range $Re = 2x10^5 - 3x10^5$ the conditions were transient and spiral erosion lines were observed, and at $Re>3x10^5$ the flow in the boundary layer became fully turbulent.

Such erosion spirals have been noted after the dissolution of rotated metal discs in metallic melts. Eremenko, Natanzon and Galdzhii (44,45), constructed an apparatus to investigate the applicability of Levich's equations for the rate of migration of a metal through an interface diffusion layer to a rotated disc in a metallic melt. In one experiment using a disc of copper 9 mm. diameter in a bath of molten lead 23 mm. diameter rotated under vacuum at speeds from 8.5 to 615.5 r.p.m. and temperatures from 400^o to 550^o, Levich's equations were confirmed from the analysis of lead samples taken during the run. After the tests the copper specimen was removed and the lead coating stripped by dissolution in molten Wood's alloy. The erosion spirals were noticed on the specimens rotated at the higher speeds, starting at a certain radius from the centre and continuing to the edge. It was thus determined that the transition from laminar to transient flow occurred at $Re>1.5x10^3$, and from transient to turbulent at $Re>3.5x10^3$, i.e. at values 100 times smaller than those previously reported (43). This difference was attributed to a slight

wobble of the disc about the axis of $\pm$0.3 mm. It must be noted that with copper and lead no intermediate phases are formed; in subsequent work (46,47), using iron dissolving in molten aluminium, in which distinct intermetallic compounds are formed, no erosion spirals were noted. Reasons for this will be discussed later.

Previous work involving the attack of zinc on steel has tended to use rather non-standard methods for relative motion. Cameron and Ormay (22), attempting to simulate the agitation in a galvanising bath traversed the specimens along a vertical axis with an amplitude of $\frac{1}{2}$ in. to 1 in. twice a second. Hodge, Evans and Haskins (29), in an investigation into classes of materials resistant to molten zinc, tied test samples with tungsten wire to tungsten rods fixed vertically around the edge of a horizontal disc 4 in. in diameter and revolving at 12 r.p.m., giving a velocity of about 64 mm. sec^{-1}. Weight loss was reported as percentage loss after 50 hours in molten zinc at 440° C or 700° C. Velocities of this order are not likely to produce attack rates differing much from static conditions.

In a series of papers Kosaka, Kato and Minowa (48,49,50) reported the results of their tests using cylinders of iron rotated in molten zinc or aluminium. The specimen diameters varied from 2 mm. to 10 mm. and the bath diameter was 53 mm. For zinc the temperatures varied from 480° C to 670° C, with speeds of rotation from 85 r.p.m. to 1200 r.p.m. Unfortunately there are some errors in their initial assumptions which render their results somewhat suspect. It seems

that they were using a thirty year old copy of the relevant phase diagrams, and that these were considerably inaccurate with respect to the low iron liquidus lines. Thus in an early experiment to determine the diffusion coefficient of iron in liquid zinc they used an iron-zinc alloy which they expected to be wholly liquid at that temperature, but which should in fact contain solid particles of zeta phase intermetallic compounds. It would seem that these settled out under gravity, against a concentration gradient, and caused much dismay when the system was sectioned and analysed.

Later, when attempting to use the formula

$$V = D \frac{n_s - n}{\delta \rho}$$

where V = rate of solution, (cm/sec)

n = concentration of iron in bulk of soln (gm/cm^3)

n_s = saturation concentration of iron

ρ = density of iron

D = Diffusion coefficient (cm^2/sec)

and δ = Boundary layer thickness

with $\delta = f(Re, Sc, d)$

d = specimen diameter

Re = Reynolds number

Sc = Schmidt number ν/D

the saturation concentration of iron in zinc was taken as 1.7 wt.%, at 600° C whereas a more correct value would be 0.9 wt.%, so that the difference between n_s and n may be considerably in error. They also took

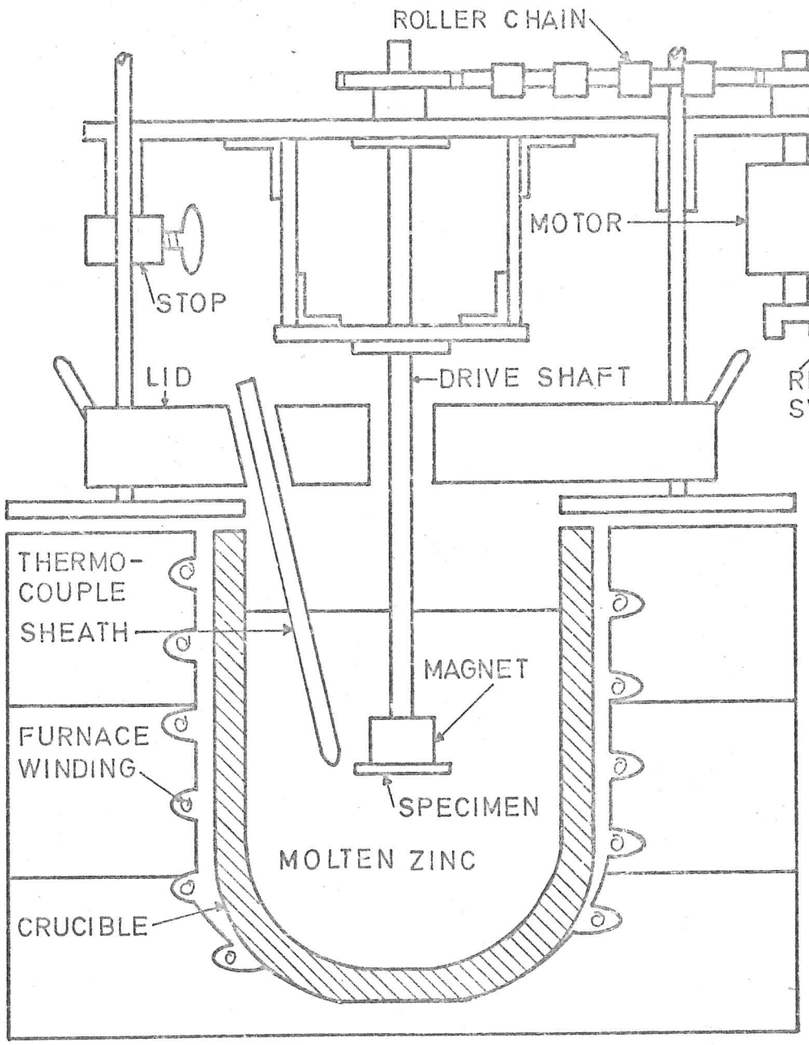

FIG.10 ROTATING DISC APPARATUS (DIAGRAMMATIC)

Re = xu/ν, where x = specimen length, u = surface velocity. Most other workers would feel that the length of the cylinder is not the relevant dimension for Reynolds number. Further, they observed erosion spirals on some of their specimens rotated at 1200 r.p.m. and dismissed the possibility of these being caused by turbulent vortex currents, feeling that they were due to a change-over from a liquid diffusion controlled reaction to an interface controlled reaction. While they might have felt that this change was due to the changing flow pattern, the difference between laminar and turbulent flow was not discussed. In view of these sources of inaccuracy the conclusions presented in these papers cannot be accpted as they stand.

3:3 This work

3:3:1 Experimental Method

It was decided that a rotating disc system would give useful results which could be applied to other systems. It was realised that Reynolds number and the onset of turbulence would vary with the radius being considered, but it was felt that this could be clarified by a mathematical analysis of the results.

Two sets of apparatus were constructed on similar lines, for the rotating disc experiments, Fig. (10,11,12) These consisted of a large salamander crucible, about 6 in. (155 mm.) internal diameter, and 9 in. (230 mm.) deep which was set in a hollow cut out of refractory bricks. Into the sides of the bricks was cut a spiral groove, consisting of about 6 complete circuits and into this groove was set a spiral winding of electrical resistance wire, held in by wire ties taken through the

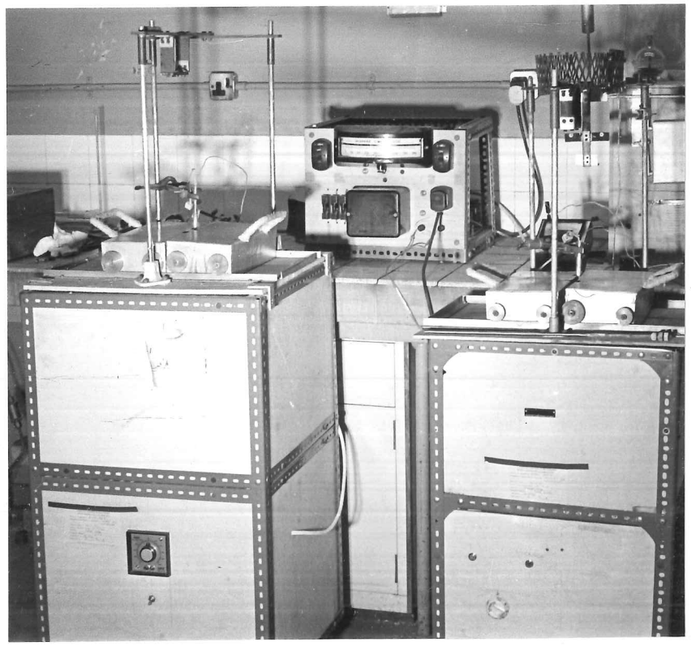

Fig. 11 Zinc baths used for rotating disc experiments.

thickness of brick. The windings did not protrude from the grooves within which they were set, but for safety the outside of the crucible was protected from electrical contact by a wrapping of asbestos fabric.

Above the crucible was constructed an assembly which could be raised or lowered on 3 supporting posts. This assembly carried an electric motor, which was connected via sprocket wheels and roller chain to the vertical drive rod, to which the disc was attached. The crucible was covered by two sliding lids, and by opening these the drive assembly could be lowered and the disc immersed in the zinc. It was thus possible for the disc to enter and be removed from the zinc while spinning.

The specimen disc was attached to the drive rod in one of two different ways. In some initial experiments at low speeds the rod was of tungsten (tungsten not being attacked by molten zinc (29)), with a $\frac{1}{4}$ inch B.S.W. thread at the end. The specimens had a suitable central hole and were bolted on between two tungsten washers with a tungsten nut. The drawbacks were that the central area of the specimens was not being used, and thus the start of erosion lines could not be traced back to their origin if this was under the tungsten washers. Indeed the presence of the nut and washers was bound to disturb the flow pattern. Although the specimen was firmly gripped it was possible for molten zinc to penetrate under the washers and so cause extra attack which could not be quantified.

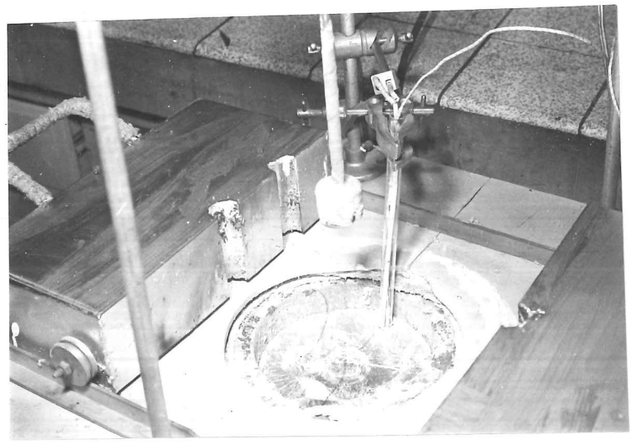

(a)

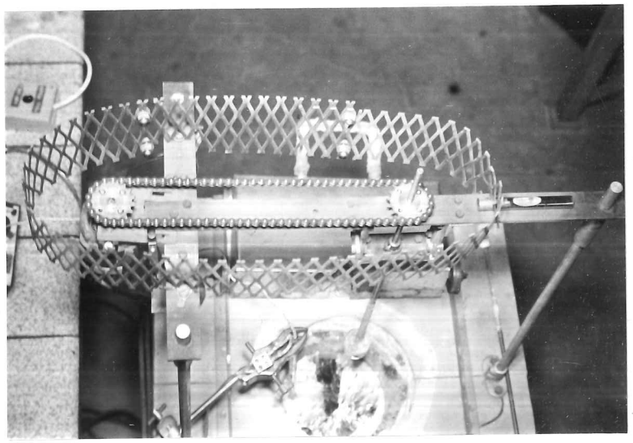

(b)

Fig. 12 Rotating disc apparatus. (a) Close-up of magnetic holder. (b) Drive assembly.

Having only one such rod meant that there were considerable delays while the assembly was cooled after use, the adherent zinc removed with hydrochloric acid and the specimen removed.

While using such a system investigation was made of other non-mechanical fastening methods, and it was discovered that commercial Alnico magnets retained their properties seemingly undiminished at temperatures greater than 500° C, which was the highest temperature to be used. It was thus found possible to use a magnet grip, and this was used with considerable success for most of the remaining runs.

For these runs the drive shaft was of stainless steel and the pot magnet was bolted to the end of this. To prevent attack on the magnet and drive rod these were protected by several layers of "Gun-Gum", painted on as a diluted slurry and thoroughly dried between coats. To bring the specimen into close enough contact with the magnet, and to ensure that it was mounted in a horizontal plane, it was necessary to grind down the "Gun-Gum" from the active faces of the magnet as it had some tendency to swell and blister on drying, and again on immersion in the zinc. This effect was minimised by baking each coat at 150° C once thoroughly dry. Nevertheless it was felt advisable to keep to a minimum thickness of "Gun-Gum" between the magnet and the disc.

The specimens were discs of about 2 mm. thickness and 11.1 mm. radius cut from a rod of En 1a free-machining steel, whose composition is displayed in the table

This steel was chosen largely because it was available to hand in a convenient size, but it was also felt that its chemical composition was reasonably typical of a range of widely used steels.

TABLE 3

Composition of Steel En 1a

Carbon	0.07-0.15%	Phosphorous	0.07% Max
Silicon	0.10 Max.	Manganese	0.8-1.2%
Sulphur	0.20-0.30%		

As will be seen later, the manganese sulphide inclusions present in this steel would not be expected to have much influence on the attack rate. The silicon content is well down in the "insignificant" range (4).

The rod was first lightly machined to remove surface oxide and scale, and the discs cut off and surface ground to a finish corresponding roughly to that produced by a 220 mesh paper. As had been established in Chapter 2 although there may be some difference in the attack rate and amount of zinc adhering to the surface between polished and very rough specimens when galvanised for short periods (11) this difference becomes too small to detect when periods as long as 1 hour are involved. This is presumably due to the smoothing effect which is especially noted at sharp corners.

These specimens were measured and weighed, degreased and given two thin coats of diluted "Gun-Gum", each coat being baked at 120° C when dry. The back and sides

of each specimen were coated, and any coating which reached the front face was gently scraped off. Blanking-off the active face with lacomite or sellotape was tried but proved to be somewhat less than perfect. It was sometimes necessary to apply a third coat to the edges of the disc so as to produce a layer of adequate thickness in this region.

Immediately before use the active face of the disc was given a thin coating of a proprietary resin flux. It was then attached to the magnet with its active face down, and manually centered. The motor was then run up to the speed at which the test was to be carried out to check that the disc was adequately centered and would not be thrown off at speed, and to check visually that the lower face was in a horizontal plane. It was felt that if these conditions were met before entering the zinc, then once immersed the up-flow of zinc to the disc would help to hold it in place, and that any blistering or swelling of the "Gun Gum", although likely to tilt the specimen, was unavoidable.

When these checks had been carried out the two lids of the furnace were drawn back and the drive assembly lowered, with the disc spinning, until a few millimeters above the surface of the molten zinc. It was held here for a few moments to allow the specimen to warm up somewhat and throw off the surplus flux, which might otherwise have charred and stuck to the surface. The assembly was then lowered further until the disc was roughly in the centre of the bath. The lids could then be closed

and the motor speed adjusted to compensate for the drag caused by the viscosity of the zinc.

Some 30 mm. of freeboard had to be allowed so that the agitated zinc did not spill over the top of the crucible. The depth of zinc was therefore about 180 mm. corresponding to a weight of around 14 Kg. The zinc was of high purity (99.99% Zn, 0.007% Cd, 0.0001% Cu, 0.002% Fe, 0.003% Pb) and was saturated with an excess of pure electrolytic iron at the temperature of the test and allowed to equilibrate for at least 24 hours before starting a series of tests. Because of the large mass of zinc involved relative to the total amount of steel dissolved in the series of tests it was felt that there would not be any significant build-up of undesirable alloying elements, and the initial charge of zinc was not replaced during the runs, although small additions were made to replace losses. These losses were due largely to the removal of zinc oxide from the surface of the bath before a run, and also to the occasional removal of the zinc-rich iron-zinc intermetallic which settled at the bottom of the bath.

The temperature of the molten zinc was controlled by a thyristor controller, using a deviation-dependent proportional control system and zero-voltage switching. This monitored the output of a chromel-alumel (T_1/T_2) thermocouple in a silica sheath immersed in the zinc so as to be close to the specimen. The control was such that any oscillations in temperature were less than $\pm 3^{\circ}C$ about the mean. The preparation and entry of the

specimen into the bath caused the temperature of the zinc to fall by perhaps 5°C. This was corrected within 10 minutes once the lids were replaced, and it was felt that any error involved, due to the lower attack rates at lower temperatures, could be tolerated. It was not really feasible to preheat the zinc to allow for this drop because it was not easy to accurately set a desired temperature on the controller. To reach a desired temperature required several slight adjustments of the setting, allowing equilibrium to be reached before any further adjustment. Nevertheless it must be emphasised that the temperature remained constant once set.

Accurate measurements of temperature were made on a Comark electronic thermometer type 167C, using an Iron-Constanton thermocouple to B.S. 1829 in the same sheath as the Cromel-Alumel thermocouple. Using this electronic thermometer it was possible to read the temperature to about $\frac{1}{2}$°C, with a guaranteed accuracy of 2°C. Because the furnace controller had no indication of actual temperature as opposed to set-point temperature it was necessary to use the Comark to indicate the true temperature of the zinc. On occasions a third thermocouple (Cromel-Alumel) was used, driving a chopper-bar type pyrometric recorder. This was used to monitor the behaviour of the controller when faced with a sudden deviation, as on the entry of the specimen, and also to give some further evidence that the temperatures during a run were within satisfactory limits.

The electric motor, of a type used for heavy duty drills, was controlled by a simple thyristor circuit, involving a degree of feed-back from the motor, which was designed to give a high torque even at low speeds. In practice there was a lower limit to the speed, below which "motor-boating" occurred, due to the motor speeding up, and then "skip-cycling" with no power input. The motor was connected to the drive rod by means of sprocket wheels and roller-chain. Various sizes of sprocket wheel were available, and the position of the motor was adjustable so as to suitably tension the roller chain. Generally the smallest wheel was used on the motor shaft, and the largest on the drive rod, giving a reduction of about 2:1, allowing the motor to run at a reasonably high speed. The largest sprocket wheel had considerable mass, and thus provided a form of flywheel. On the other hand, when run at the highest speeds the motor was capable of (~6000 r.p.m.) the balance of the wheel became very important, and if slightly off centre it caused considerable vibration.

The speed of the motor was measured by two different systems. A stroboscope was used to determine the magnitude of vibrations in the system, and was also used to measure the motor speed, using a mark on the sprocket wheel. This was a little tedious because the speed was not constant, and therefore the frequency of the stroboscope needed continual adjustment. An improvement was made by fitting a small pot magnet to the lower end of the motor spindle which then operated a fast-acting reed

switch mounted on the drive assembly frame. The closure of the reed switch contacts, produced twice per revolution by the magnet, was used to trigger the stroboscope, thus giving a frequency directly coupled to the motor speed; the speed could then be read directly off the stroboscope's scale. Unfortunately however, at high speeds the switching action became somewhat uncertain, due perhaps to contact bounce, and this system was then not fully reliable. Recourse was made to a hand held mechanical tachometer which was driven by direct contact with the drive rod. This gave results which agreed with the stroboscope at lower speeds, and were felt to be more reliable at high speeds. Most of the readings were taken from this instrument.

The motor speed did not remain constant, and needed frequent correction. The direction of drift varied, low speeds tending to increase and high ones to decrease. This was felt to be due to several effects, i.e. the warming up and loosening of bearings, and the changing electrical characteristics of the motor windings and thyristor as these became warm. If uncorrected the speed could alter by about 20% over one hour, most of this occurring in the first 20 minutes. It was therefore necessary to check the motor speed at frequent intervals, and to make adjustments as required. This resulted in an accuracy of about $\pm 5\%$.

The drive rod ran in two ball bearings set about 100 mm. apart, and extended about 250 mm. below the

lower bearing. This length was necessary to take the drive through the furnace lid to the centre of the crucible, but meant that there was a certain amount of "whip" in the system at the lower end. This was minimized by the use of stainless steel for the drive rod, with considerable stiffness, but at certain speeds there was an unacceptable degree of lateral oscillation of the disc and magnet, which could be as large as ± 5 mm. normal to the vertical axis. Some lesser degree of oscillation, ± 2 mm., was observed at other speeds. This was accentuated if the disc was mounted off centre, and could result in the disc being thrown off. As a result of this it was necessary to stick the disc on with some "Gun-Gum" if a particularly high speed was desired. However this was not always strong enough, and often resulted in the disc not being in a horizontal plane. It was found that the practical upper limit of speed was about 2500 r.p.m.

At such speeds the turbulent forces were such as to rapidly erode the "Gun-Gum" from certain areas of the magnet and it was necessary to give these regions extra protection with layers of asbestos paper between coats of "Gun-Gum". Under such conditions it was necessary to check the continuity of the protective layers after each run, instead of after every third run as at lower speeds. In no instance was there any significant erosion of the actual metal of the magnet or drive shaft, although some spots where attack had started were found. Since the runs were arranged at different speeds in a random manner, interspersed with static tests, and no anomalous

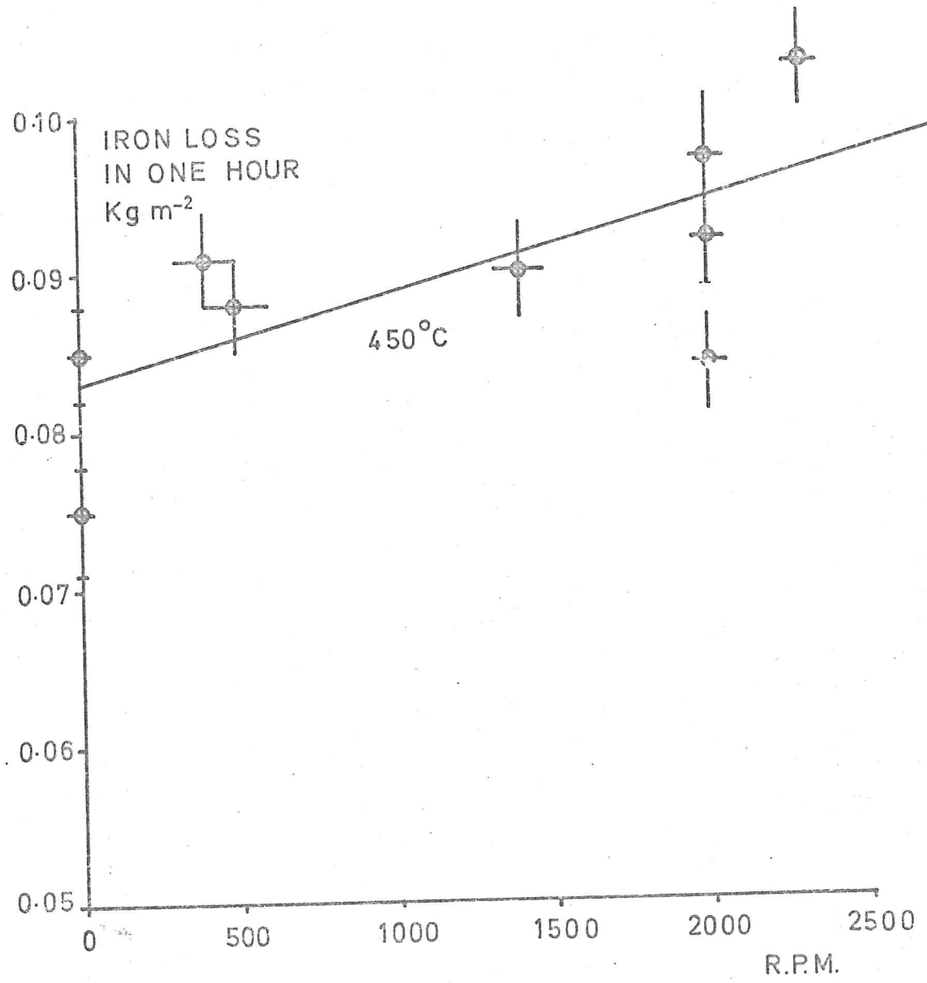

FIG. 13

results were noted, it was felt that any contamination by elements from the magnets or drive rods was too small to be significant.

All runs were of one hour's duration, and at the end of that time the disc was removed while still spinning, and the zinc and "Gun Gum" stripped off as previously mentioned. The weight loss was determined and the loss per unit area obtained by dividing by πr_o^2, where r_o = outer radius of the disc. The results are displayed in figures (13) and (14).

3:3:2 Results

It is clear that at 450° C the rate of attack averaged over one hour is scarcely affected by the rate of spinning of the disc, whereas the rate at 500° C shows a marked dependence on speed. Furthermore, examination of the surface of the specimens after removal of the zinc and alloy layers showed that many of those rotated at 500° C showed erosion spirals which extended inwards to some radius which depended on the speed of rotation, while those rotated at lower speeds or at 450° C showed no such spirals. These spirals are illustrated in Figure 15. Metallography of cross sections of some specimens showed that those rotated at 500° C at the higher speeds had only a very thin alloy layer, and that at lower speeds the alloy layer was somewhat thicker. Those rotated at 450° C produced an alloy layer whose thickness was about $\frac{1}{2}$ that produced on a static specimen, the thickness seeming independent of speed. Although

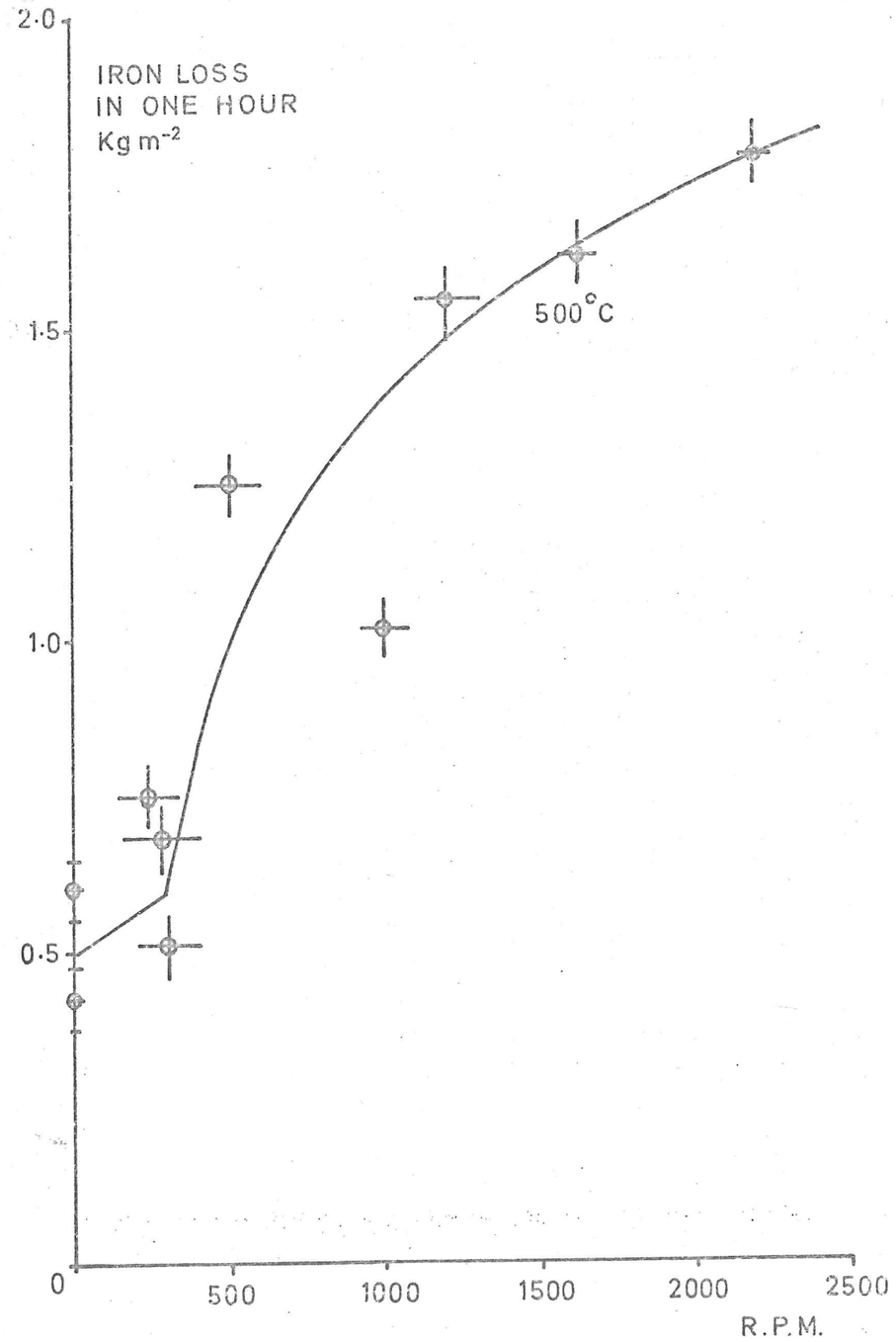

FIG. 14

no precise measurements were made it was felt that the thickness of the gamma intermetallic layer was the same on static and rotated specimens at 450° C.

3:4 Conclusions

3:4:1 The proposed model of the system

A simple model of the possible reactions occurring between iron and zinc can be constructed by considering the possible behaviour of zinc atoms moving towards the iron. The necessary stages arethus: (1) Movement through a depleted layer in the molten zinc; (2) Crossing the interface into the solid alloy layer; (3) Diffusion through the alloy layers down a concentration gradient towards the iron, crossing phase boundaries en route. This process may be speeded up by "short circuiting paths", such as cracks or grain boundaries. During this diffusion the zinc may react with iron moving in the opposite direction; (4) Eventually crossing the boundary from the alloy layers into the iron, and diffusing into the α iron. During these reactions iron atoms will be moving in a corresponding manner in the opposite direction.

Any one of the above stages might be the rate controlling reaction under particular conditions. Indeed they have all been individually suggested as the controlling reactions under normal circumstances (2). Many workers feel that it is the diffusion rate in the gamma layer which is the important rate controlling step at 450° C, and perhaps the absence of such a layer at 500° C

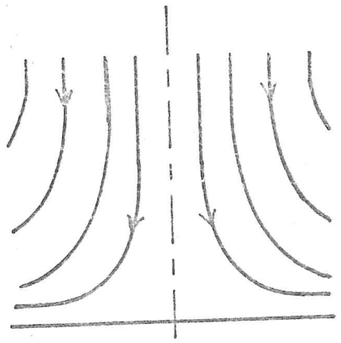

(A)

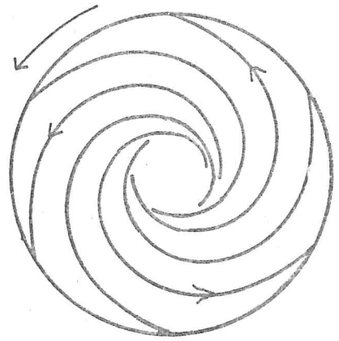

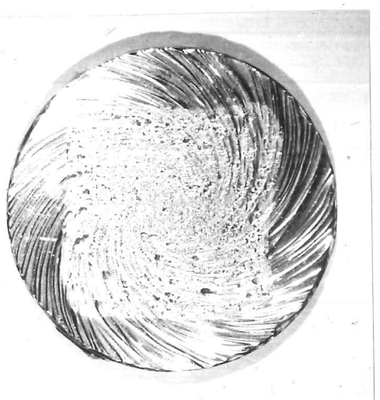

(B)

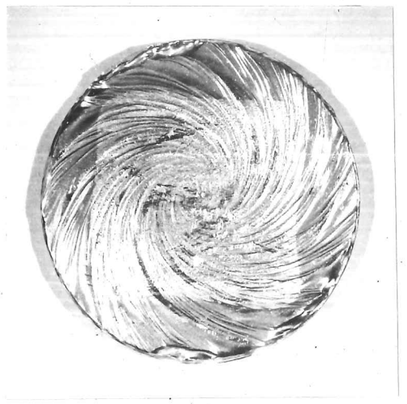

FIG.15 (A) FROM REFERENCE (40)
(B) SPUN IN ZINC AT 500°C
X2

which causes the more rapid attack at this temperature.

This work would seem to support the hypothesis of control by the diffusion in the gamma layer at 450°C. At this temperature the alloy layer is dense and coherent, with a somewhat irregular boundary between the zeta and the zinc. Gradual increase of the speed of rotation of the disc through the laminar and into the turbulent régime would be expected to decrease the thickness of any depleted boundary layer ($\delta \propto 1/\omega^{\frac{1}{2}}$ in the laminar region), and thus increase the attack rate if this was governed by diffusion in the liquid zinc. Loose or protruding zeta would be swept away, and the overall thickness of zeta reduced. When turbulence set in the outer surface of the alloy layer would be subject to considerable scouring by eddy currents, and these might form stable erosion spirals on the surface of the alloy layer. However, because of the strength and coherence of the intermetallics at this temperature they would appear to resist any great overall attrition and thus the underlying Gamma layer is virtually unaffected and the overall attack rate is unaltered.

The same argument does not apply to the hypothesis of control by the delta layer, because this was observed to be noticeably thinner on the rotated specimens relative to the static ones. It would seem that the thickness of this layer is closely related to that of the zeta layer. When the zeta layer is thinner due to the attrition of its irregular outer surface then the underlying delta layer is also thinner. Since this seems to have little effect on the overall attack rate then

presumably neither of these layers can be considered to be the rate controlling one.

Working on this basis it can therefore be expected that the relative velocity of the molten zinc over the iron surface at 450°C will have no distinct effect until the velocity is high enough to cause such violent eddies and turbulence that the zeta and delta layers are eroded down to a thickness similar to that of the gamma layer. This work would suggest that the velocity required for this is high, perhaps 5 metre per second.

At 500°C the conditions are very different. The alloy layer is very fragmented and lacks coherency. It is possible that it possesses sufficient strength to resist attrition under lamina conditions, but certainly once turbulence sets in the fragmented delta is swept away, leaving a thin layer of coherent delta, with possibly a very thin layer of gamma underneath (4). Under such circumstances it is not clear what is controlling the rate of reaction. It may be the gamma layer, whose presence is disputed, and whose thickness is possibly determined by that of the delta layer (4), or alternatively by the thickness of the delta layer itself. A third possibility is that the reaction at some interface becomes rate controlling. If diffusion through an alloy layer is rate controlling then under a particular flow condition the thickness of the alloy layer will be such that the rate of diffusion, and hence the overall reaction rate, is such as to replace the alloy layer at the rate that the outer surface is

suffering attrition. Thus the alloy layer will reach a certain constant thickness, and the attack rate will be linear with respect to time, but varying with flow rate. On the other hand, if an interface reaction is the controlling step, the rate will be linear and independent of flow rate.

The fact that erosion spirals are observed on the steel surface supports the diffusion hypothesis. Stable eddies first form on the surface of the intermetallic layer, and cause greater erosion, thereby thinning the alloy layer underneath them. This results in more rapid attack on the steel substrate underneath, thus duplicating the pattern. If an interface reaction was involved this should be independent of flow velocity or thickness of intermetallic layer, i.e. a constant rate at all points on the surface, and there would be no method for producing the spirals on the steel.

3:4:2 Mathematical relationships

The results at 450° C require little analysis. The static results agree quite well with Horstmann's figures (23) for various similar alloys, 73×10^{-3} to 109×10^{3} Kg m^{-2}. There would seem to be little point in saying other than that this rate of attack is effectively constant with varying speed. A least squares linear regression for all the points gives: (Weight loss in 1hour, Kg m^{-2})$\times 10^{3}$ = 0.0057 r.p.m. + 83.

The results at 500° C are more complex, and because of the nature of the rotating disc system, more difficult

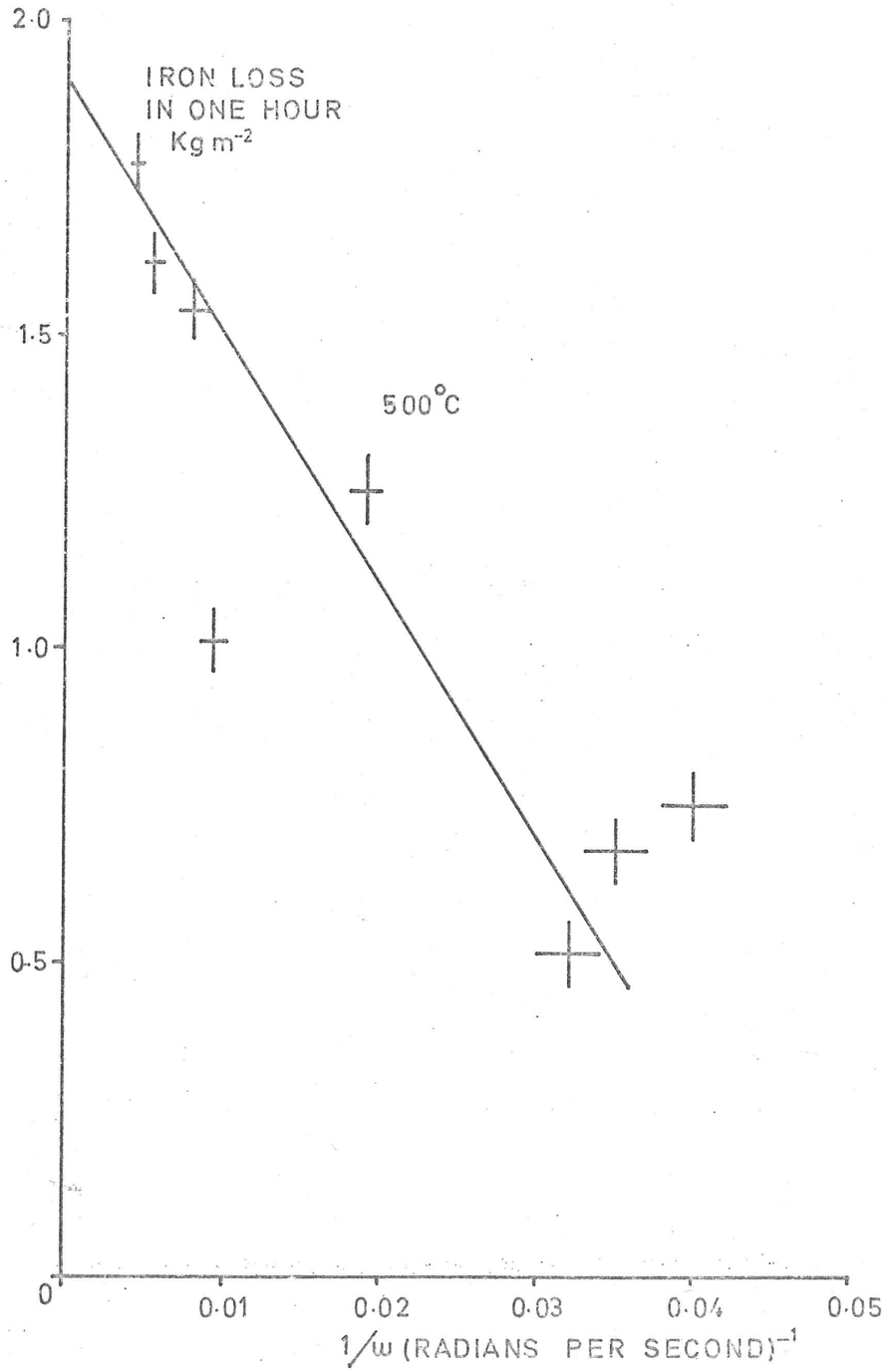

FIG.16

to analyse. At low speeds the flow over the entire surface is laminar; as the speed increases so the turbulent region moves in from the edge towards the centre, but in theory there is always a certain region in the centre which remains lamina. Thus there are two regimes present on the same specimen, and to separate the effect of these some simplifications have to be made.

It thus seems reasonable to assume that the attack rate in the lamina region (A) is independent of the velocity of the disc. The flow over the whole disc is lamina up to about 200 r.p.m., but no readings could be taken in this region because of the poor stability of the motor at low speeds. The attack rate in the turbulent region (B) may well depend on the angular velocity, ω, but the evidence of Fig. 14 is that such a dependence is not very marked and for simplicity we can take B as independent of ω.

The situation now is that from the centre out to a certain radius r_c the flow is lamina, with attack rate A; and from r_c to the edge at r_0 the flow is turbulent, with attack rate B. The overall measured weight loss per unit area is thus:

$$\frac{\Delta W}{a} = \frac{\pi r_c^2 A + \pi B(r_0 - r_c^2)}{\pi r_0^2} \qquad r_c < r_0$$

where $r_c^2 = \dfrac{Re_c \eta}{\omega \rho}$ $\qquad r_0 = 11$ mm.

Thus $$\frac{\Delta W}{a} = \frac{r_c^2}{r_0^2}(A-B)+B = \frac{Re_c \eta}{r_0^2 \omega \rho}(A-B)+B$$

Plotting $\dfrac{\Delta W}{a}$ vs $\dfrac{1}{\omega}$ as in Fig. 16 gives

Slope $= -40 \pm 7$ $\qquad$ Intercept (=B)=1.9 Kg m^{-2} hr^{-1}

Taking $\rho = 6.59$ gm cm^{-3}, $\eta = 3.67 \times 10^{-2}$ poise (12) and assuming that rate "A" is similar to the rate when static, i.e. ~ 0.5 Kg m^{-2} hr^{-1},

then $Re_c = (6 \pm 1) \times 10^3$

3:4:3 Measurements from erosion spirals

Direct measurement of r_c, taken as the point at which the erosion spirals could be seen to start gave values of Re_c between 1000 and 2000, similar to those found by Eremenko et.al. (46). The difference between these values and those found above by the graphical method is probably because they are measures of different transition points. Between the fully lamina and the fully turbulent regions there is a transition region where the lamina flow is not fully stable, and may become turbulent. It would seem that the attack rate in this region is similar to that in the fully turbulent region, but that the eddy currents are not stable and do not produce distinct erosion spirals. Taking ω=100 radions sec^{-1} we have:

$$Re_c = 2 \times 10^3 \rightarrow r_c = 3.3 \text{ mm}$$

$$Re_c = 6 \times 10^3 \rightarrow r_c = 5.8 \text{ mm}$$

It is thus clear that this transition region occupies only a small region, comparable with the uncertainty in the determination of the point at which the erosion spirals start.

3:4:4 Reconciliation with other work.

As previously mentioned, the above results for Re_c

are in agreement with those of Eremenko et.al. (46), but differ from those of Gregory, Stuart and Walker (43). There is no reason to believe that the flow over a disc should differ between molten metals and air, and it is therefore necessary to establish what factors cause the different results. In both this work and that of Eremenko et.al. there was a lateral wobble of the disc which is quite likely to disturb the lamina flow pattern and promote turbulence at a lower speed than on a better balanced system. To eliminate this wobble would require a bearing for the drive rod, together with supporting frame, very close to the disc, possibly even in the molten metal. This is likely to present certain problems.

Another relevant factor is the roughness of the surface of the disc, i.e. the outer intermetallic layer. Carnet, Lewis and Kappesser (51) cast discs of monel on sandpaper, and then spun them in aerated sodium chloride solution and determined the Reynolds Number for transition from lamina to turbulent flow. This was found to decrease markedly as the roughness increased:

Polished	$Re_c = 2.6 \times 10^5$
No. 80 grit	$Re_c = 6.5 \times 10^4$
No. 16 grit	$Re_c = 2.8 \times 10^4$

The discs used in the molten zinc started off quite smooth, but under static conditions the outer surface of the alloy layer could be quite rough and uneven. When spun such high spots would suffer greater attrition

thus tending to produce a smooth surface, but it is possible that the growth and protuberance of large intermetallic crystals could help the transition to turbulent flow.

It is felt that the specimen wobble is the one factor most likely to have effectively lowered the speed at which turbulence starts. Nevertheless there would seem to be no reason to doubt that the attack rate observed in such tubulent conditions is the same as that which would be produced by turbulent flow under other conditions. Thus in other systems knowledge of the relevant Reynolds Number relative to that for tubulent flow in such a system, together with the results evaluated here, should make it possible to estimate the attack rate with some degree of accuracy.

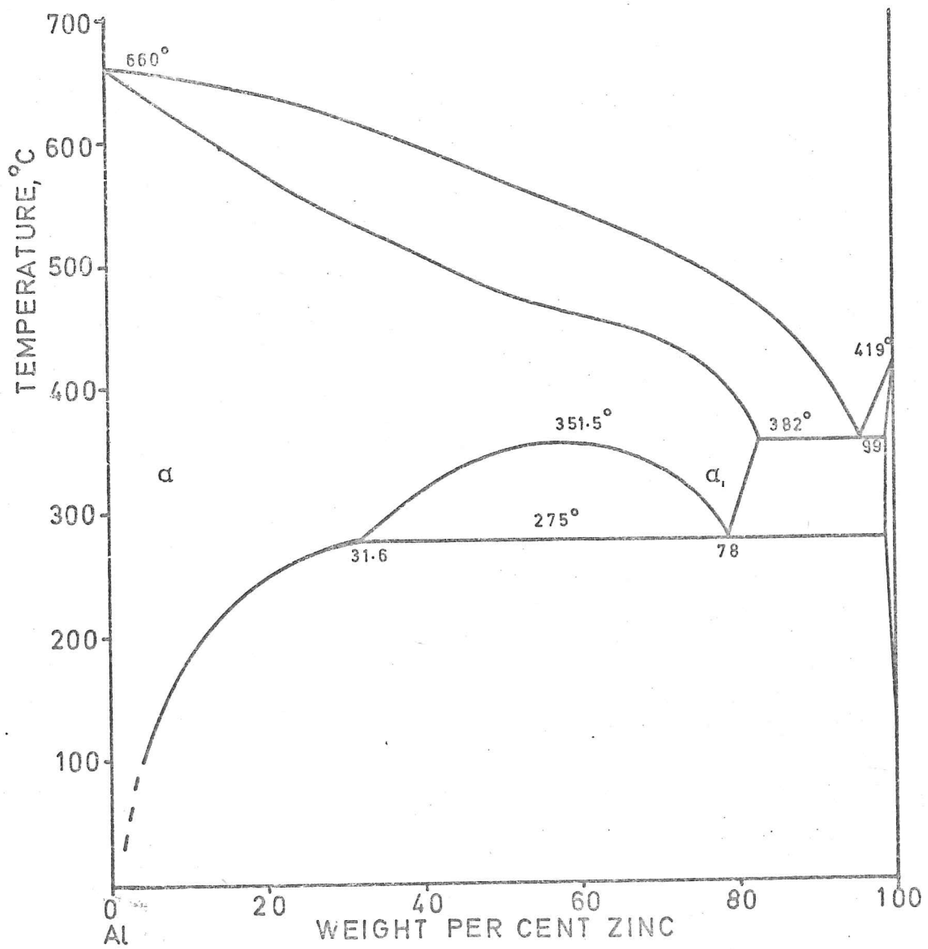

FIG·17 FROM REFERENCE (5)

CHAPTER 4

EFFECT OF ALUMINIUM IN ZINC

4:1 Background

Die-casters using the "Zamak" type zinc alloys containing 3.5 - 4.3% Aluminium and operating at temperatures around 400° C report very low rates of attack and erosion on the steels used for dies, nozzles, plungers etc., but there is no evidence to say if this is due to the lowered operating temperature relative to zinc (see Fig. 17), or to the high aluminium content.

As stated in Chapter 1 aluminium is widely used by galvanizers at a much lower concentration to inhibit the normal alloying behaviour while the steel is passing through the bath. Some galvanizers have complained that the addition of aluminium to the bath causes an increase in the rate of attack on the bath structure. It is generally agreed that after the inhibition period the attack is very rapid and linear with time, but Bablik (11) suggests that this may then slow down so that after 24 hours there is no difference between the weight loss in a pure zinc bath and one containing 0.5% Aluminium. Horstmanns results (35) also suggest that the rapid attack may diminish after some hours. Because of the lack of data on attack over long periods, and the potential protection produced initially by iron-aluminium alloy layers a series of tests were carried out involving

additions of aluminium to the molten zinc.

4:2 Experimental methods.

The tests were carried out in the baths used previously for the rotating disc work. These were charged with known weights of 99.99% purity zinc, and calculated additions of 99.5% purity aluminium were made to give the required analyses. Because of the interaction of iron and aluminium within the bath only small quantities of pure iron were added, so as to saturate the bath with this without excessive removal of aluminium as iron-aluminium intermetallics.

Frequent samples were taken from the bath at different levels between runs, using a specially designed pyrex pipette. These were analysed for iron and aluminium using a Pye-Unicam SP 90 Atomic Absorption spectrophotometer, using cold cathode lamps. This method measures the total content of the element in the sample, both that dissolved in the zinc and that combined as intermetallics. Samples taken from the middle of a bath left standing overnight generally showed an aluminium content some 10% below that nominally present, with the iron content very low. Samples taken from the bottom of the bath had higher aluminium contents, around twice the nominal value, together with perhaps 0.2% iron. This presumably represents the inclusion of iron-aluminium intermetallic crystals; stirring the bath mixed these up with the zinc and gave higher measurements of iron and aluminium from the middle of the bath. It was

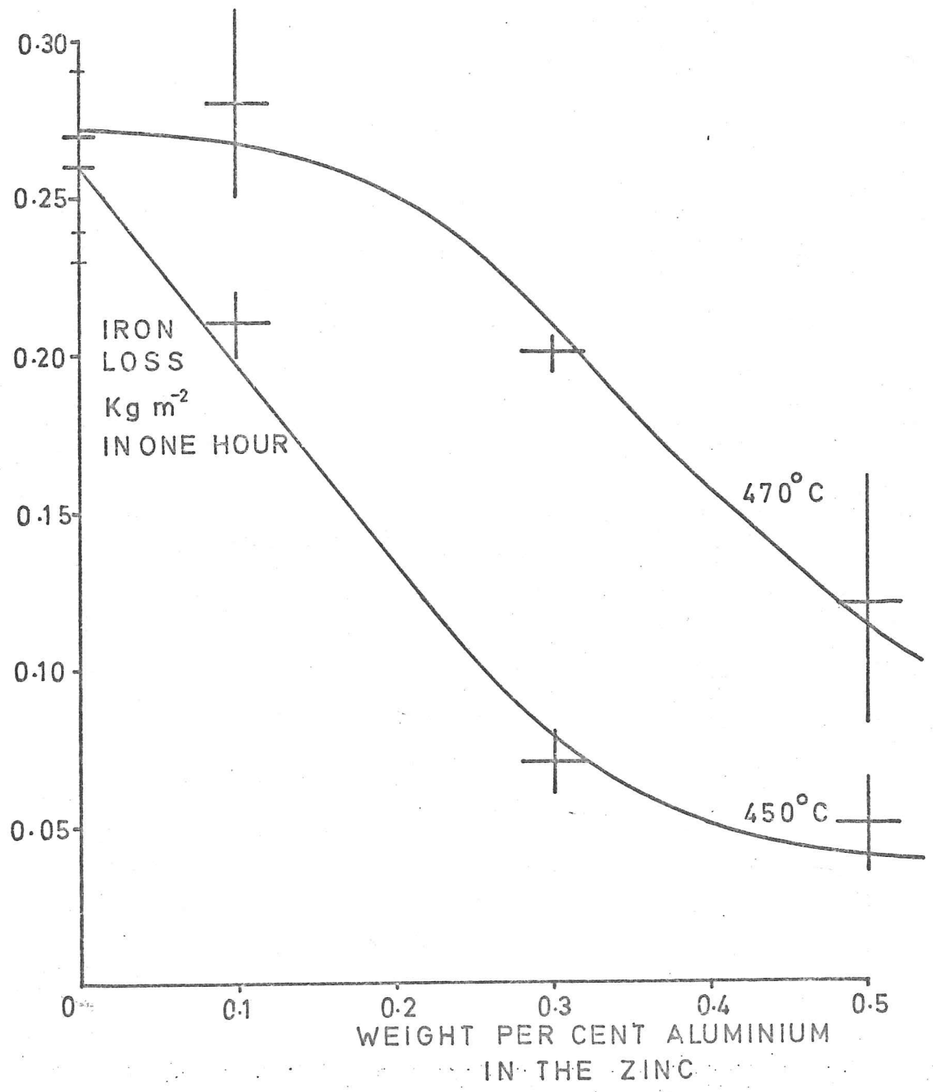

FIG.18

also found that the oxide and dross formed on the bath surface was rich in aluminium.

The steel specimens used came mainly from a hot rolled low carbon steel bar, $1\frac{1}{8}$" diameter (29 mm) supplied by B.I.S.R.A., code "BB". The analysis of this as quoted by B.I.S.R.A. was:

0.12% C 0.69% Mn 0.22% Si 0.054% S 0.039% P 0.09% Ni 0.06% Cr.

This corresponds to En 32b, and was selected as being a readily available steel with relatively low impurity levels. This wassawn into slices about 3 mm. thick and was ground flat on both surfaces to a finish corresponding roughly to that produced by a 220 mesh paper.

4:2:1 <u>One hour runs</u>.

In the first phase of the investigation some of these discs were weighed, measured, and coated on one flat face and round the edge with "Gun-Gum" as for the rotating disc experiments. They were lightly fluxed, stuck onto the magnetic holders used previously and immersed in the zinc bath for one hour. Most were held static, but some were rotated at 1500 r.p.m. On removal they were stripped and re-weighed as before. Those rotated in aluminium-containing alloys generally showed a somewhat lower rate of attack than those kept static. This was probably due to local depletion of aluminium around the static discs. This phenomena was not further explored, and the results for each set of conditions have been averaged together, and are displayed in Fig. 18, each

point being the mean of some 5 individual results. The values obtained for weight loss/area in pure zinc are rather higher than expected for a low carbon steel; Horstmann quotes around 0.1 Kg m^{-2} (23). This may be due to the effect of the manganese and silicon impurities acting together, or some systematic error, perhaps in the measurement of the specimen areas. It is possible some attack occurred around the protected edges of the specimen, where the "Gun-Gum" was weakest, and that some of the principle face was obscured by stray traces of "Gun Gum".

4:2:2 Longer runs.

Attempts to extend the method used satisfactorily for one hour to tests lasting several days proved to be unsuccessful. After 1 or 2 days the discs had a very thick layer of alloy adhering to them. The loss of iron was considerable, and attack had frequently taken place between the steel and the "Gun Gum" coating, resulting eventually in alloy formation on the back of the disc which pushed it off the magnet. Added to this was the large uncertainty in the effective surface area.

The magnetic suspension system and "Gun Gum" coating were thus abandoned, and future tests were carried out using discs suspended by tungsten wires or resting freely on the bottom of the bath; excessive dross was removed between runs. The tungsten wires were fixed through small holes drilled in each disc, thereby increasing to

some degree the surface area, and resulting in slower stripping because of the extra time required to remove the zinc from inside the hole. The whole area of the disc was used as a reacting surface, i.e. 2 flat faces plus the curved edge.

These modifications proved to be successful, and a series of satisfactory runs were carried out for up to 5 days, with aluminium up to 5% and temperatures between 400° C and 530° C. A subsidiary series of tests were carried out on some small squares cut out from some thin stainless steel sheet, probably 18% Cr 8% Ni. Because of the danger of contaminating the main bath these tests were carried out in a small crucible in a muffle furnace. The results of all these runs are displayed in Figs. 19 - 26. It should be noted that the attack rate at 530° C with 5% aluminium was so rapid that discs were totally consumed within 24 hours, giving a minium weight loss in that time of around 11 Kg m^{-2}.

4:2:3 Sources of error

Because of the large loss of iron under certain conditions the mass, and hence the area of the discs can change considerably during a run, so that attack rates based on the original area became inaccurate. However, with the thickness of discs used the change in area is very much less than the change in mass until the disc becomes of the zero thickness. Ideally the disc should be measured before and after attack, and some

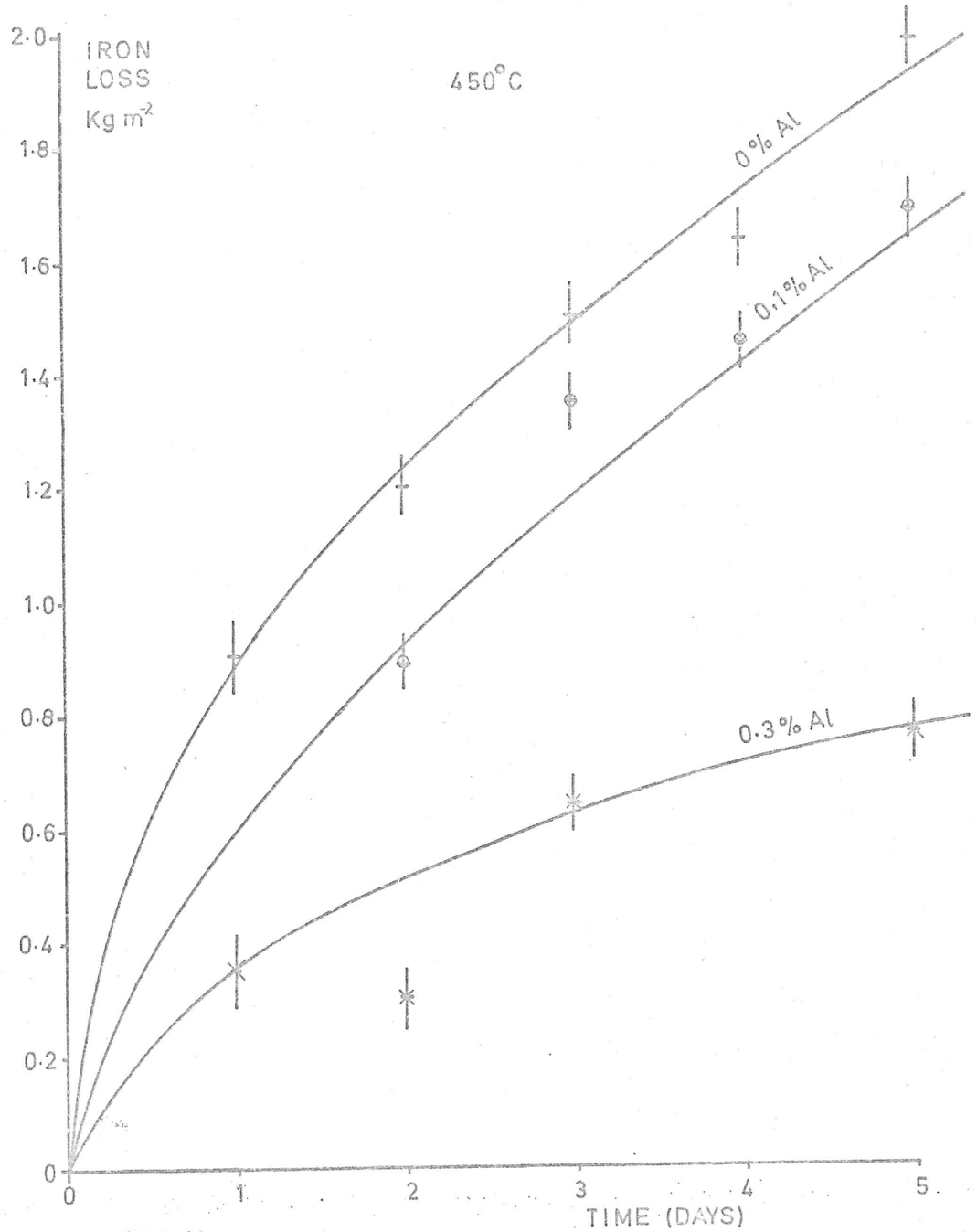
IRON
LOSS
Kg m⁻²
450°C
2·0
1·8
1·6
1·4
1·2
1·0
0·8
0·6
0·4
0·2
0
0% Al
0·1% Al
0·3% Al
0
1
2
3
4
5
TIME (DAYS)

FIG. 19

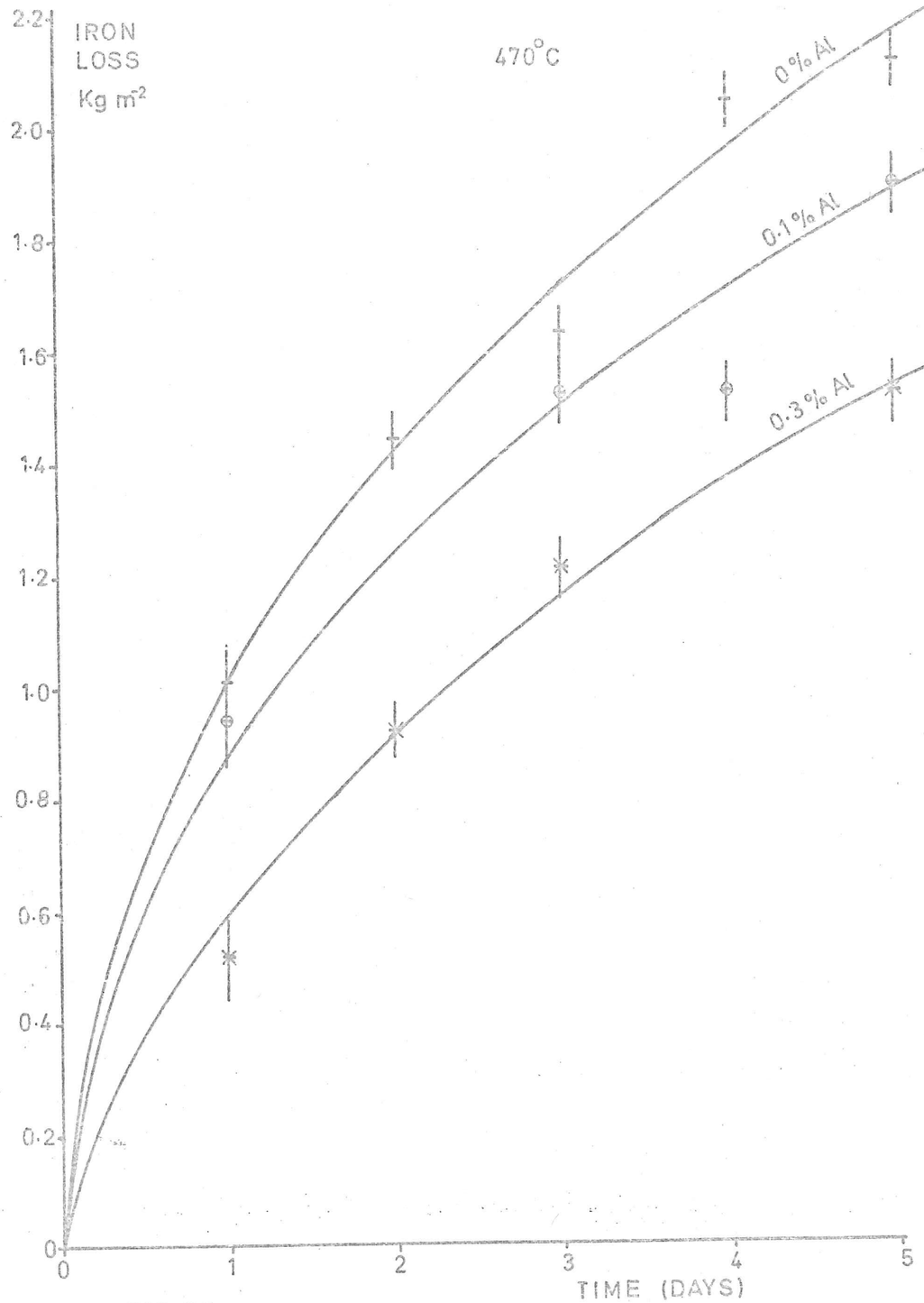
IRON
LOSS
Kg m²
470°C
0 % Al
0·1 % Al
0·3 % Al
2·2
2·0
1·8
1·6
1·4
1·2
1·0
0·8
0·6
0·4
0·2
0
0
1
2
3
4
5
TIME (DAYS)

FIG. 20

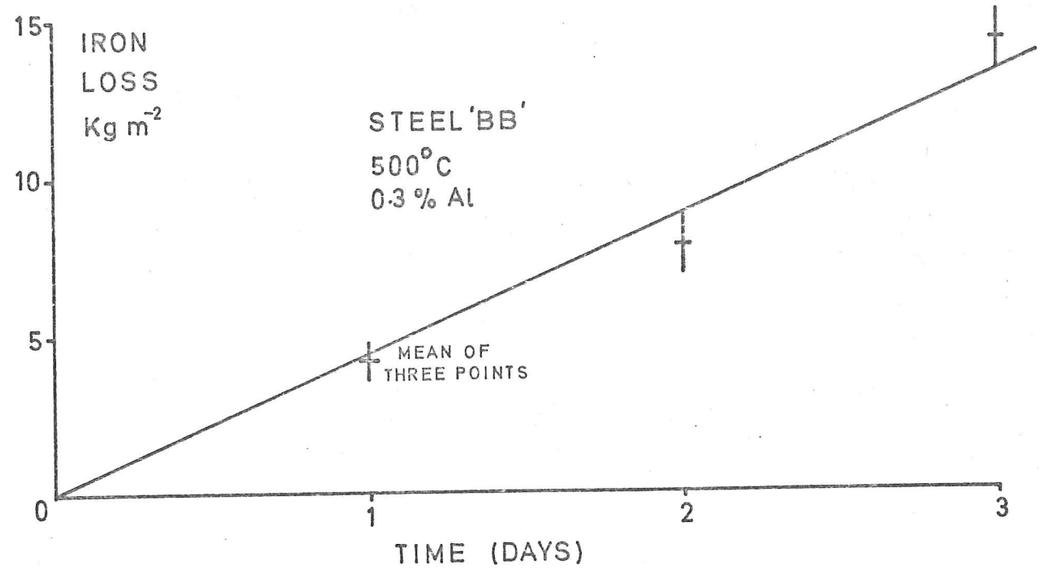
15
10
5
0
IRON
LOSS
Kg m^{-2}
STEEL 'BB'
500°C
0·3 % Al
MEAN OF
THREE POINTS
1
2
3
TIME (DAYS)

FIG. 21

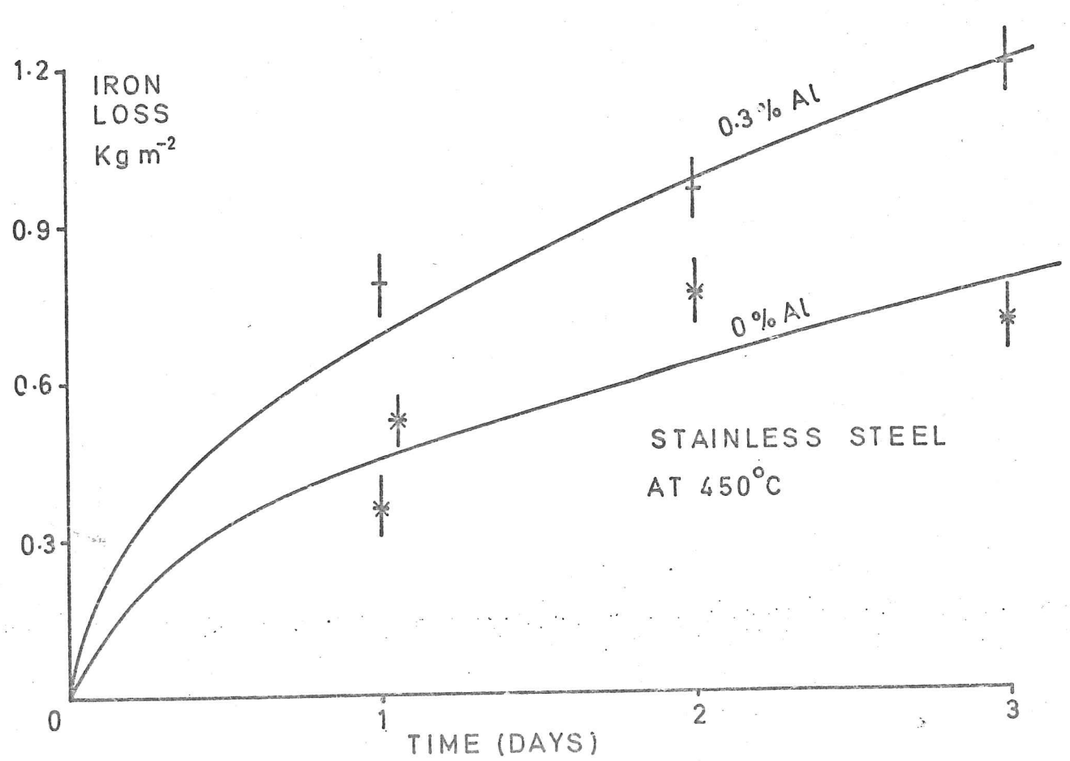
1·2
0·9
0·6
0·3
0
IRON
LOSS
Kg m^{-2}
0·3 % Al
0 % Al
STAINLESS STEEL
AT 450°C
1
2
3
TIME (DAYS)

FIG. 22

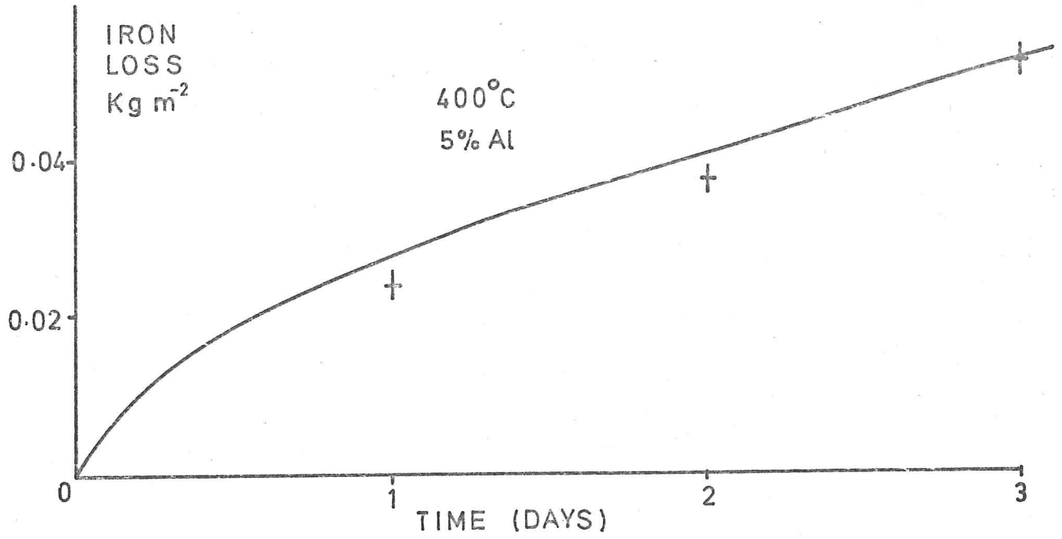
IRON
LOSS
Kg m^{-2}
400°C
5% Al
0·04
0·02
0
1
2
3
TIME (DAYS)

FIG. 23

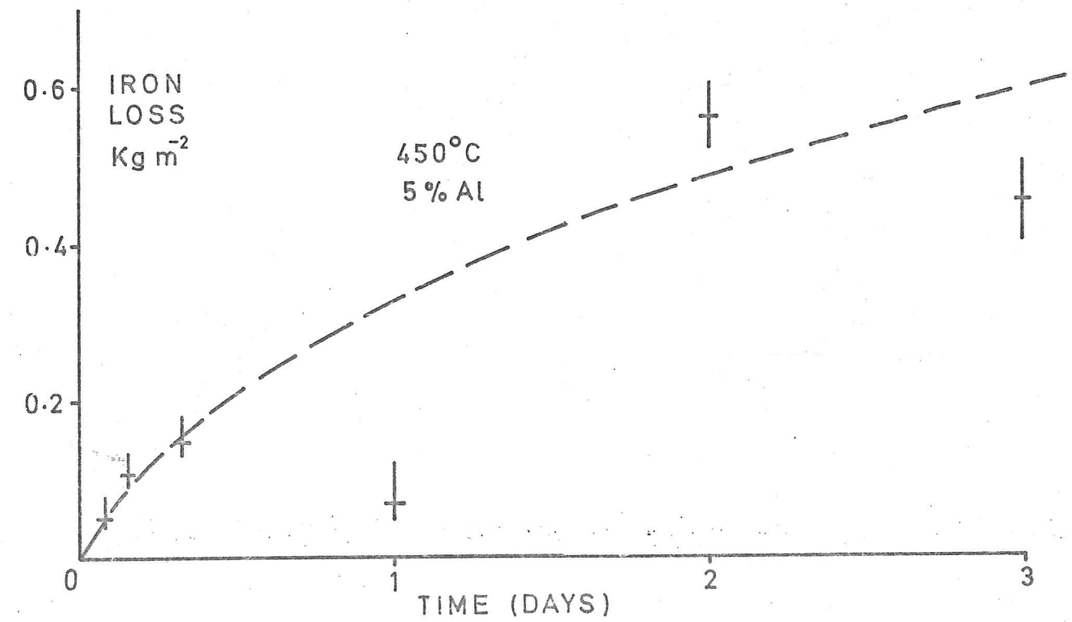
0·6
IRON
LOSS
Kg m^{-2}
450°C
5% Al
0·4
0·2
0
1
2
3
TIME (DAYS)

FIG. 24

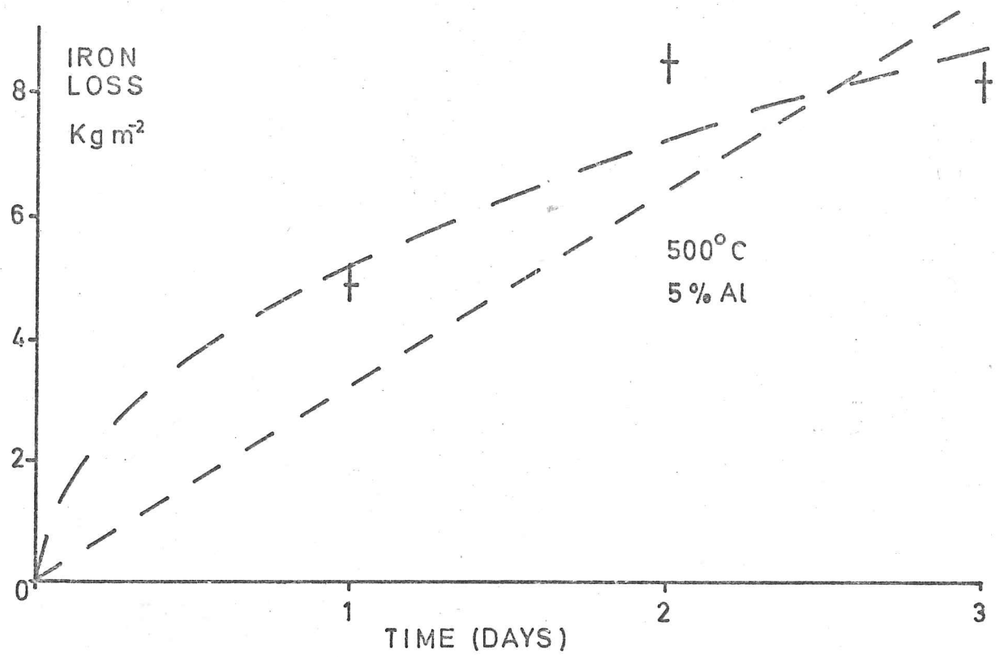

FIG. 25

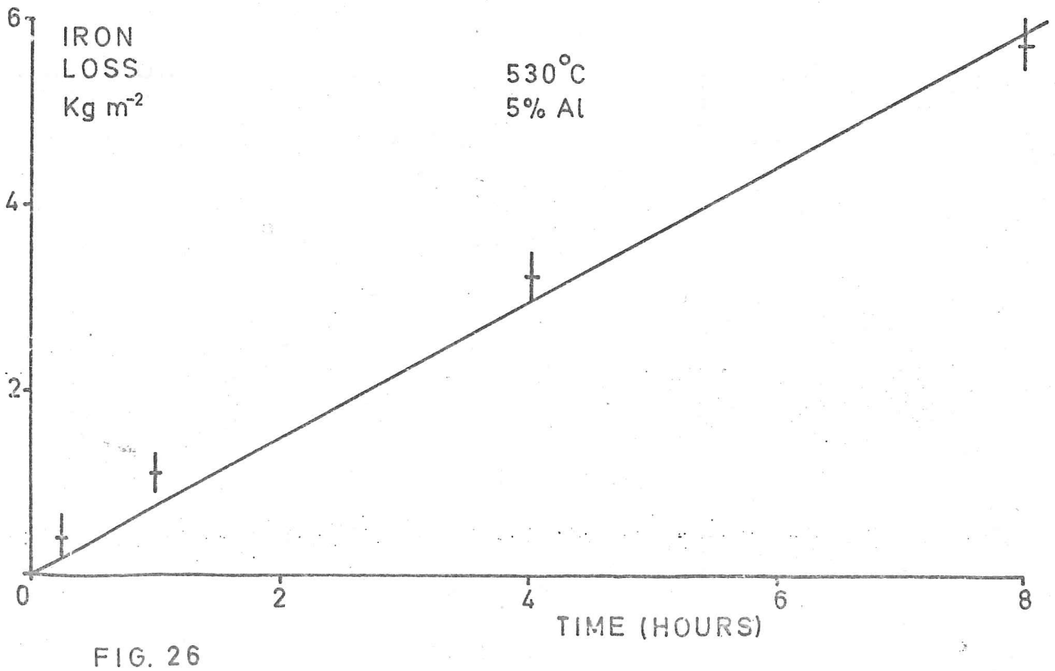

FIG. 26

average area used, but this was not in fact done. The runs were in general of relatively short duration so that the change in area is not too large, but the higher weight losses have been consistently underestimated.

With the runs of one hour duration there may be some error involved due to the cooling of the bath on the addition of the cold magnet assembly; this should not be of great significance.

One unknown factor is the state of combination of aluminium within the bath, which was not revealed by the analysis method used. The total iron lost from the specimens into the low aluminium baths might be sufficient to remove all the aluminium as iron-aluminium dross, which is presumably ineffective in inhibiting attack. However most, if not all, of the iron lost ends up in the iron-zinc alloy layer on the specimen and therefore is unlikely to have much effect on aluminium dissolved in the bath. This may not be true at 500°C, or at higher aluminium concentrations, but there is then a larger absolute quantity of aluminium in the bath. This is one of the advantages of using a large mass of zinc with relatively small specimens. It might be possible to separate the molten zinc-aluminium from the iron-zinc-aluminium alloy crystals by filtration, but attempts to do this through glass wool were unsuccessful, the crystals probably being small and easily broken.

4:3 Results

As well as the weight-loss data displayed earlier

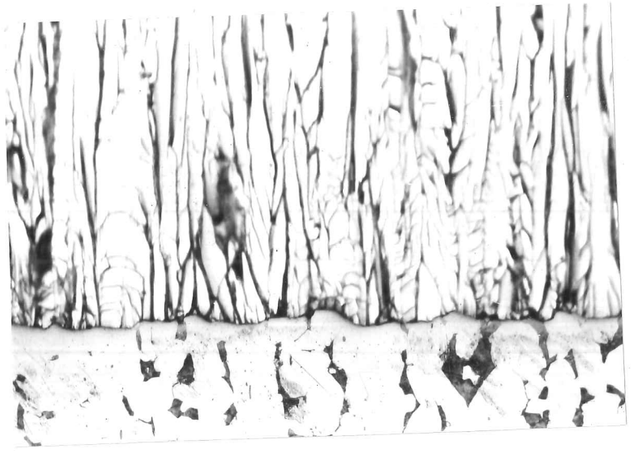

Fig. 27 Compact layers on steel "BB" after 4 days at 450° C in zinc with 0.3% aluminium. Picral etch, x 170.

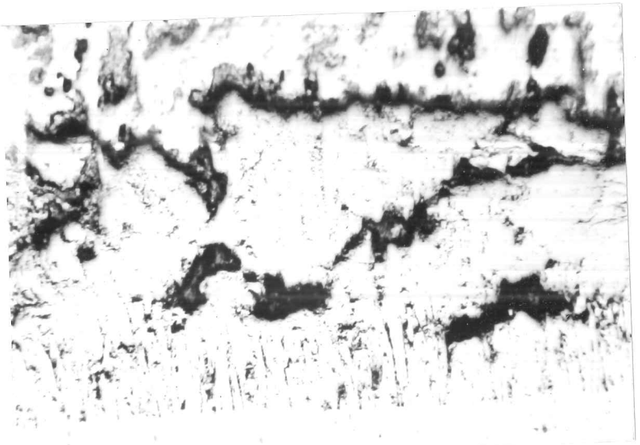

Fig. 28 Loose layers on steel "BB" after 1 hour at 450° C in zinc with 5% aluminium. Unetched, x 70.

some specimens were sectioned metallographically and examined both optically and with the electron micro-probe, a Cambridge Scientific Instrument Ltd. Micro-scan 5. Metallography on these specimens was not very easy because of the considerable hardness difference and etching had to be done carefully if all the alloy layers were to be revealed. A 5% picral solution was found to be the most satisfactory (14).

In some cases insufficient results were available and it is not possible to be certain what class of behaviour is being observed. The microstructures can be divided into three broad categories: (a) compact and dense (but perhaps cracked) similar to those produced in pure zinc in the Lower Parabolic Range, i.e. Fig. 27, (2) Broken-up structures, similar to those normally produced in the linear range, as in Fig. 28, and (3) structures containing a coherent layer of an iron-aluminium compound on the surface of the iron, as in Fig. 29. Use of the electron micro-probe showed that the structures (1) and (2) generally contained little aluminium, perhaps half the concentration in the molten zinc, but the iron-aluminium layers, if present, had high concentrations of aluminium. One specimen, after 4 hours in molten zinc at 450° C containing 5% aluminium had a layer on the surface some 20 microns thick which, after computor corrections to allow for fluorescence, absorption and other known factors was shown to have an analysis of 5.5% zinc, 58.5% aluminium and 36% iron. Another specimen, after

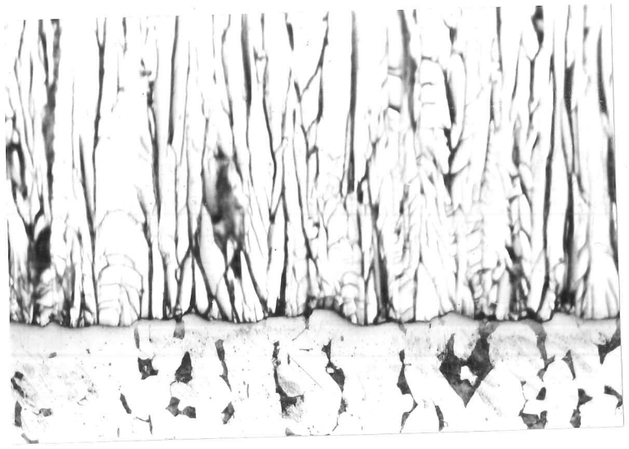

Fig. 27 Compact layers on steel "BB" after 4 days at 450° C in zinc with 0.3% aluminium. Picral etch, x 170.

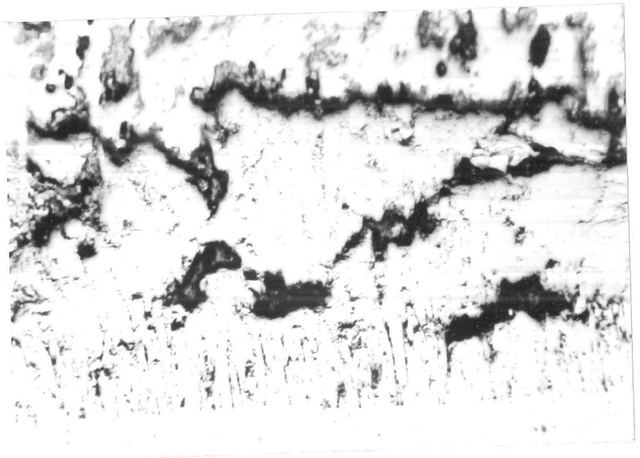

Fig. 28 Loose layers on steel "BB" after 1 hour at 450° C in zinc with 5% aluminium. Unetched, x 70.

some specimens were sectioned metallographically and examined both optically and with the electron micro-probe, a Cambridge Scientific Instrument Ltd. Micro-scan 5. Metallography on these specimens was not very easy because of the considerable hardness difference and etching had to be done carefully if all the alloy layers were to be revealed. A 5% picral solution was found to be the most satisfactory (14).

In some cases insufficient results were available and it is not possible to be certain what class of behaviour is being observed. The microstructures can be divided into three broad categories: (a) compact and dense (but perhaps cracked) similar to those produced in pure zinc in the Lower Parabolic Range, i.e. Fig. 27, (2) Broken-up structures, similar to those normally produced in the linear range, as in Fig. 28, and (3) structures containing a coherent layer of an iron-aluminium compound on the surface of the iron, as in Fig. 29. Use of the electron micro-probe showed that the structures (1) and (2) generally contained little aluminium, perhaps half the concentration in the molten zinc, but the iron-aluminium layers, if present, had high concentrations of aluminium. One specimen, after 4 hours in molten zinc at 450° C containing 5% aluminium had a layer on the surface some 20 microns thick which, after computor corrections to allow for fluorescence, absorption and other known factors was shown to have an analysis of 5.5% zinc, 58.5% aluminium and 36% iron. Another specimen, after

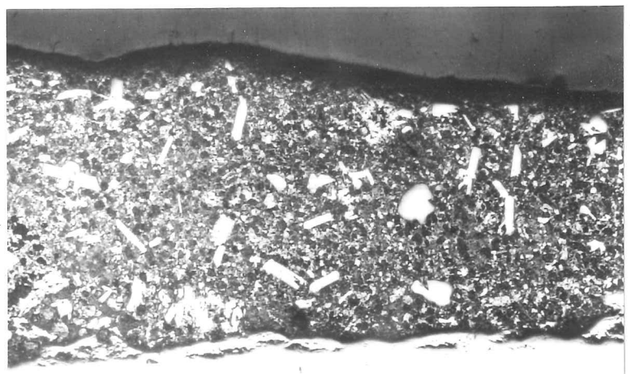

Fig. 29 Iron-aluminium layer on steel "BB" after $\frac{1}{2}$ hour at 500° C in zinc with 5% aluminium. Unetched, x 70.

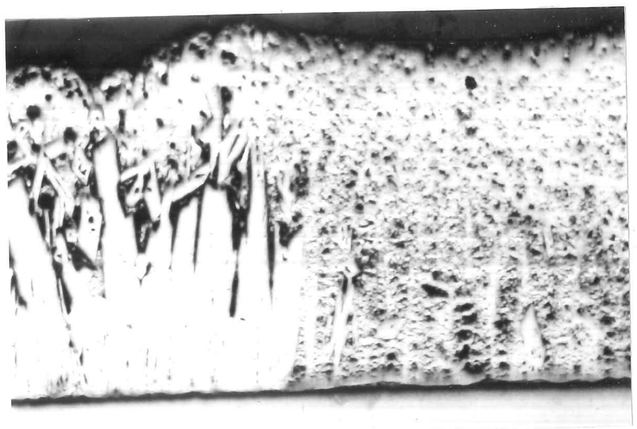

Fig. 30 Two different structures on steel "BB" after $1\frac{1}{2}$ hours at 470° C in zinc with 0.3% aluminium. Unetched, x 45.

1 hour in zinc at 500° C with 5% aluminium had a layer with 8.9% zinc, 46.9% aluminium and 44.2% iron, while a third specimen, after 4 days in zinc at 450° C with 0.3% aluminium had a layer some 22 microns thick with about 18% zinc, 45% aluminium and 37% iron.

It is difficult to correlate these types of structure with the rate of attack because the same specimen could show two different structures side by side, with no obvious difference in the degree of attack on the steel substrate. Thus Fig.30 shows structures (1) and (2), and from the other results it might be expected to behave parabolically, while Fig. 31 shows a compact layer, type (1), breaking away and being succeeded by type (3). No aluminium rich layer is visible under the type (1) layer (Fig. 27), but on the other face of the same specimen only structures of type (3) are found. (Fig. 32). This specimen should also be expected to show parabolic behaviour.

At 530° C, with 5% aluminium, the iron-aluminium layer is very thin, with a thin iron-zinc-aluminium mixture above it, and the attack is linear and very rapid. On the other hand, at 500° C with 5% aluminium the layer is much thicker, although seemingly spalling off (Fig. 33), and the rate is much slower and may be parabolic (the least squares method shows a parabola or straight line fit the three points on Fig. 25 equally well).

There is some evidence that these different structures may be due to interaction with differences in the steel base. The specimens stripped after several days in 0.1% or 0.3% aluminium showed pitting at certain points

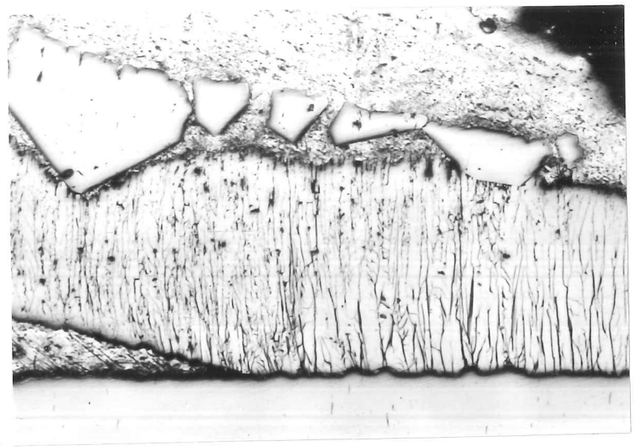

(a)

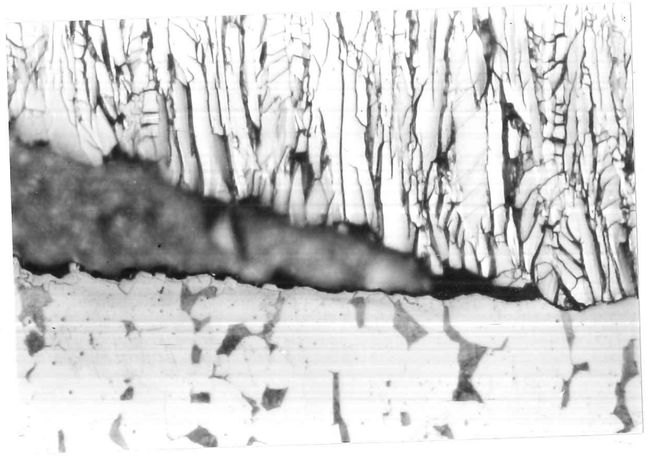

(b)

Fig. 31. Compact layer coming off steel "BB" after four days at 450°C in zinc with 0.3% aluminium
(a) Nital etch, x70 (b) Picral etch x270 showing iron-aluminium layer starting to form.

on their surface, and this was particularly concentrated in a central square region with sides about as long as the radius of the disc. (Fig. 34). It was later discovered that there was a slight degree of segregation between the square and the region outside it, probably representing segregation in the original ingot which had not been broken up by the rolling process. An analysis carried out by Tube Investments Ltd., at Hinxton Hall, showed there to be 0.13% carbon and 0.049% sulphur in the inner square region, and 0.14% carbon and 0.054% sulphur in the outer region. Since measurements of other properties, such as grain size and inclusion content showed no differences it may be that such slight alterations of the basic material are enough to materially alter the rate of attack. This question will be further developed later.

It may explain the anomalous behaviour of the stainless steel, attack increasing with the increasing aluminium content of the zinc. However, it must be pointed out that this experiment was subject to special systematic errors arising from the use of a relatively small volume of molten zinc, which would become increasingly contaminated with the alloying elements present in the steel.

4:4 Conclusions

Because of the complexity of the possible reactions and the relative lack of evidence as to their progress it is not possible to make more than rather vague general statements on the effect of aluminium in the zinc. It

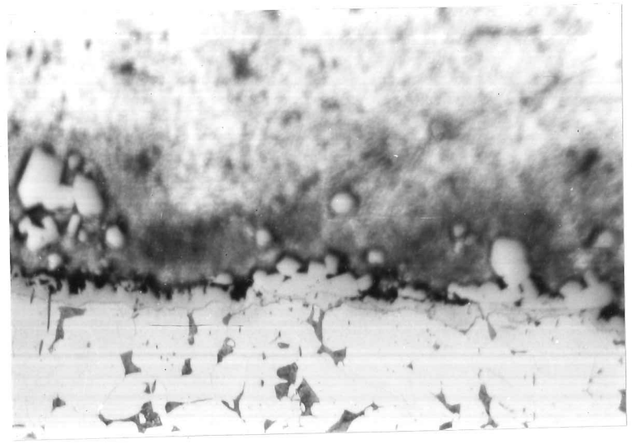

Fig. 32 Iron-aluminium layer on steel "BB" after 4 days at 450° C in zinc with 0.3% aluminium. Picral etch, x170.

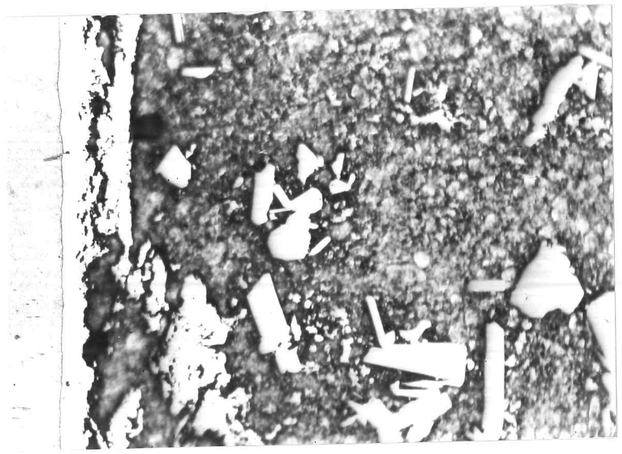

Fig. 33 Iron aluminium layers spalling-off steel "BB" after ½ hour at 500° C in zinc with 5% aluminium. Picral etch, x170

is clear that with the steel used addition of aluminium generally resulted in a slower rate of attack, reducing as the aluminium was increased but increasing as the temperature was raised. This is clearly summarised in Fig. 18. It has not been possible to establish whether the iron-aluminium-zinc layer sometimes observed is protective in the sense of reducing the attack rate; its behaviour may well depend on temperature. Bearing in mind the protection produced by an iron-aluminium layer in the first few minutes after entry into the bath, the ternary layer might be expected to produce similar protection at low temperatures; however it can certainly be present even when the attack is very rapid (i.e. 530° C, 5% Al).

It seems that aluminium does not affect the attack rate law obeyed at a given temperature, except perhaps at 530° C with 5% aluminium which is linear and not parabolic. However, bearing in mind the errors and lack of results for some conditions, it is sometimes difficult to determine if a linear or parabolic law is being followed.

It is clear from the work previously quoted (4,11,35) that in the Lower Parabolic Range, after the initial very slow rate of attack due to the presence of an iron-aluminium layer, there is a period of rapid attack while this layer is destroyed by the zinc, with formation of loosely attached iron-zinc layers. (Regions I and II on Fig. 35). Our work makes it clear that after a longer period of time the iron-zinc layers became more

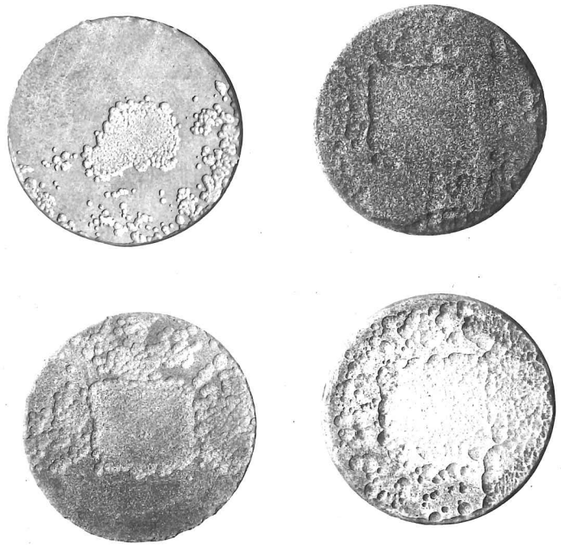

(a)

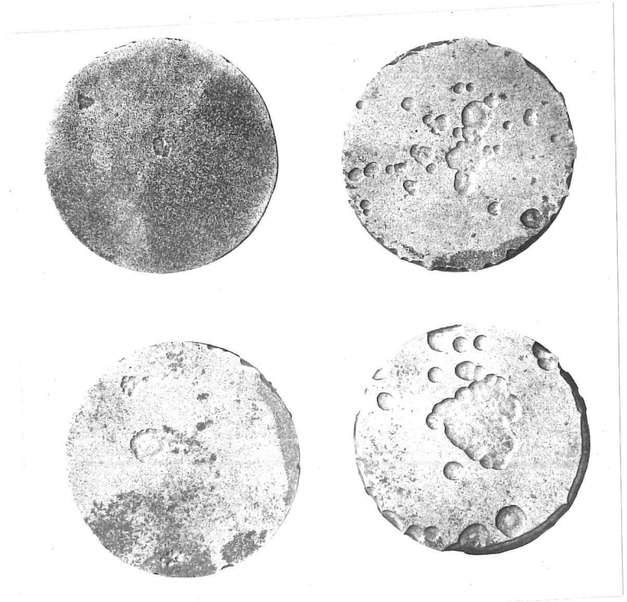

(b)

Fig. 34 Discs of steel "BB" after removal of zinc

(a) $\frac{2|3}{4|5}$ Days at 450° C in zinc with 0.1% aluminium, x $\frac{1}{2}$.

(b) $\frac{1|2}{3|5}$ Days at 450° C in zinc with 0.3% aluminium, x $\frac{1}{2}$.

compact, and the attack rate becomes parabolic again, as would be expected at these temperatures (Region III, Fig. 35). If the alloy layer were now to spall-off, or in some manner crack, allowing the melt to come into contact with the iron again, then the iron-aluminium layer would be expected to reform and the process repeat itself. This is probably what has happened in Fig. 31. It might be that as the iron-zinc alloy layers thicken and the rate at which the iron interface is attacked decreases, the rate of diffusion of the aluminium through these layers is not much affected. Eventually sufficient aluminium might reach the iron surface so as to form the iron-aluminium alloy again, and effectively choke-off the competing iron-zinc reaction. Repeated cycles of formation and dissolution of the iron-aluminium layer would give rise to a pseudo-linear behaviour, as in Fig. 36. The overall rate of this attack would vary depending on the proportion of time spent with the protective layer, but could be much slower or much faster than the corresponding parabolic rate.

Such a behaviour, for whatever reason, proceeding at slightly different rates over the specimen surface could explain the different microstructures seen side by side, as in Fig. 30, but with no gross differences in the position of the iron interface between the two types of attack. If a high carbon content in the steel made the iron-aluminium layer more defective, and hence more easily broken down by the zinc, this could explain the pitting observed on some specimens.

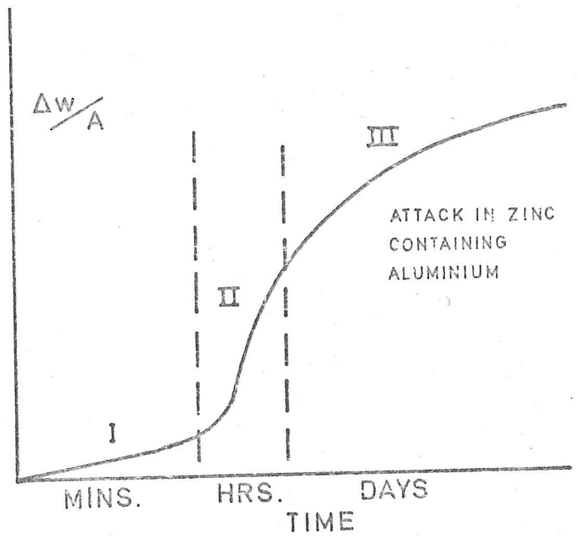

FIG. 35

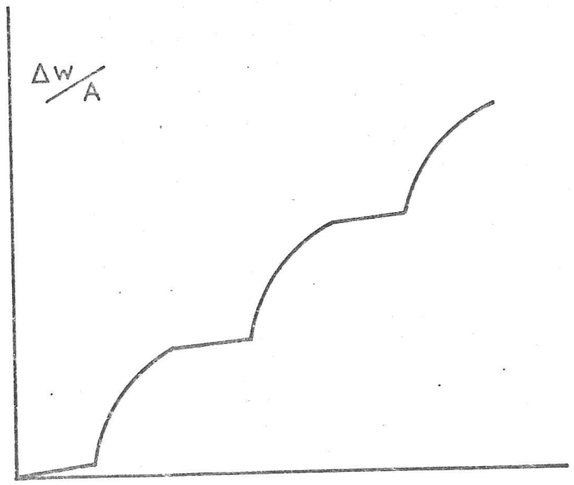

FIG. 36 PSEUDO-LINEAR ATTACK

Another possibility is that after stage III the layer which forms is a ternary iron-zinc-aluminium, and that this remains at a roughly constant thickness due to the spalling-off of the outer surface. Probe analysis showed that some of the broken-off crystals in Fig. 33 were identical to the iron-aluminium-zinc base layer. (Fig. 37). This may give rise to a linear rate of attack. In no case was any distinctly crystal form found over such an iron-aluminium layer. Any coatings over such a layer were very amorphous-looking, consisting possibly of iron-zinc crystals in a matrix of the zinc-aluminium. This is presumably formed by reaction of the zinc-aluminium melt with the solid iron-aluminium layer.

Obviously these hypotheses as to the possible reactions are based on surmise rather than a full understanding of the facts, but all workers in this field agree that the system is complex and confusing. Only at the higher temperature or aluminium contents do the microstructures seem consistent and repeatable. This may represent the predominance of thermodynamic factors over kinetic factors, but before predictions can be made on this basis a lot more needs to be known about activities of the components of the iron-zinc-aluminium system, and the effect of traces of further elements.

It is however clear that the concentrations of aluminium normally met with in galvanising should not have any disastrous long term effect on the galvanising bath unless this is overheated, a mistake which is potentially dangerous even without the presence of aluminium. This may not be true of structures made of

specially alloyed steel.

(a)

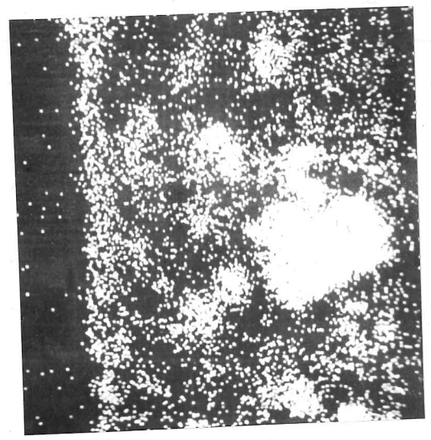

(b)

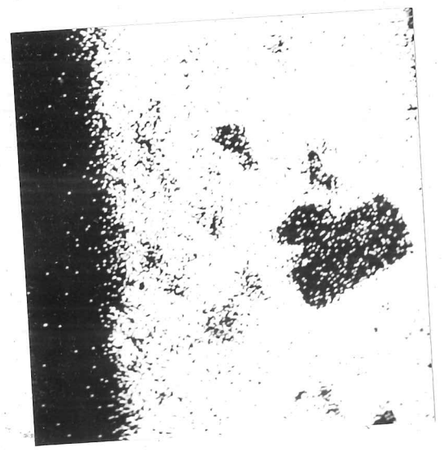

(c)

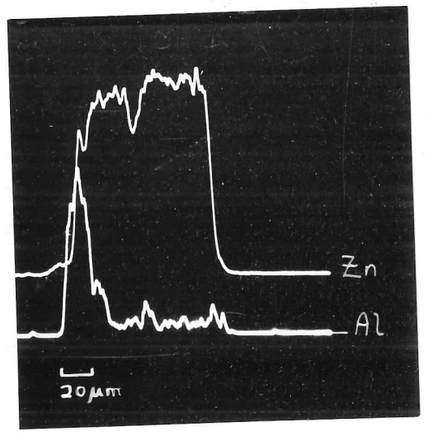

(d)

Fig. 37 Electron micro-probe X-ray images of steel "BB" after 15 mins. at 500°C in zinc with 5% aluminium x 300.
(a) Iron (b) Aluminium (c) Zinc
(d) Line scan for zinc and aluminium across alloy layer.

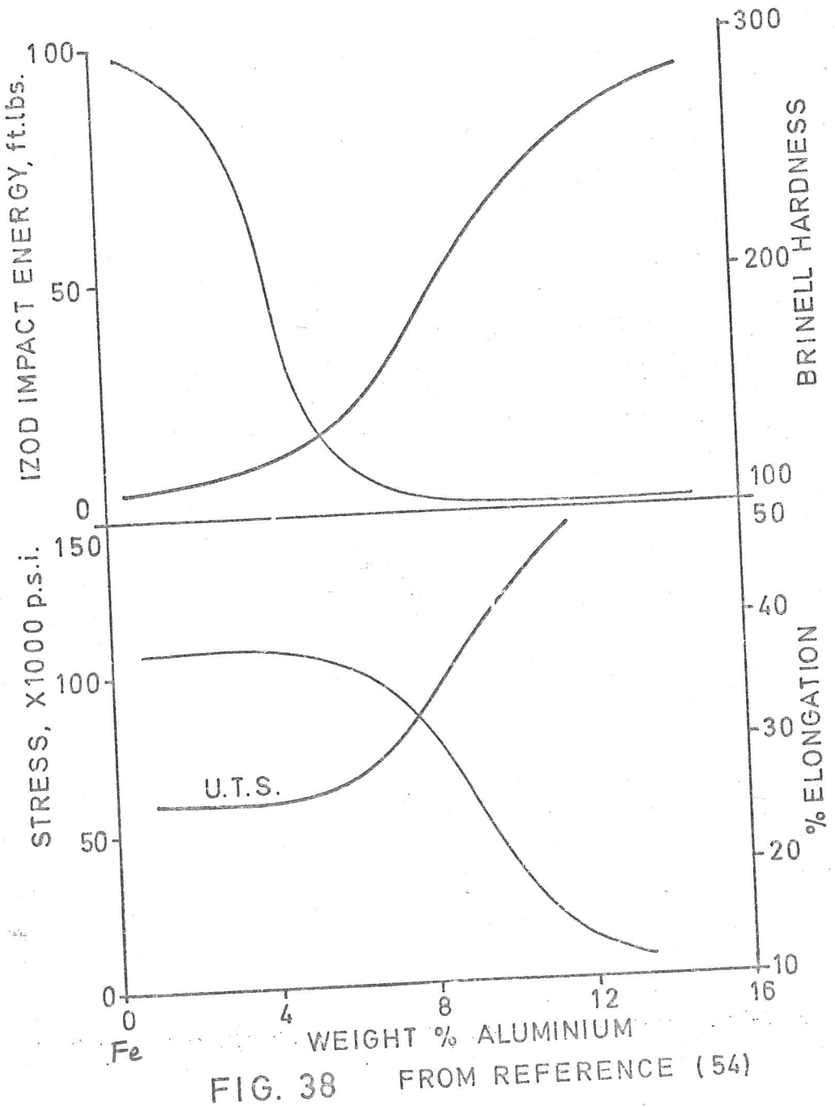

FIG. 38 FROM REFERENCE (54)

CHAPTER 5

EFFECT OF ALUMINIUM IN IRON

5:1 Introduction

As discussed in the previous chapter, the formation of an iron-aluminium (Fe_2Al_5) layer on the iron surface effectively protects it against zinc attack for some short time, but a ternary compound containing some zinc may not be protective. It was felt that the protective nature of the Fe_2Al_5 layer should be investigated with a view to producing a layer showing longer life.

In 1928 Russell, Goodrich, Cross and Allen (52) tested some materials for 3¾ hrs. in molten zinc at about 512°C and found that all those investigated showed some degree of attack, except for a calorized mild steel, which was not wetted or attacked in this period. Unfortunately further work on this was not encouraging (53) and has not been repeated.

It was therefore decided that it would be worthwhile to make a full investigation of a range of iron-aluminium alloys, and to correlate their behaviour with those of iron-aluminium coatings on steel prepared by various methods.

5:2 Properties of Iron-Aluminium alloys.

Most of the available data is for compositions with small quantities of the other element. As can be seen from Fig. 38 iron becomes hard and brittle when more

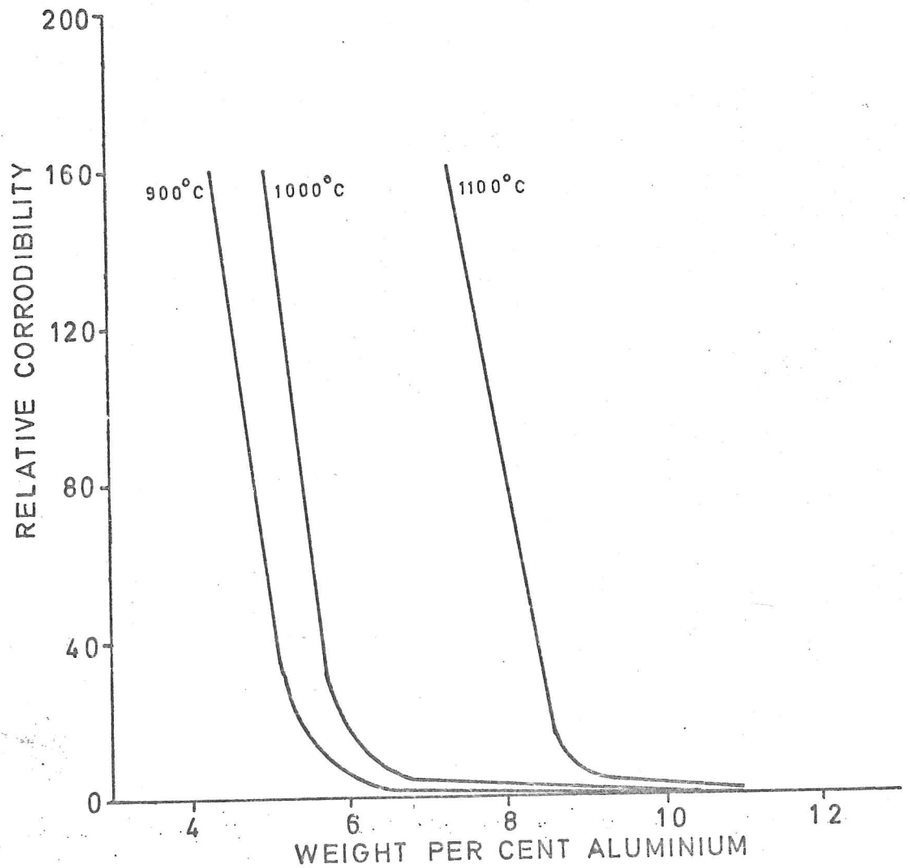

FIG. 39 FROM REFERENCE (55)

than about 6% Aluminium is present. Sykes and Bampfylde (55) found that iron-aluminium alloys could be cold worked, with increasing difficulty, up to about 5% aluminium and up to about 16% they could be hot worked. Cast irons with 20-24% Aluminium are said to be machinable and have good mechanical properties (56).

The addition of a small amount of aluminium to iron markedly reduces its rate of oxidation at elevated temperatures (Fig. 39). Alloys oxidising at the high rates produce a dense black scale, and the resistant alloys have a smooth surface covered with a fine powdery oxide, while those of intermediate composition show pitting. The oxide film is reddish at all temperatures up to 1000° C. At 1100° C the high aluminium alloys (13-15%) give a greenish white powder, while at 1300° C alloys which resist oxidation often give a perfectly white oxide layer. X-ray analysis of such an oxide shows it to be virtually pure Al_2O_3. (55) It would seem that at the lower temperatures the iron may be the first to oxidise, and aluminium cannot diffuse at a sufficient rate to reduce this oxide back to iron; this is however possible at the higher temperatures and aluminium contents. A protective layer of alumina or the spinel $FeO.Al_2O_3$ may form, and iron ions diffuse through this layer; the protection is due to the diffusion being slower in alumina or the spinel than in the iron oxides.

All these compositions are within the alpha phase region, i.e. up to 36% aluminium (Fig. 40). It seems that little data is available for the actual intermetallic

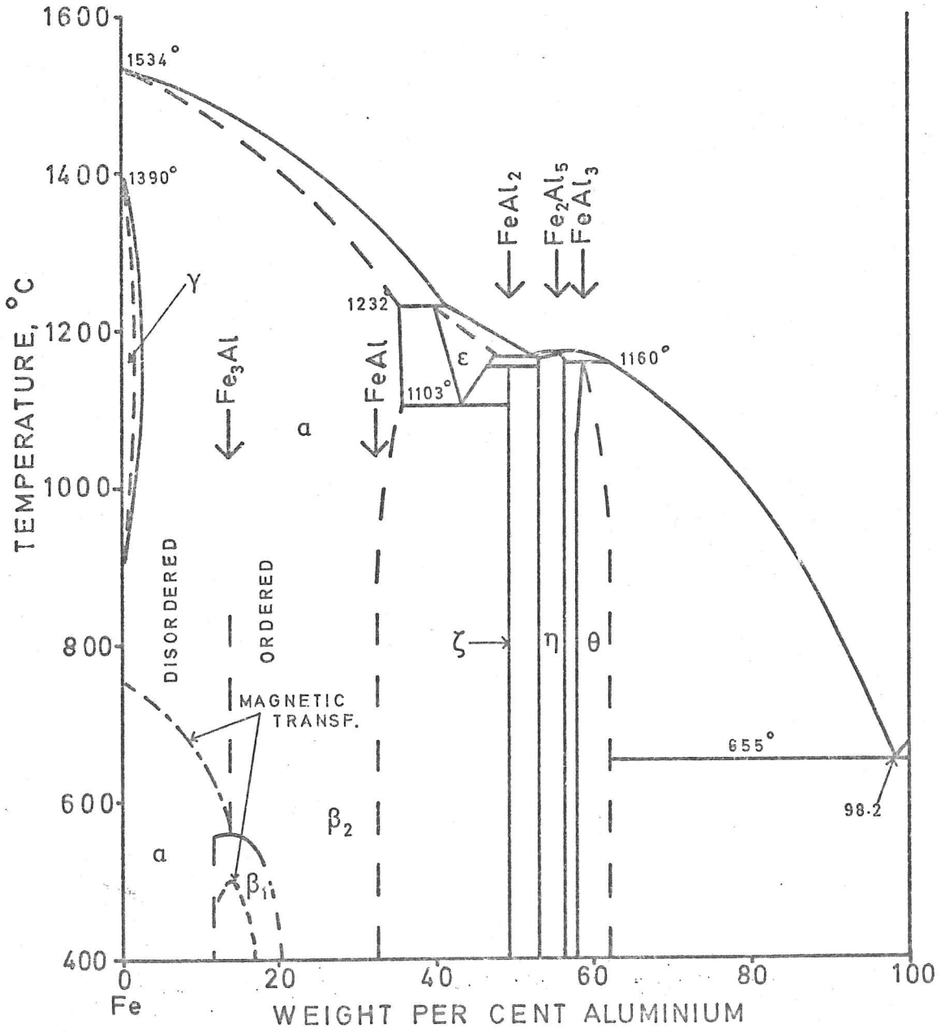

FIG.40 FROM REFERENCE (5)

compounds, but the hardness of $FeAl_3$ is quoted as 730 V.P.N., and that of Fe_2Al_5 as 1000 V.P.N. (57). Obviously these materials can be fabricated only by casting and grinding, and would be of little use as engineering materials. If they have special properties which it is desired to exploit this would only be possible if they were in a thin layer on the surface of some more suitable alloy. Obviously one way to do this is to coat iron with aluminium, and then heat to allow a reaction to proceed, resulting in a layer of the desired alloy.

5:3 Methods of coating iron with aluminium

The principle methods by which coatings may be applied are as follows:

1. Spraying
2. Cladding or roll-bonding
3. Electroplating
4. Casting aluminium round steel, or hot dipping
5. Calorizing
6. Decomposition of aluminium compounds on iron surface
7. Vacuum deposition

Each method has specific advantages and drawbacks which may effectively limit the choice of method. Thus hot dipping, calorizing and vapour decomposition involve the use of heat while the aluminium is being applied, resulting in some thickness of iron-aluminium alloy layer. There may be a thick layer of aluminium over this, as in the case of hot dipping, or thin or non-existant as with calorizing. Vacuum deposition is a very slow process,

limited to relatively small items.

Spraying or metallising can be by means of a plasma, arc or oxyacetylene torch, using either aluminium wire or powder. The resultant layer is porous, contains much alumina, and is mainly bonded mechanically to the previously roughened surface. "Aluminising" requires subsequent painting with a bituminous paint to exclude oxygen, followed by heat treatment at about 780° C to bond the aluminium to the iron with formation of an alloy layer.

Calorizing produces a similar result by packing the article to be treated into an air-tight box with powdered aluminium (50%), alumina to prevent caking (48%) and some 2% of ammonium chloride. This latter ingredient vaporises and flushes out any oxygen, and acts as a carrier, forming aluminium chloride which decomposes on the iron surface and recycles. After heating to about 900° C for 4 - 6 hours a coating 20-150 μm thick may be formed; this can be increased to 350-600 μm by further heating for 12 - 48 hours. This reduces the aluminium content to about 25%. Originally the coating consists of an outer layer of oxide (alumina) over $FeAl_3$ and alpha solid solution; subsequent heating allows further diffusion resulting in the elimination of the brittle $FeAl_3$. The calorizing process results in excellent protection against oxidation and sulphurous gases at elevated temperatures.

The thickness of the alloy layer formed on hot dipping depends, among other factors, on the size and temperature

of the specimen, time in the aluminium and temperature of bath, and rate of cooling after removal. A bath temperature of 900° C is said to produce a coating in which all the aluminium is converted to alloy as it cools (56). The main problem with hot dipping is getting the aluminium to wet the steel; i.e. in finding a suitable flux to remove oxides from the metal surfaces. Various mixtures of molten zinc/aluminium/ammonium chlorides and fluorides are quoted in the literature. With care excellent coatings may be obtained, well bonded to the steel base and free from included oxide. Close control of coating thickness is difficult however. If the article is subsequently heated to produce a thicker alloy layer it is found that this thickness after a given time may be rather variable. A similar effect is noted with roll-bonded specimens (54); this is presumably due to poor contact at certain points.

Electroplating is difficult because of the high negative deposition potential of aluminium which precludes the possibility of plating from an electrolyte containing hydrogen ions, but several laboratory processes have been developed. These use either fused salt baths of binary or ternary mixtures of alkali and aluminium halides, or organic electrolytes containing aluminium bromide.

It has been found (54) that the techniques required to produce successful coatings are not at all simple, and there are many practical operating difficulties which probably explain why this process has met with limited acceptance.

If it is desired to form a fairly thick iron-aluminium layer at the surface of some large article, then the best method might be to spray on aluminium and subsequently heat treat. For a smaller article calorizing might be suitable, or perhaps hot dipping or cladding followed by heat treatment.

5:4 Aluminium coatings: Methods used and Results.

It will be best to discuss together, in broadly chronological order, the methods used to produce the coatings and the results of the tests on such coatings.

5:4:1 Hot Dipping

Various fluxes were investigated in a search to find one which was effective but without giving off any corrosive fume. Fluxes tried but found to be ineffective included zinc and aluminium chlorides, glycerol, and a thin plating of copper. A mixture of 40% NaCl. 40% KCl, 10% NaF and 10% AlF_3, melting at around 700° C was reasonably effective. Two other systems, quoted by Cairns (54) were also found to be effective, i.e:-

A (1) Abrade with fine emery and degrease with acetone

(2) Dip 30 secs. in 10% HCl.

(3) Dip and agitate for 1 min. at 500° C in a flux made of 20% NaCl + 80% $ZnCl_2$.

(4) Dip and agitate in molten aluminium for 1 min.

B As above, but flux is 51% KCl, 39% NaCl and 10% Na_3AlF_6 at 500-600° C.

The material used for these dipping experiments was a low carbon mild steel in the form of thin sheet cut into rectangles about 50 mm. x 30 mm., 2 mm. thick. It was found that the flux solidified while the specimen was being transferred to the crucible containing the molten aluminium. It was then necessary to immerse it into the aluminium very slowly, allowing the flux to melt off the surface. If this precaution was not observed many spots of burnt-on flux were found in the coating. It was necessary to coat each specimen in two stages because of the difficulty of removing it from the aluminium without damaging the still molten coating. The specimens were thus half immersed in the aluminium, reversed, and the other half coated. This did not lead to very even coatings.

The best coatings produced by this method consisted of a layer covering some 98% of the specimen, but with one or two regions, about 2% of the total area, not wetted because of inadequate fluxing and subsequent oxidation, or where the flux had burnt on. Cross-sections of the coatings showed them to consist of about 80% pure aluminium over intermetallic compounds.

As coated the specimens naturally showed a behaviour in molten zinc similar to that of bulk aluminium. Thus they were not initially wetted on immersion in the zinc, due to the surface layer of alumina, but after some time, about 40 mins. at 500°C, attack started at certain points over the surface, and rapidly spread, the zinc and aluminium forming a low melting point eutectic (Fig. 17).

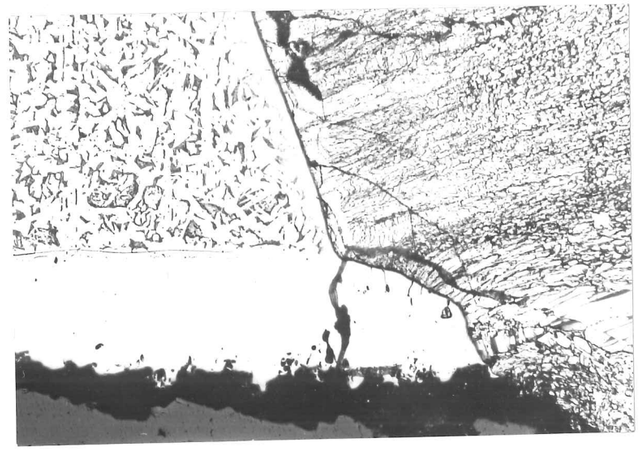

Fig. 41 Zinc attack after 6 hours at 500° C on a hot-dipped aluminium coating heat treated in air 3 hours at 650° C. Picral etch, x 55.

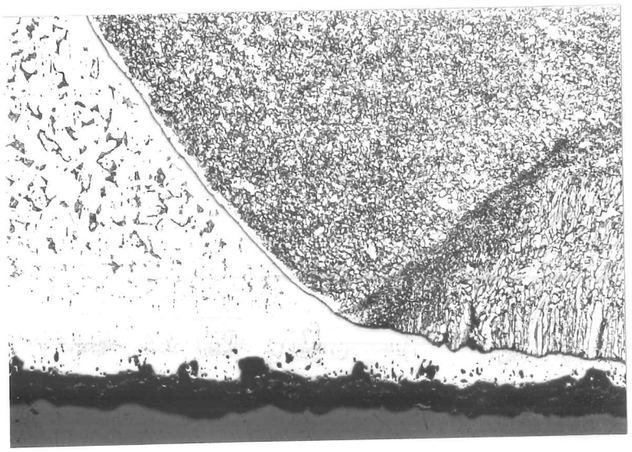

Fig. 42 Zinc attack on a calorized specimen after 4 days at 500° C. Picral etch, x 55.

Attempts to improve the protection offered by the alumina layer by anodising and sealing it proved to be unsuccessful.

Greater success was achieved with specimens heat treated in air for about 3 hours at 650° C after hot dipping. This produced a matt grey surface consisting of an oxide layer over a thick alloy layer. Even when heavily fluxed this oxide layer could not be wetted by molten zinc, but failure eventually occurred in all cases, generally after about 6 hours in molten zinc at 500° C. It was not clear whether this failure was due to pre-existing flaws in the oxide film which allowed isolated attack which eventually spread underneath the oxide, or whether it was due to a slow overall attack by the zinc on the oxide, eventually resulting in failure at the thinnest point. It was obvious (Fig. 41) that the iron-aluminium layer beneath the surface, although resistant, was not un-attacked by the zinc.

Four further hot dipped specimens were heat-treated for 6 hours at 1100° C, two in air and two under hydrogen. It was hoped that these would reveal a difference between a thick and a thin oxide film. In fact both types were rapidly attacked by zinc at 500° C. The criterion of failure in these and other similar tests was when distinct iron-zinc alloy formation could be visually detected on the specimen surface, as distinct from a layer of zinc which might be held on mechanically and removed by scraping while still hot, or by peeling-off once solidified. It will be appreciated that this is rather a crude way of assessing the material's resistance, but

no other method (such as weight loss or gain) was appropriate. The only quantification comes in the time of immersion before attack was observed.

Attempts to anodise in 10% sulphuric acid specimens dipped and then heat treated for 6 hours at 1100° C proved inconclusive. There was no evidence of a thickening oxide layer being produced, and the current in the anodising cell dropped very slowly. Such "anodised" specimens showed no greater resistance in the zinc, and these specimens treated at 1100° C were only slightly more resistant than unprotected steel.

It would seem that 6 hours at 1100° C is too long a treatment, and results in a low concentration of aluminium near the surface, and an oxide layer containing non-protective iron oxides.

At this stage it was felt that since it was not always possible to produce flawless hot dipped coatings, then it was not possible to evaluate subsequent heat treatments because these might be observed to fail because of flaws in the original coating rather than in the method of heat treatment. It was therefore decided to investigate other forms of aluminium coatings.

5:4:2 Calorized coatings

A mixture of about 5 grams of coarse aluminium powder, with 0.5 g. aluminium chloride and 0.5 g. alumina was prepared, and four cleaned specimens in the form of discs about 4 mm. thick cut from the bar of steel "BB" and

surface ground were packed with this in an open crucible and heated at 900° C for 64 hours. On removal it appeared that no reaction had taken place and that the surfaces were heavily oxidised, but sectioning and micro-examination showed a very distinct layer, about 0.3 mm. (12 thou.) thick, of an iron-aluminium mixture with a porous oxide layer above it about 0.06 mm. thick.

A repeat run for four hours at 900° C gave a very similar result, suggesting that after perhaps one hour the mixture became exhausted and all reactions ceased except slow inward diffusion and oxidation. Subsequent annealing in air for 24 hours at 900° C resulted in only a slight increase in the width of the iron-aluminium layer; it would seem that the aluminium concentration profile becomes flattened quite rapidly once the supply of aluminium to the surface ceases, and inward diffusion becomes slow. The specimens were sufficiently thick that the inward (uphill) diffusion of carbon consequent on the ferrite formation by the aluminium should be of little significance.

One of the specimens calorized for 64 hours was immersed in zinc at 500° C and inspected at intervals. After 36 hours some attack was observed on one face and at the edges, and after 4 days it was completely perforated at some points, although still untouched at others. On removal and sectioning it was again clear that the iron-aluminium layer was not itself immune to attack. It would appear (Fig. 42) that the stresses produced by the formation of the iron-zinc alloys might

be sufficient to break off the resistant iron-aluminium layer.

The failure of this specimen was attributed to an uneven and inadequate supply of the calorizing mixture at the specimen's face and edges. A further 4 specimens were therefore calorized at 900° C. for 3 hours, paying greater attention to the preparation and packing of the mixture around the specimens.

The specimens were subsequently given an individual treatment as follows:

No. 1. Given an anodising treatment in 10% sulphuric acid. Keeping the current constant at 0.2 amps ($\equiv 200\,A\,m^{-2}$) the voltage slowly rose to about 0.5 v., indicating some thickening film, but then dropped. The specimen was removed after 10 mins.

No. 2. Heat treated in air at 900° C for 24 hours, giving a red/brown oxide. Also "anodised" as above, showing a slow fall in voltage followed by a rise.

No. 3. Calorized again in a fresh mixture to try to increase the aluminium concentration at the surface.

No. 4. Calorized again in a fresh mixture, and also "anodised" as above; voltage remained steady at 0.5 v.

All four specimens were boiled in distilled water for 20 mins. to attempt to seal the "anodised" layer.

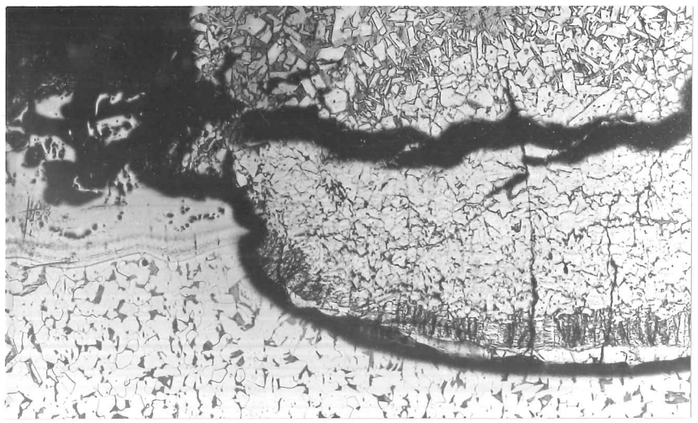

Fig. 43 Zinc attack on specimen calorized twice, after 24 days at 500° C. Picral etch, x 60.

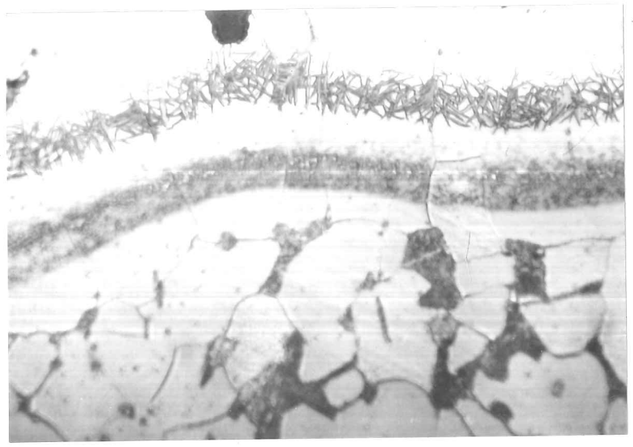

Fig. 44 Detail of ordered, needle-like band produced by prolonged heating at 500° C. Picral etch, x 300.

They were subsequently given a coating of "Gun-Gum" around their edges because it was felt that the edges were rather vulnerable to poor calorizing conditions and were best given some extra protection. The flat faces were to be the main test areas.

After being lightly fluxed they were immersed in molten zinc at 500° C, being suspended by a loop of tungsten wire held on a metal frame above the surface of the zinc. They were inspected every fourth day for signs of attack.

After 20 days it was noted that specimen (1) was perforated at the centre of the flat face, and that (2) was being attacked at the centre of one face. (3) and (4) showed no visible attack.

Because of industrial action, during the next 4 days the electric power was cut off twice for several hours, causing the zinc to solidify. At the end of this period, i.e. after a total of 24 days in the zinc, all the specimens were removed. Specimens (3) and (4) now showed attack at certain points and were cross-sectioned and examined. Again it was clear that the iron-aluminium layer was not itself immune from attack. It was obvious from examination of specimen (3) that an oxide film was present, and was probably the main mechanism for protection (Fig. 43). It may be that solidification of the zinc around the specimens caused stresses which ruptured this oxide, thereby promoting eventual failure.

On this specimen, and also on others which were sectioned after a long period in the molten zinc, it was noted that a structure developed in the iron-aluminium layer, close to the interface with the unaffected iron, which was not observed on similar specimens before the prolonged heating at 500° C. This structure is best described as a band of irregularly orientated needle-like crystals (Fig. 44). It was felt that this might be the ordered structure predicted by the phase-diagram (Fig. 40).

Scans by the electron microprobe showed that considerable differences in the width of the iron-aluminium layer could occur between specimens treated similarly, and even between different faces of the same specimen. Thus one specimen, calorized for 1 hour at 950° C showed on one face a region about 270 μm wide with iron and aluminium at a constant level (53% Fe, 47% Al, corrected values), and a region with a uniform concentration gradient up to pure iron, with width about 300 μm. On the other face the plateau region was about 540 μm. wide (with the same concentrations), and the gradient region about 150 μm. wide. These differences presumably indicate differences in the supply of aluminium to the surface during calorizing.

Because of this variation it was not possible to say if a significant degree of diffusion had taken place during the 24 days at 500°. The width of the layers on specimen (3) was within the above limits. Hardness

indents on either side of the needle-like band made it possible to analyse this region as containing about 78% iron, thereby confirming that this was probably an ordered structure. It might be expected that this band of ordered structure would act as a barrier to the diffusion of iron or zinc because its complex superlatticestructure would make the passage of extra atoms more difficult. This would have the desirable effect of tending to stabilise and confine the surface coating of aluminium so that the maximum concentration of aluminium would not decrease so rapidly during prolonged exposure to elevated temperatures.

It is also clear (Fig. 43) that this ordered region is rather more resistant to the attack by zinc than is the material of similar composition on either side of it. It therefore tends to protrude into the iron-zinc layers. It may be that the composition of this region i.e. Fe_3Al is inherently more resistant, and would show such behaviour even without the presence of a superlattice, or else it represents additional resistance consequent on the extra hardness and bond strength produced by the superlattice.

To check the probe analysis of the calorized coating samples were taken and analysed on the atomic absorption spectrophotometer. This involved considerable dilution of the original solutions to give a working strength, and the overall accuracy was not very high, the result being 42 ± 10 wt.% Fe, 47 ± 7 wt.% Al. This may indicate the inclusion of some oxide in the original

sample, but broadly confirms that the surface of the layer consists of iron-aluminium compounds with about 50% iron. (Fe_2Al_5 has 45.3% Fe, $FeAl_2$ 50.9%). The hardness of the coating further confirmed this composition.

To correlate the behaviour of these laboratory treated specimens with commercial calorizing the Calorizing Corporation kindly supplied some rectangular samples, about 60 mm. x 40 mm. x 10 mm., either calorized or aluminised (i.e. aluminium sprayed, then heat treated out of contact with air). Four of these were tested in the molten zinc at 500° C, suspended as before by tungsten wires.

After 19 days all four were found to be suffering attack, most showing sever attack over a large portion of their surface. Some areas of one calorized specimen were however untouched. Sectioning again showed that the protection was mainly, if not entirely, due to the presence of an oxide layer. These specimens had been heavily shot blasted before treatment, giving a rough surface which should produce a good mechanical bond, but it might be that certain crevices received a thinner coating of aluminium, or produced a thinner oxide film, than others, resulting in early failure. Alternatively it might be that the commercial process, preventing as it does the access of air, results in a thinner oxide film, or perhaps is designed to give a lower surface concentration of aluminium (25% ?) which produces a film

less protective in molten zinc.

It was therefore felt that calorizing showed promising results, but that more data were needed to establish the best conditions.

5:4:3 Sprayed coatings of aluminium

The Metallisation Co. sprayed aluminium to a thickness of about 10 thou. onto shot blasted discs of steel "BB" by means of a gas torch and also an open arc between two aluminium wires. Metallography showed the arc sprayed specimens to have a rougher but denser coating, with less included alumina. Before testing the specimens they were given a subsidiary treatment as specified below:

No. 1 Arc sprayed; as received.

No. 2 Arc sprayed. "Anodised" for 5 mins. in 10% sulphuric acid at 10 volts, current dropping from 0.75a to 0.2a . Sealed by 10 mins. in boiling water.

No. 3 Arc sprayed. Heated in air for 5 hours at 600° C.

No. 4 Arc sprayed. Heated in air for 1½ hrs. at 900° C.

No. 5 Gas sprayed; as received.

No. 6 Gas sprayed and "anodised".

They were inspected daily, and after one day it was seen that specimens (1),(3),(5) and (6) were being heavily attacked but (2) and (4) were unaffected. After

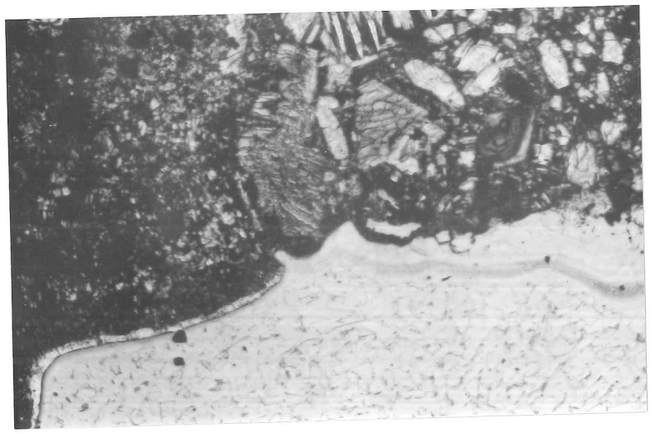

Fig. 45 Attack on aluminium arc sprayed specimen, heated in air for 1½ hour at 900° C, after 7 days in zinc at 500° C. Picral etch, x 135.

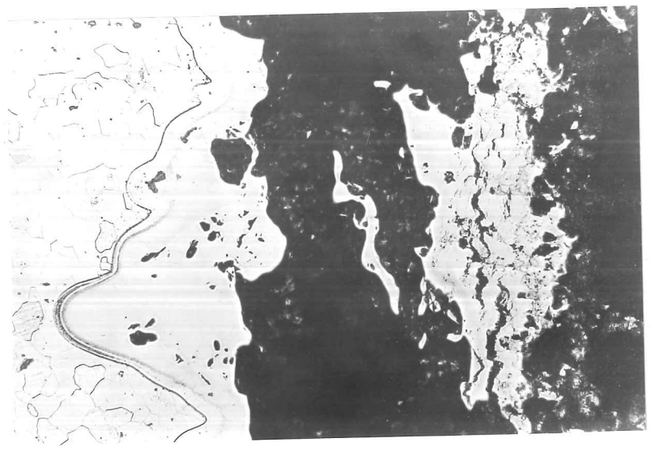

Fig. 46 Thick layer of alumina (black) separating zinc from aluminium arc sprayed specimen, heated in air for 1 hour at 900° C, after 19 days in zinc at 500° C, x 85.

2 days specimens (1),(3) and (5) were obviously being attacked all over and were removed, as were (2) and (6), which had heavy but localised attack.

Specimen (4) was unattacked at this time, but was removed after seven days when it was found to have suffered attack at one point on the curved edge. (Fig. 45). This shows attack occurring on the aluminium layer from the outside, seemingly concentrated on high spots on the shot blasted surface. Such spots might have had a thinner layer of aluminium over them. It also seems that blobs of alumina formed during the heat treatment in the "valleys" produced by the shot blasting. These blobs were identified by electron probe analysis.

It was concluded that the above specimens failed because of an inadequate thickness of alumina. A further set of specimens were sprayed by Metco Ltd. to investigate this further. Three different coating systems were supplied on grit blasted discs of steel "BB" and specimens of each were given a subsequent treatment.

The coatings were:

No 1 About 10 thou. (~250 μm.) thick alumina.

No 2 As (1), but over a ~ 10 thou. sprayed layer of aluminium.

No 3 As (1) but over a ~ 4 thou. sprayed coating of a mixture of 80% nickel, 20% chromium. This was said to improve both the bond and the oxidation resistance; it was said that zinc would not penetrate the alumina, and that the life of a treated galvanising tank was about 2½ years, compared with 6-8 months if untreated.

The method of spraying was not quoted.

The subsequent treatments were:

(a) As received

(b) As received, but with two deep parallel lines scored across one face, with a heavy blow with a ball hammer below them. This was to simulate potential mechanical damage.

(c) Heat treatment for 10 hours in air at 500° C

(d) Heat treatment for 1 hour in air at 900° C

There was thus a total of 12 different specimens. These were all immersed in a bath of zinc at 500° C being suspended by tungsten wires. Some tended to float with a small portion above the surface, but it was possible to cover these with a film of molten zinc. The bath by now contained some aluminium from the dissolution of previous coatings, but it was felt that this would not much affect the life of these specimens.

After one day specimens 1 (a), 1 (b), 1 (c), 1 (d), 2 (a), 2 (b), 3 (a) and 3 (b) were suffering sever attack and were removed. Some slight attack was observed on specimen 3 (d), but 2 (c), 2 (d) and 3 (c) were unattacked. After the second day specimen 3 (d) was severely attacked on one side, and 2 (c) all over. These were removed. 3 (c) and 2 (d) were still unaffected, but by the third day 3 (c) showed slight attack around the edges, and by the fourth day was very heavily attacked.

However specimen 2 (d) ($Al+Al_2O_3$ heated in air for 1 hr. at 900° C) showed complete immunity to attack. After 18 days it was decided that failure should be speeded up

because of a lack of time. Two lines were gouged through the layer using a vibratory engraver with hardened tip, hoping that attack would start on the metal thus exposed, but no such attack was detected after 24 hours. The specimen was then finally removed and sectioned. The structure was similar to others previously examined, with a distinct "ordered" bond which was not present on another specimen heat treated in a similar way at 900° C but not immersed in zinc. The oxide layer was very thick and intimately mixed with the aluminium alloy surface (Fig. 46).

To confirm some of the above results repeat samples of 2 (a) and 2 (d) were prepared and tested as before. 2 (a) failed within 24 hours, the oxide layer being lifted off the metallic surface in large chunks. The second 2 (d) specimen was attacked from a flaw in the coating at one edge after 11 days, and attack subsequently spread under the oxide layer, lifting it off as it spread.

These results confirm other work (58) to the effect that sprayed coatings of alumina, silica or even tungsten do not in themselves protect the underlying steel. It would seem that some specific intermediate layer is required to bond the alumina to the substrate. This will be discussed further later in the chapter.

5:5 Attack on Iron-Aluminium alloys

A series of binary iron-aluminium alloys were prepared by melting calculated quantities of pure electrolytic iron together with 99.5% aluminium in a crucible with a radio-frequency induction furnace. No special precautions were taken to prevent losses by oxidation, but analysis

TABLE 4

Attack by molten zinc on iron-aluminium alloys

% Iron by weight	Run 1 at 500° C	Run 2 at 450° C $(\frac{\Delta W}{A})x10^3$	Run 3 at 500° C $(\frac{\Delta W}{A})x10^3$; appearance	
0	Not tested	Not tested	>4000	completely dissolved
2	⅓ dissolved	470	?	completely dissolved
10	very slightly attacked	600	1420	60% attacked
20	slightly attacked	370	920	100% attacked
30	not wetted	340	1480	10% attacked
40	not wetted	140	-	not wetted
50	attacked all over	110	-	not wetted
90	attacked all over	320	160	100% attacked
100	not tested	not tested	400	100% attacked

of each melt using the atomic absorption spectrophotometer showed the compositions to be as desired.

They were cast into shallow moulds machined in a graphite block, giving disc-shaped specimens about 10 mm. diameter and 4 mm. thick, with the lower surface flat and the upper surface generally convex. Most compositions were too hard to attempt to machine or even grind to a more precise shape and the discs were used as cast. Measurement of surface area was thus rather inaccurate.

It was intended that these specimens should be tested for one hour in molten zinc, and a figure for the weight loss/area determined, but there were certain problems. Many of the alloys were less dense than the zinc and floated with most of their surface above the zinc. For the first run they were not adequately weighted and it was felt to be inappropriate to determine $\Delta W/A$ for such specimens, some of which had been completely immersed, and others not. Attack was therefore evaluated in term of the area of each specimen which showed wetting and/or attack by the molten zinc.

The two subsequent runs enabled more useful figures to be obtained, but stripping with diluted hydrochloric acid caused considerable attack on the iron-aluminium alloys, resulting in rather heavy weight losses for certain alloys in the second run. For the third run more care was taken, and specimens removed from the acid as soon as all visible zinc alloy was removed. Only those showing attack were subjected to the stripping process. The results are displayed in Table 4.

There are several anomalies, and the quantitive results are subject to large errors, but it was not felt to be worth the effort to produce a method of assessing attack applicable to the whole range of alloys from pure iron to pure aluminium. Further, it was clear that measurement of area would be difficult unless every specimen was machined to a constant shape. It was found that the specimens showed distinct segregation and many had a large number of cracks, formed by contraction on cooling. These would obviously potentially increase the surface area.

It was felt that as they stood these results suggested that certain alloys around 50% iron were resistant, at least in the short term, to attack by molten zinc. To check whether this was again due to protection by the oxide film one disc of 50% iron was scratched on one face with a hardened scriber beneath the surface of molten zinc at 500° C. This produced no immediate attack, but after 3 days the whole specimen showed intense nodular attack at certain points, as if the oxide had failed there, perhaps because of segregation.

5:6 Attempts to reduce the oxide layer

It was thought that additions to the molten zinc of other elements having a greater affinity for oxygen than aluminium might reduce the oxide layer and hence speed up the start of attack. From the Ellingham diagram calcium or magnesium would appear suitable.

Unfortunately the addition of small quantities of

these elements causes a very large increase in the rate of oxidation of molten zinc (59). The addition of calcium also has the effect of raising the melting point of the alloy (5), so that with 5% calcium the melting point is around 700° C.

The addition of 1% magnesium to the zinc was found to produce a very thick layer of oxide within ½ hour, presumably consuming all the added magnesium. The addition of some 1% aluminium with the magnesium seemed to prevent this, perhaps by formation of an alumina film or a spinel, $MgO:Al_2O_3$. If this was the case then obviously the magnesium was not reducing the alumina as hoped. Actual tests with this alloyed zinc on laboratory calorized specimens were uninformative because although no attack was observed it was not clear if any magnesium was still present in the melt, or if its access to the specimen was hindered by oxide films.

5:7 Diffusion of zinc vapour through porous membranes

Sprayed coatings of alumina will tend to be porous, although sufficient thickness may result in most pores being blocked at some point. Thermal stresses may cause cracks in such coatings and also in natural air-formed oxides. The vapour pressure of zinc is quite high even at its melting point (60), and increases rapidly with temperature. Actual figures are:

405° C	0.08 mm Hg
440° C	0.024 " "
470° C	0.62 " "
491° C	1.07 " "
545° C	3.69 " "
650° C	28.1 " "

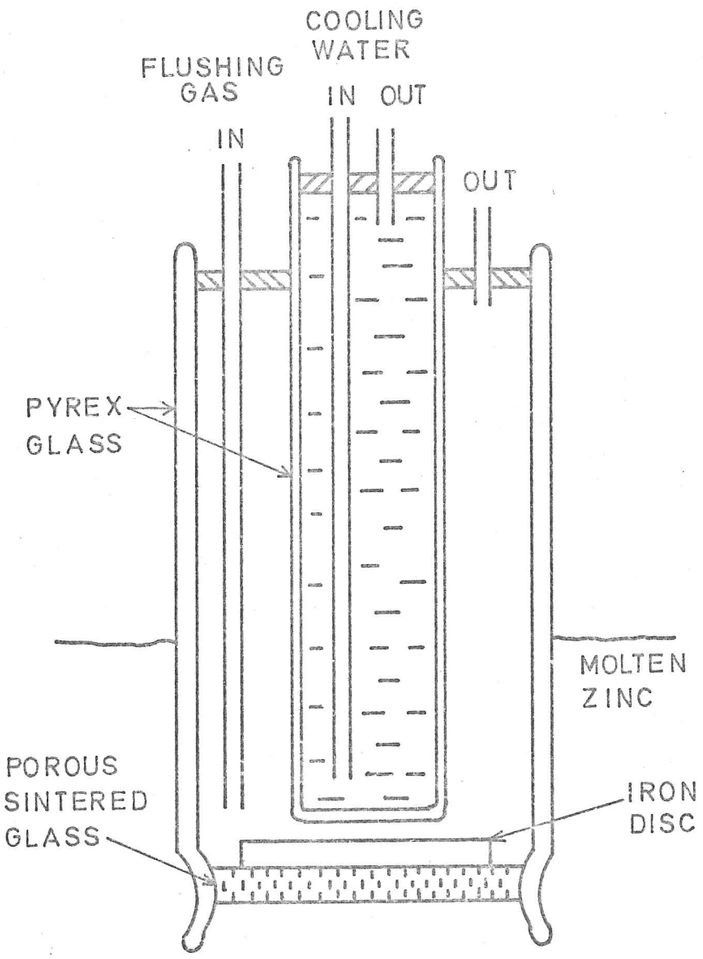

FIG. 47 APPARATUS USED TO INVESTIGATE ZINC PENETRATION THROUGH A POROUS DISC

Crude calculations (Appendix 1) on the basis of Knudsen effusion through narrow tubes, length 10 mm. radius 0.1 mm., with a pore area of 10^{-2} mm^2 per mm^2 of total area, assuming a monatomic vapour, would suggest a flux of some 10^{-3} gms. per hour per cm^2 of total area. It was felt that this might be detectable, and might allow a significant rate of attack on a substrate, eventually lifting off the porous layer.

To investigate this a sintered porous pyrex glass filter was set at the bottom of a pyrex tube and immersed in the molten zinc to a depth of some 50 mm. The glass not being wetted by the molten zinc, no penetration by the liquid occurred. To trap and detect the flux of zinc vapour a small disc of steel rested on the inside of the porous glass, and was cooled by a water cooled finger (Fig. 47). The whole apparatus was flushed with nitrogen and hydrogen before immersion, but oxygen rapidly diffused in and oxidised the steel, although mainly on its upper surface. Tests with a thermocouple showed the temperature of the inside of the glass filter to be close to that of the molten zinc, with the steel some 100° C cooler.

The first run was for 11 days at 450° using a No. 4 porosity filter, i.e. a pore size of 5-10 μm. During this run the steel suffered considerable oxidation, but on removal it was clear that the lower surface was still bright. However, examination with the electron-microprobe showed that no zinc could be detected on this surface. It was difficult to estimate the sensitivity of

this analysis because it would be difficult to detect a thin layer of zinc on a thick iron block, but it probably indicates that less than 1 μm thickness was present, i.e. $< 10^{-3}$ gm. per cm^2.

Similar negative results were obtained after runs for 10 days using a No. 1 porosity filter, i.e. 100-120 μm pore size, at 450° C and 500° C. This latter run showed some slight penetration by the zinc into the filter. This may have been due to the lower surface tension.

It is not immediately obvious what would happen if a vapour whose liquid does not wet the material is passed through such a tortuous diffusion path. Any tendency to condense onto the walls of the passage would be counteracted by the lack of attraction between the liquid and solid. This might mean that the vapour passes through very rapidly, or else perhaps with great difficulty. It is also possible in this experiment that evaporation was hindered by the presence of an oxide film, or that oxidation occurred within the passages - however these were not found to be blocked after a run. Alternatively the assumptions made in the calculations might not be valid, and the theoretical flow rate on a better model might be much lower. In any case it suggests that rapid diffusion of vapour through similar porous barriers, such as sprayed alumina, is not likely to cause rapid failure.

5:8 Discussion of results

If an oxide formed over an iron-aluminium layer is to be protective it seems that the surface composition

of the layer should be about 50% iron. If this is to remain constant for a long period then the rate of diffusion of the aluminium must be kept low; this may provide an upper limit to the service temperature of such a coating. Shreir (61) quotes 700°-750° C as the temperature at which diffusion becomes important. Most of the diffusion data available is for temperatures between 850° C and 1100° C (62,64), and it is not necessarily valid to extrapolate such figures to galvanising temperatures because aluminium is far more soluble, and hence diffuses easier, in alpha iron rather than gamma. The results presented above suggest that the rate of diffusion at 500° C is insignificant. It could probably be reduced further if desired; this could be advantageous during heat treatment of the coating. The intermetallic compound Fe_2Al_5 is monoclinic, and is found to have a high proportion of vacant lattice sites along the "C" axis (62). This explains the directionality of the resultant crystals, and also the high rate of diffusion and the preponderance of this phase in the layer. Addition of silicon tends to fill these vacant sites and formation of Fe_2Al_5 is hindered.

Further modification could be produced by the introduction of nickel so as to produce a layer of the intermetallic compound NiAl, which acts as a barrier to diffusion (63). Specimens clad with NiAl by diffusion impregnation ("calorizing") at 900° C using a powdered alloy of NiAl showed excellent oxidation resistance and stability against further diffusion at 950° C (63).

Certain other aspects need further investigation. The resistance of oxide films to erosion by flowing zinc has not been investigated, nor has the resistance to mechanical damage. Although alumina is hard it is not necessarily well bonded to the substrate. This substrate is however also hard and not likely to deform much under impact. The bond would thus not be severely tested. Resistance to flowing zinc may not be so good however.

Observation of the early stages of failure of the various coated specimens showed that attack often started at an edge or corner, and spread under any sprayed alumina film. In some cases it could be positively established that the point of initial failure was where the specimen had been in contact with the furnace while being heat treated. Removal from the furnace may have broken off an oxide coating adhering to the furnace walls.

Frequent removal of the specimens for examination might have allowed oxygen to heal weak points in the oxide film, whereas in service oxygen might be effectively excluded for long periods. It was hoped that failure could be detected by an alternative method, i.e. the breakdown of the insulating oxide between the metallic specimen and the molten zinc. However it was found that even when sound this resistance was very low, around $0.04\ \Omega\ mm^{-2}$, and an even lower figure was obtained for calorized specimens in mercury at room temperature. It is difficult to reconcile these figures with the low oxidation rate of such materials, and the protection they offer against molten zinc.

5:9 Investigation of some other coatings

Apart from aluminium several other chemical conversion coating systems are commonly applied to steel to increase surface hardness or corrosion resistance. Those frequently used include phosphates, chromates, nitrides, borides and silicides. Borides and silicides are known to be resistant to molten zinc (29); it was hoped that some of the other systems might also prove to be protective.

Samples of oxide, phosphate, chromate, silicide and borax coatings were prepared on armco iron discs (For methods used see Appendix 2). Nitriding was not attempted because of the lack of suitable equipment, and boriding was not carried out because of the difficulty in obtaining a suitable source of boron.

None of these proved at all satisfactory. The phosphate and chromate specimens were wetted all over within $\frac{1}{2}$ hour at 500° C (no flux used). The oxidised specimen was not fully wetted for 6 hours, while the silicon treated specimen was wetted over $\frac{3}{4}$ of its surface in 10 hours. The borax specimens were rather variable, depending perhaps on whether the coating was fully continuous, but none resisted attack for more than 15 hours.

It was felt that silicon treatment, boriding or alumino-boriding (treatment with boron and aluminium together) had potential to produce a protective coating, but that this would require a further series of experiments to establish the optimum treatment.

5:10 Conclusions

It has been shown that an alumina-type oxide film formed over an iron-aluminium alloy with about 50% iron has considerable resistance to molten zinc, and it seems that this resistance may increase with the thickness of the oxide. A similar oxide film sprayed directly onto the iron shows no such resistance, nordoes an alumina film on aluminium even when thickened by anodising or low temperature oxidation. Several possible reasons can be advanced to explain these results. It may be, for example, that a considerable thickness of oxide is needed to provide an impermeable barrier, and that this can only be provided by a thick sprayed coating, whose looser structure might be expected to absorb thermal shocks without producing gross cracks, but that this is not as adequately bonded to the substrate as is a naturally formed alumina film. The combination of the two allows perhaps the bonding of the sprayed coating to the substrate by the growth and intimate penetration of the natural alumina film.

It is also clear that a natural film formed on an iron-50% aluminium alloy is more resistant than one on pure alumina. It may be that the oxide formed on such an alloy is the spinel hercynite ($FeAl_2O_3$), and that this has particularly desirable properties. The molar volume of hercynite is 39.6 cm^3, some 46% greater than the sum of the molar volumes of alpha iron and aluminium (59), whereas the molar volume of alpha alumina is about

50% greater than the aluminium which forms it. Thus the hercynite would be under less compressive stress than would alumina. However these figures are for room temperature, and assume that the molar volumes of iron and aluminium in the alloy are the same as for the pure metals.

There is a lack of data to calculate the effect of raising the temperature of the alloy-oxide system, but it is known that the coefficient of thermal expansion of aluminium is high, 26×10^{-6} between 20° C and 400° C, whereas that of iron is low, 12×10^{-6} between 0° C and 100° C. The figure for alumina is 8×10^{-6} between 25° C and 800° C (12). It may be that the expansion of the spinel is better matched to that of the alloy than is that of alumina to aluminium, and that the stresses produced by thermal shock or cycling are thus reduced.

It may therefore be possible to improve the behaviour of the system by modification of the components in many ways. Chemical or physical stability of the oxide might be modified by addition of a third metallic element, and the molar volume or coefficient of expansion of the alloy could perhaps be similarly improved by further alloying additions.

It is felt that a suitably prepared and heat treated duplex coating of sprayed aluminium followed by alumina, or alternatively a calorized coating could provide suitable protection in an industrial situation and that its behaviour could be improved by further modifications. Other oxide coatings might prove satisfactory if adequately bonded

and matched to the substrate. Sprayed coatings of mixed oxides as $MgO + Al_2O_3$, $BeO + Al_2O_3$, $FeO + TiO_2$ or $MnO + TiO_2$ might have suitable physical and chemical properties.

Sprayed coatings might have advantages over naturally formed films because their degree of porosity can be varied over a wide range, and this gives some benefits in thermal shock resistance. If the pores are fine enough they should not be penetrated by the zinc.

CHAPTER 6

EFFECT OF CARBON IN STEEL

6:1 Previous work

It has long been known that an increase in the carbon content of steel increases the rate of attack by molten zinc (52), and that for long service galvanising baths should thus be constructed of a low carbon steel, together with low silicon (27,65). Bablik (11) quoted data to show that the effect of carbon depended very much on the form in which it occurred. Heat treatment of a certain steel with 0.78% C, 0.39% Mn and 0.14% Si to give different structures was carried out, and these tested in zinc at 440° C for one hour. The weight losses, in $g.m.^{-2}$ $hr.^{-1}$ were:-

Globular pearlite	680
Lamellar pearlite	740
Martensite	120
Quenched and tempered	110

It was noted that these weight losses were roughly proportional to the weight losses in dilute sulphuric acid at room temperature. It was also realised that the martensitic specimen was undergoing tempering while being held at 440° C. Graphite inclusions seemed to have no influence on the velocity of dissolution, and very coarse cementite needles, as in pig iron, did not much

affect the rate.

Horstmann, in his investigations into the effect of alloying additions in the steel (16,23), determined the effect of carbon content and structure on both the transition temperatures between rate laws and the rate constants for the laws. When carbon was present as lamellar pearlite, the temperature range for the rapid linear rate law widened from 495-515° C with pure iron to 480-525° C at 0.9% carbon. With still higher carbon contents this range narrowed again back to 495-515° C at 2% carbon. With globular pearlite however, although a similar widening of the band occurred this did not narrow again. Carbon as troostite had little influence.

In the Lower Parabolic Range, the effect of carbon again depended on the form in which it occurred. With lamellar pearlite the attack rate increases greatly up to a carbon content of about 0.88%, and diminishes again beyond that point. If present as globular cementite the attack rate is lower and increases to a maximum at about 1.4% C and then declines. This decline was explained by the presence of grain boundary cementite impeding attack. In the troostite state carbon has an insignificant effect.

In the Linear Range attack on lamellar pearlitic structures increases up to 0.88% carbon, and then decreases, so that at 2% carbon the rate is similar to that of a low carbon iron. Globular pearlite and troostite however show attack increasing constantly with carbon

content. The temperature of maximum attack remained in all cases at around 500° C.

Some work done at Battersea (66,67,68) has been along slightly different lines, but being in the form of short projects there were frequently experimental problems which could not be solved in the time available. Nevertheless such quantative results as have been produced agree with Horstmann, i.e. that increasing carbon content, in the form of fine pearlite, increases the width of the rapid attack region, and increases the rate of attack in the lower parabolic range (66).

Alloy layers were formed at a low temperature (450 or 460° C) on various steels, and then attacked for varying periods at 500° C. Subtraction of the weight loss expected at the lower temperature gave the rate of attack at the higher temperature. It was found that layers formed at 450° C on 0.4% carbon steel survived for some 12 hours at 500° C, but those on 0.8% carbon steel were dissolved in less than one hour. (67). Other elements, particularly high silicon and phosphorous levels in the different steels, made exact comparison difficult.

6:2 Initial Observations

The first observations indicating the effect of carbon in the steel were made on the discs of steel En 1a used for the rotating disc experiments (Chapter 3). It was noticed that many of the discs which were heavily attacked, i.e. at 500° C, showed a square pattern on the attacked face, resulting from more severe attack on a

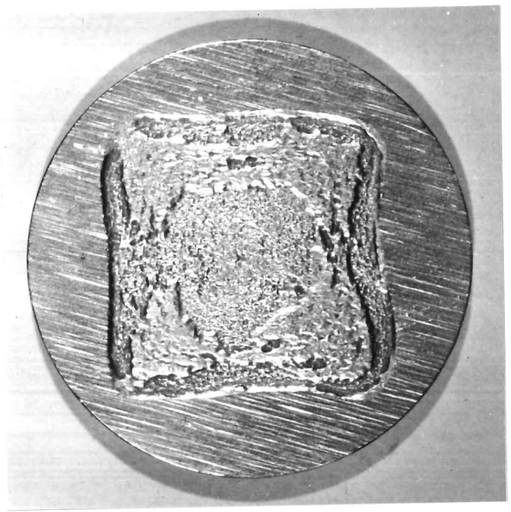

(a)

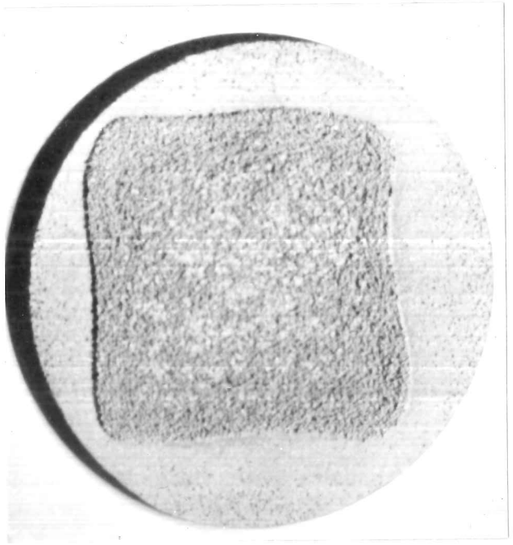

(b)

Fig. 48 Segregation revealed in steel En 1a
(a) after 1 hour in zinc at 500° C, zinc then removed x 2.5
(b) after heavy etching in conc. nitric acid. x 2.5

central square region. This extra attack was sometimes sufficient to blur the erosion spirals, making it difficult to see where they started (Fig. 15). The shape and nature of this square region was most beautifully revealed on one specimen attacked for 1 hour at 500° C but not rotated. (Fig. 48). It could also be revealed by macro-etching with nitric acid diluted 1:1 with water at 80° C. After one hour of this treatment , some 2 mm. of steel having been removed by the acid, the inner square region was revealed as a dark brown rough region, surrounded by a lighter coloured smooth region (Fig. 48).

It was clear that this square pattern was indicative of some form of segregation, but this could have been segregation of any of the major or minor components in the steel, or a difference in the composition or form of the inclusions. If the original ingot was square in cross-section, then the equiaxed zone, into which much of the segregation would take place, would be roughly circular if small enough. This is because of the more rapid cooling and hence growth of columnar grains from the corners of the ingot. If this ingot was now worked into a circular cross-section, the circular region would become a square (Fourier transforms).

The segregation in this particular steel was not further investigated because it was felt to be a curiosity arising from a particular steel-making practice, but a similar phenomenon was observed on the discs of steel used for investigation into the effect of aluminium in the zinc.

This steel, B.I.S.R.A. code "BB", was reported by B.I.S.R.A. to reveal, by sulphur printing and macro-etching, a slight degree of segregation, but the nature of this was not quoted, and no other workers using this steel had commented on it.

As reported in Chapter 4, it was observed that discs of this steel, when attacked in molten zinc containing some aluminium at 450° C, showed attack in the form of pitting which was particularly concentrated on the inner square region (Fig. 34). This effect was more distinct at the lower level of aluminium (0.1%), but was not observed in pure zinc. It was thought that this represented some form of segregation which was causing a temporary or permanent disruption of a protective alloy layer, allowing more rapid attack to occur. Steps were therefore taken to identify the nature of this segregate.

Initial observations were not very enlightening. Hardness values in the inner and outer region proved to be the same, 133 ± 2 V.P.N., and micro examination showed the structures to be very similar, fine pearlite and ferrite. Macro-etching revealed a line around the square, and after a very long etch slight differences could be detected across this boundary. Observation of a polished but un-etched longtitudinal section revealed many inclusions, mainly of the manganese sulphide and manganese oxide type. There was a high density of these, with many long or broken specimens, at the boundary between

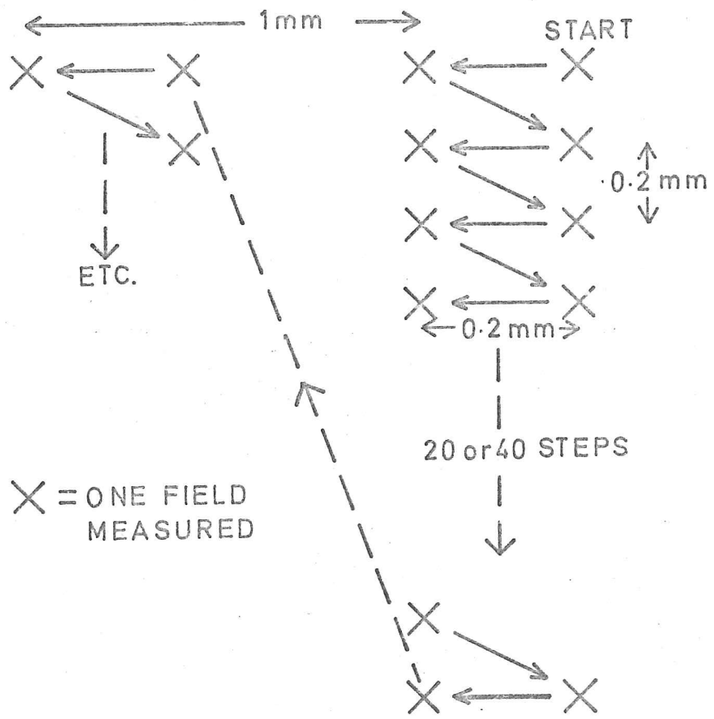

FIG. 49 RASTER PATTERN USED ON QUANTIMET

the two regions, and a smaller concentration at the centre of the bar.

More precise measurements were made with an image analysing microscope, the Metals Research Ltd. Quantimet "B". Considerable skill and practice was needed in specimen preparation and machine operation in order to achieve consistent results across a specimen $1\frac{1}{8}$" wide. Most of the work was done on longtitudinal sections, cut across a diameter of the bar so as to intersect the sides of the square at 90^{o}, taking some 20 or 40 frames in a raster pattern parallel to the axis of the bar, then moving on a small distance normal to this direction, as shown in Fig. 49. Use of this method to count a number of frames in a small region, measuring length and number of area of inclusions showed no significant difference across the specimen, except at the concentrations mentioned above.

It was difficult to measure the pearlite content of the steel because of the difficulty of etching it uniformly across the specimen. Over etching meant that grain boundaries were counted, whereas under-etching lost some of the smaller pearlite colonies. After several abortive attempts it was possible to obtain results as in Fig. 50, measuring the total pearlite content in a given number of frames around a certain point. This could be converted to a % carbon, knowing the area of "blank frame". This pattern was reproducible, but the absolute concentration of carbon determined in this

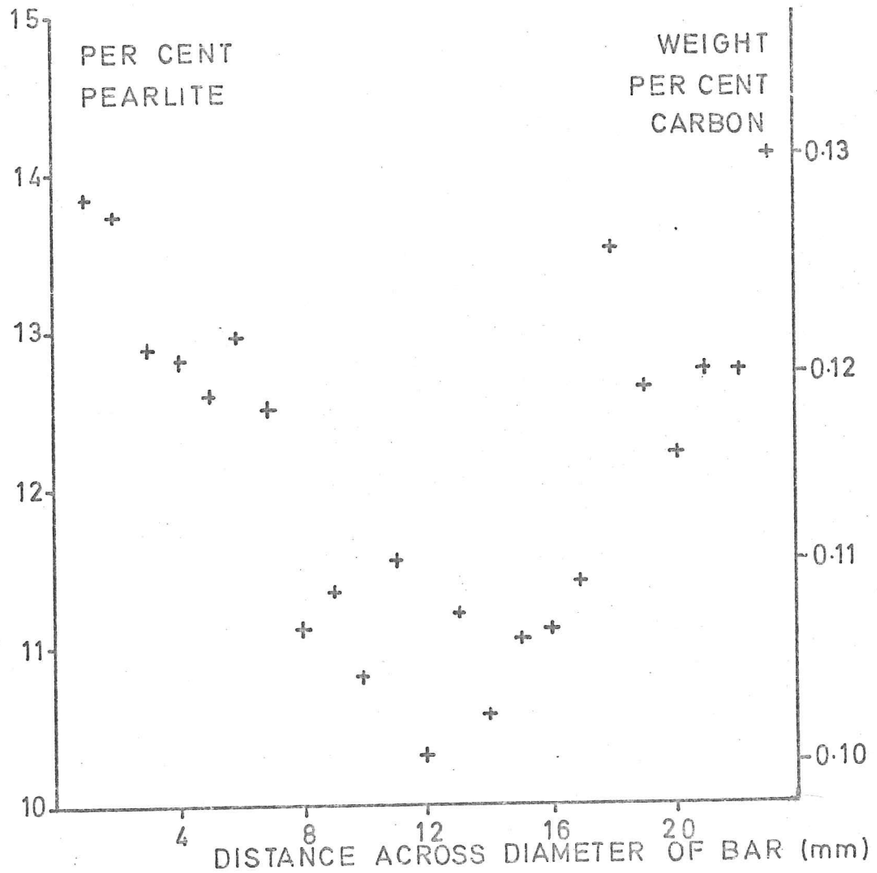

FIG.50 TYPICAL RUN ACROSS STEEL 'BB' ON THE QUANTIMET; EACH POINT THE AVERAGE OF 20 FIELDS

manner was variable, depending on the settings of the "threshold" and "minimum size" controls. It was not possible to measure right up to the edges because the polishing was imperfect in this region, but any decarburized skin was certainly quite thin. Such measurements as were made suggested that the changing quantity of pearlite was due to a variation in the number of colonies rather than in the size of each colony.

A difference in the carbon content between the inner and outer regions of about 0.014% seemed rather small to account for the distinct difference in attack noted in zinc plus aluminium. Samples were therefore sent to Tube Investments at Hinxton Hall for spectrographic analysis, concentrating on the elements known to be present in quantity and likely to affect the attack rate. The results, together with the B.I.S.R.A. analysis were:-

	C	S	P	Si	Mn
T.I. Inner Square	0.13%	0.049	0.039	0.19	0.67
T.I. Outer region	0.12	0.054	0.040	0.19	0.68
B.I.S.R.A.	0.12	0.054	0.039	0.22	0.695

The analyst felt that the difference in sulphur content might be significant. It will be seen that the carbon levels are the opposite of what were found with the Quantimet. This may represent the error arising from the method of analysis. It was clear that the only certain segregation was of sulphur or carbon. Although the differential attack reported above might have been due to some other element not investigated (perhaps titanium?) it was felt worthwhile to investigate the

Table 5

Attack of molten zinc on two different microstructures produced from the same steel.

Microstructure	weight loss per unit area ($Kg\ m^{-2}$)$\times 10^3$	steel surface after stripping
1 hour at 450° C.		
Pearlite	930	Uniformly roughened
Pearlite	842	" "
Martensite	92	Smooth all over
Martensite	92	" " "
1 hour at 500° C		
Pearlite	1386	Uniformly roughened
Pearlite	1282	rather more blotchy
Martensite	669	Rather blotchy
Martensite	883	One side smooth, the other blotchy.

effect of carbon in greater detail.

6:3 Investigation into the effect of carbon in steels

It was decided that it was not feasible to prepare and analyse purely binary, homogeneous, iron-carbon alloys, and that investigations would have to be confined to the preparation of different microstructures in one particular steel, and to the carburization of pure armco iron, producing a carbon-rich skin of unknown composition. Efforts were first concentrated on the effects of microstructure.

It was hoped to use a near-eutectoid composition, so that effects would not be masked by a quantity of ferrite. Initially a steel was used containing several alloying elements, but having the advantage of a full analysis, i.e.: 1.02%C, 0.01%S, 0.017%P, 0.36%Mn, 0.27%Si, 0.14%Ni, 1.38%Cr, 0.04%Mo, 0.14%Cu, 0.019%Al. This was austenized at 1000° C for 10 hours, then cooled to ~820° C and one specimen quenched into water. The other specimen was cooled from 820° C to 690° C at about 10° C per hour, then furnace cooled. The structures produced were martensitic or medium coarse pearlite, both with some decarburization despite protection from an inert atmosphere in a silica tube. Specimens cut from these samples were attacked in pure molten zinc saturated with iron at 450° C and 500° C, being suspended by tungsten wires. The results are displayed in Table 5.

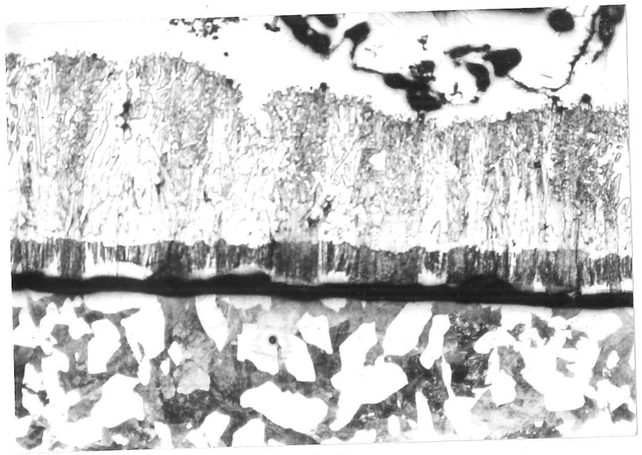

(a)

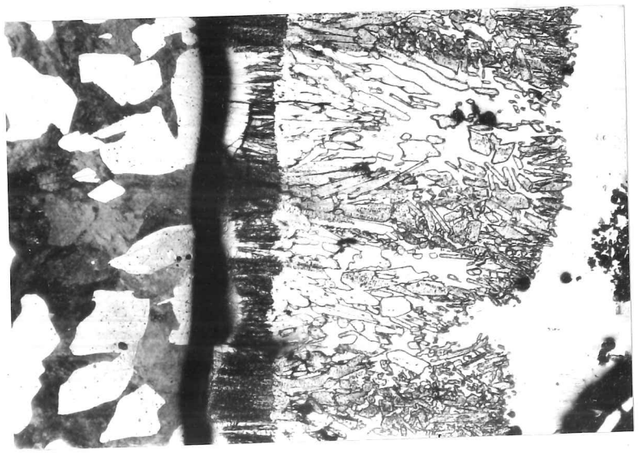

(b)

Fig. 51 Alloy structures on a pearlitic steel after 1 hour in zinc at 450° C. Picral etch
(a) x 70 (b) x 110

It is clear that the effect is of the same order as reported for other steels at 450° C (11), but less marked at 500° C. The surface of the steel when stripped showed a distinct roughened granular effect on the pearlitic specimens which was not apparent on the martensitic ones.

Another steel, of unknown composition but lower carbon content, was heat treated to produce large colonies of pearlite, and was examined metallographically after one hour in zinc at 450° C and 500° C, Figs. 51 and 52. Various etchants were investigated in order to reveal the steel structure right up to the zinc alloy interface. Boiling 1% nitric acid in isopropyl alcohol, electrolytic etching in nital, and masking the zinc with lacomite proved unsuccessful, but a long etch (90-180 seconds) in 5% picral revealed the steel structure up to the boundary, although at the expense of somewhat over etching the zinc, which may then appear out of focus.

It was quite clear however that the attack on the pearlite differed from that on the ferrite. At 450° C the palisade delta layer was much thicker over the pearlite, and was covered by a thicker and more compact zeta layer. The whole layer had a smoky effect, as if containing many fine particles. The steel interface was somewhat undulating, suggesting a greater attack on the pearlite areas. The effect at 500° C was similar but not as clear because of the more broken up structure. The structures on the martensitic specimens etched very rapidly and were uninformative, particularly at 500° C (Fig. 53).

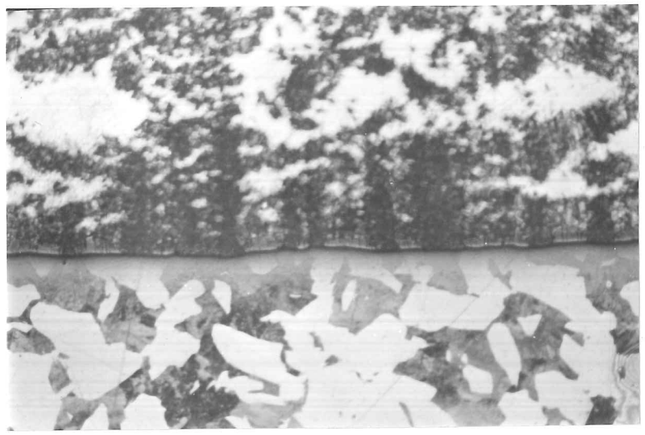

Fig. 52 Alloy structure on a pearlite steel after 1 hour in zinc at 500° C. Picral etch, x 85.

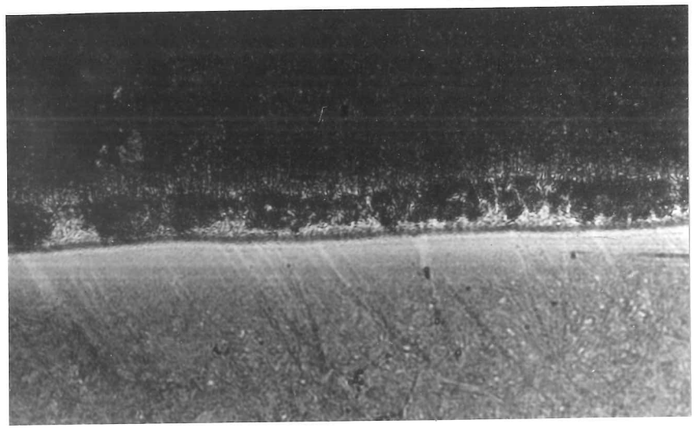

Fig. 53 Alloy structure on a martensitic steel after 1 hour in zinc at 500° C. Picral etch x 375.

A disc of armco iron was carburized at 950° C for 8 hours in a proprietary compound and then slowly cooled. Being quite thin the composition was virtually uniform across the specimen, and consisted of coarse pearlite with some massive globular cementite. When attacked for 1 hour at 450° C and subsequently examined the cementite was seen to be rather more resistant to attack than the ferrite (Fig. 54).

It is thus not clear why the attack rate on pearlite steels should increase with carbon content, since this is increasing the amount of a more resistant component. Three hypotheses can be suggested:

1. An increase in the surface area between the phases, i.e. ferrite and cementite. This could be a direct contribution from surface energy, the surface energy between these two phases being rather high, ~1350 ergs. cm^{-2} (69). Alternatively the phase boundaries could provide channels for rapid attack into the steel, increasing the effective surface area.
2. An electrochemical effect, as would be invoked to explain a similar phenomenon in aqueous corrosion. The cementite would have to be cathodic, with the reaction under cathodic control. It is difficult to postulate a workable mechanism for the attack in zinc, an electronic conductor, because of the lack of an ionic circuit.
3. Modification by the carbon of the alloy layers, resulting in a more rapid attack. This could be brought about by the Fe_3C breaking up the continuity of the layers.

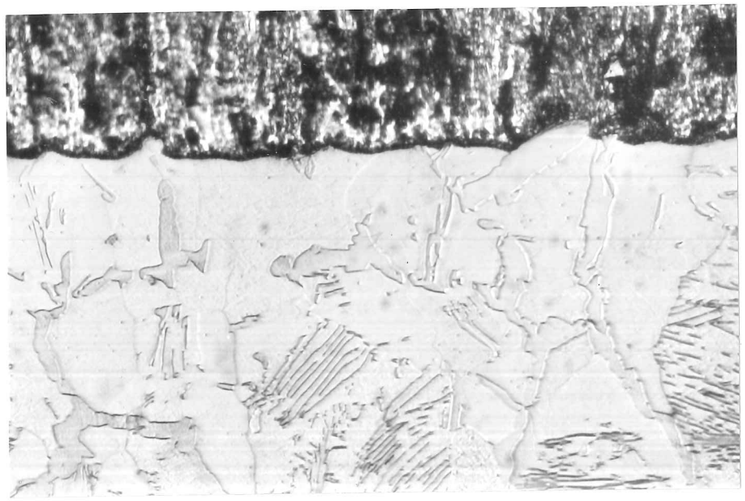

Fig. 54 Attack on carburized armco iron after 1 hour at 450° C. Picral etch x 375.

Further experiments were carried out to distinguish between these possibilities.

6:3:1 Effect of transformation temperature

If the surface area or energy was a significant factor it would be expected that fine pearlite would be attacked more readily than coarse. Taking this to its limit it would be suggested that martensite, a metastable structure, should be attacked more heavily than stable pearlite. Nevertheless it was felt worthwhile to investigate fully a range of structures produced at different temperatures from the same steel.

To this end a rod ~$^3/_8$" dia. of a pure eutectoid steel was obtained, with 0.80% carbon and total impurity content less than 0.09%. This was water quenched after $\frac{1}{2}$ hour at 1200° C, austenized at 1050° C for $^3/_4$ hour and then isothermally transformed in a bath of molten tin at various temperatures as in Fig. 55. To prevent decarburization the specimens were sealed off in silica tubes under argon until water quenched, but in order to get the necessary rapid change of temperature for the subsequent transformations (~5 secs. at 550° C) it was found necessary to heat the specimens in air. The decarburization was in fact undetectable. Some further specimens were spherodized by heating for 3 days at 700° C.

After heat treatment the specimens were lightly ground to remove oxide and sliced up to give discs 0.15" thick; these were then ground on 180 paper, measured and weighed.

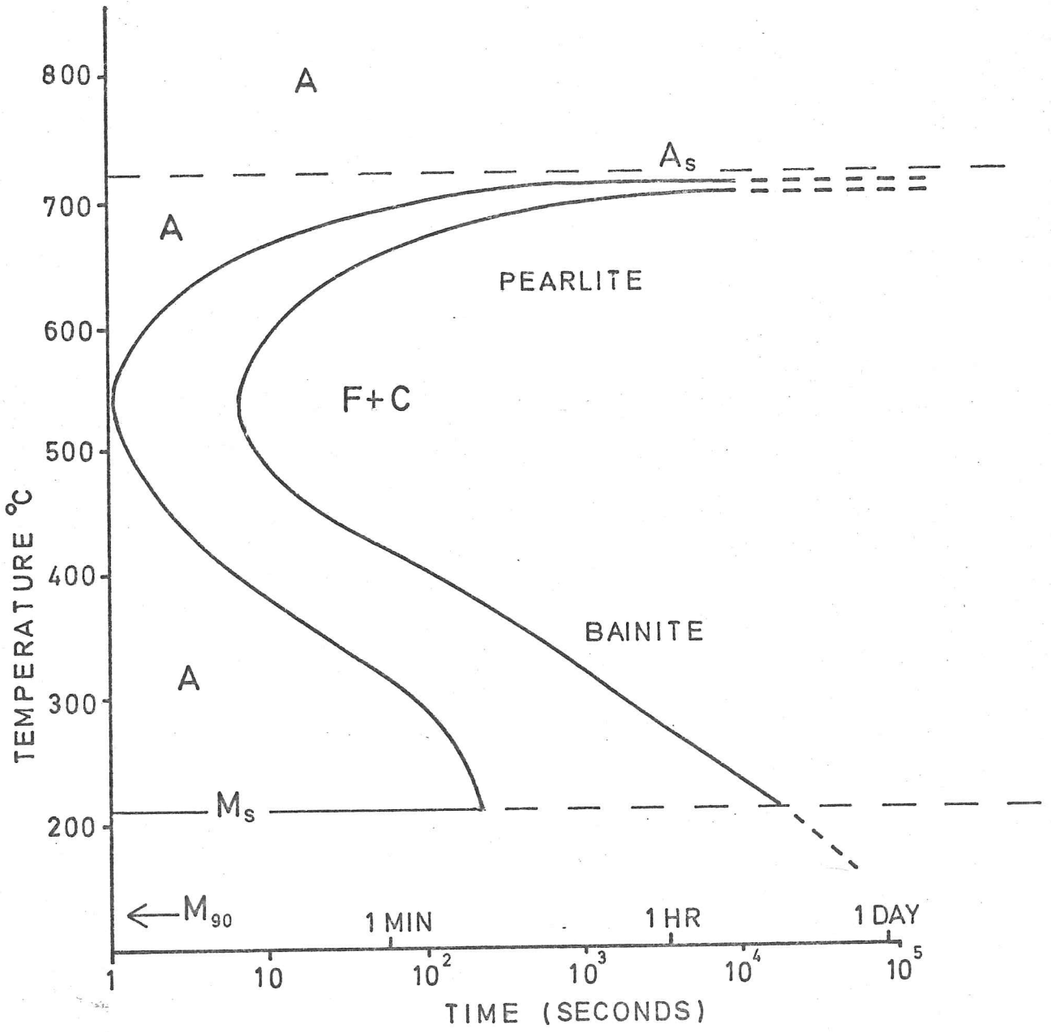

FIG.55 ISOTHERMAL TRANSFORMATION OF EUTECTOID STEEL FROM REF.(70)

They were suspended by tungsten wires, fluxed with "Bakers soldering fluid" and attacked in zinc at 450° C or 500° C for one hour. It was originally intended to correlate the attack with the pearlite spacing measured on the scanning electron microscope using the method of Pellisier et.al. (71), i.e. measurement of the smallest observed spacing on a given section. However when the results were known (Fig. 56) it was clear that this was not worth the effort.

The rather large degree of scatter in the results at 450° C might have been due to inaccuracy in the measurement of the rather small specimens, or, more likely, to imperfect fluxing causing some areas to be inadequately wetted. The lower values of weight loss would thus be suspect.

It is clear that the greatest attack occurs on the coarsest specimens, i.e. those spherodized, consisting of coarse pearlite with massive globular cementite. There is then a decline in the attack rate roughly proportional to the pearlite spacing, i.e. to the transformation temperature, down to about 500° C, which was both the nose of the curve and also the temperature of the bath. It was thus not clear whether the attack on the different bainitic structures was the same, or whether these all tempered to a constant structure during their immersion in the zinc.

To check that the measured weight losses were not due only to the different rates of attack by the acid used to strip the alloy Specimens were also tested in diluted acid for $\frac{1}{2}$ hour, about 3 times the time required

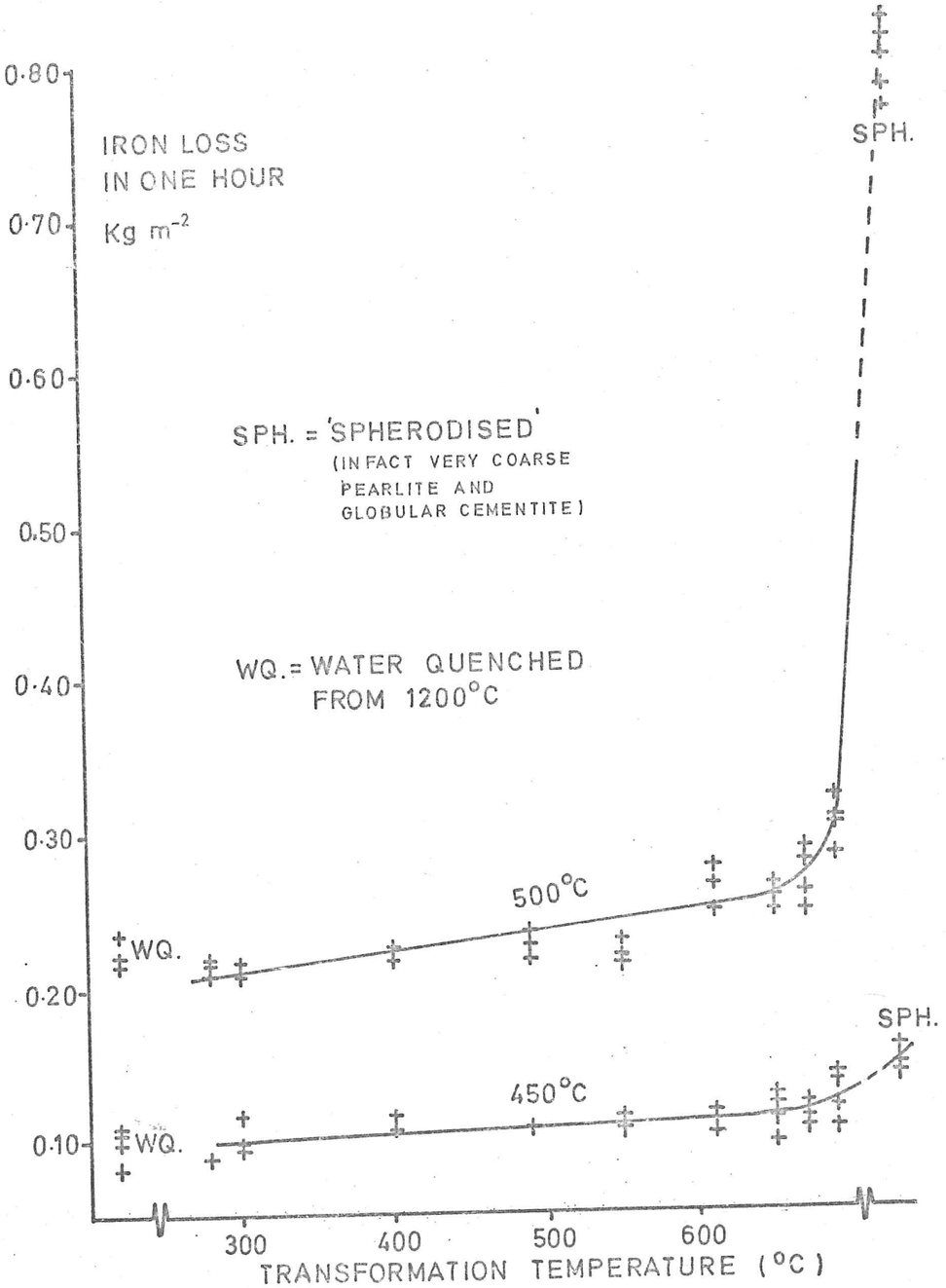

FIG. 56 ATTACK RATE ON DIFFERENT MICRO-STRUCTURES

for stripping. The trend was in the same sense as for attack by zinc, but the absolute level was too low to be significant, i.e. 3 to 6% of the weight loss after 1 hour at 450° C.

It was felt that the rapid attack on the coarser structure must disprove the surface energy hypothesis, but it was still possible that penetration at the phase boundary was of significance. The coarser structures would have less such boundary reaching the zinc, but it would tend to penetrate the steel to a greater depth. No such penetration could be observed however.

As a subsidiary experiment armco iron specimens with different grain sizes were prepared. Discs about 4 mm. thick were cut from a bar $1\frac{1}{8}$ dia., and were cold rolled to reduce this thickness to 2 mm. These specimens, now elliptical, were recrystallized under a vacuum at 600° C for 1 hour, then grain growth produced at 1100° C for $\frac{3}{4}$, 3, 5 or 10 hours, or 1 hour at 900° C. After treatment the specimens were weighed and measured using the formulae:

Area of ellipse = $2\pi ab$, circumference = $\pi(1.5(a+b)-\sqrt{ab})$, where a and b are the lengths of the major and minor axes. Grain sizes were measured by counting the number of grains intersecting a given length on a projection microscope at a suitable magnification.

Weight losses per unit area after one hour at 450° C and 500° C showed a good correlation with grain size, which could be plotted as average grain diameter, grain boundary length per unit area on a cross section, or

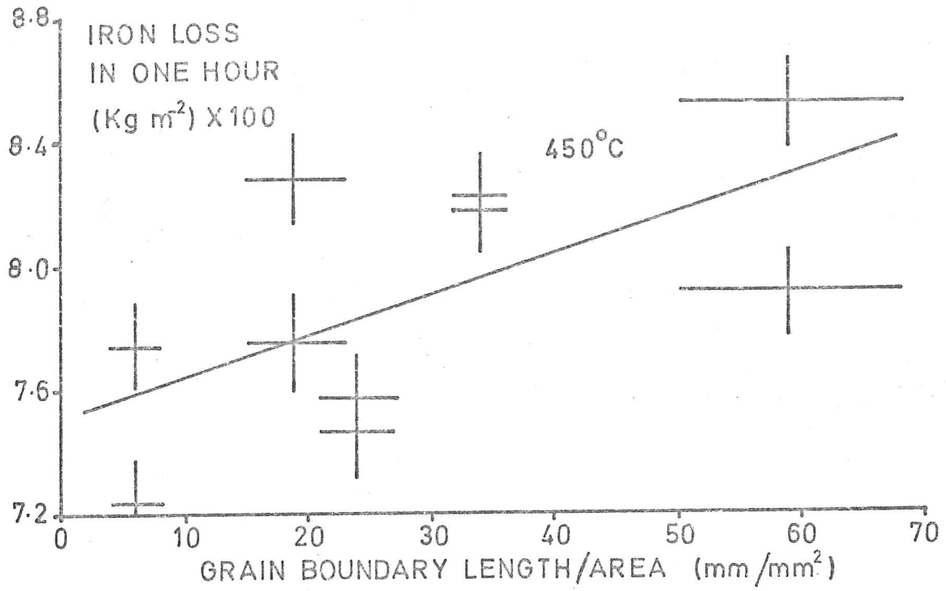
IRON LOSS
IN ONE HOUR
(Kg m^2) X100
450°C
8·8
8·4
8·0
7·6
7·2
0
10
20
30
40
50
60
70
GRAIN BOUNDARY LENGTH/AREA (mm/mm^2)

FIG. 57

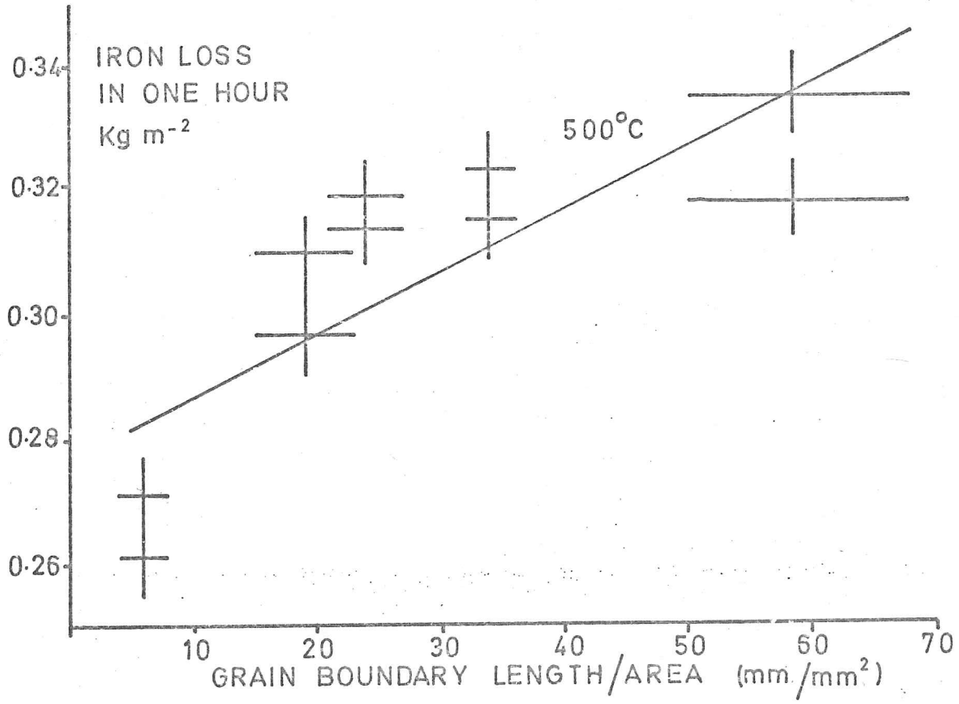
IRON LOSS
IN ONE HOUR
Kg m^{-2}
500°C
0·34
0·32
0·30
0·28
0·26
10
20
30
40
50
60
70
GRAIN BOUNDARY LENGTH/AREA (mm/mm^2)

FIG. 58

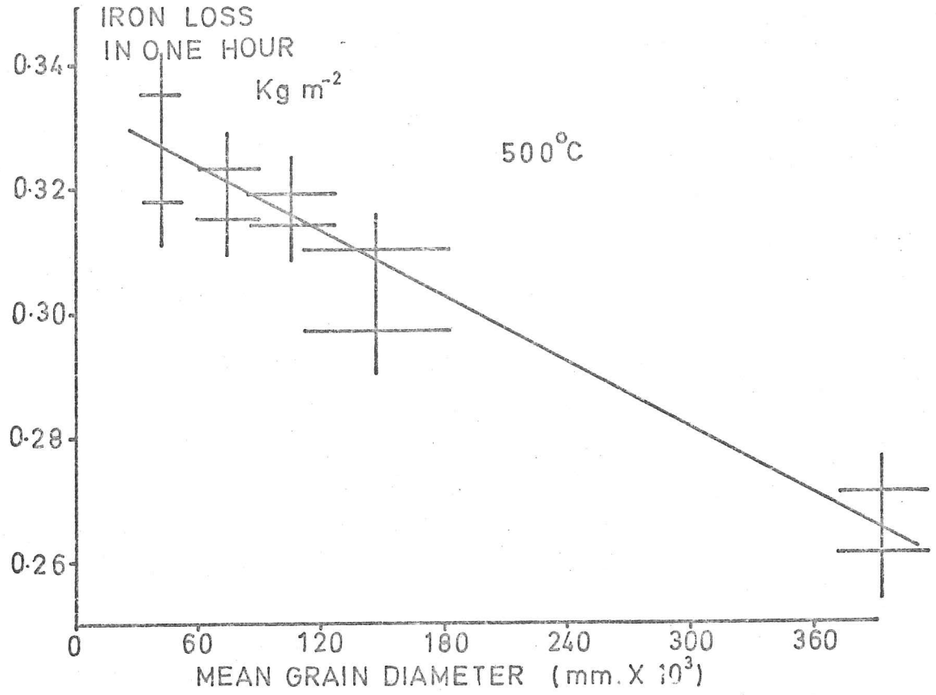

FIG. 59

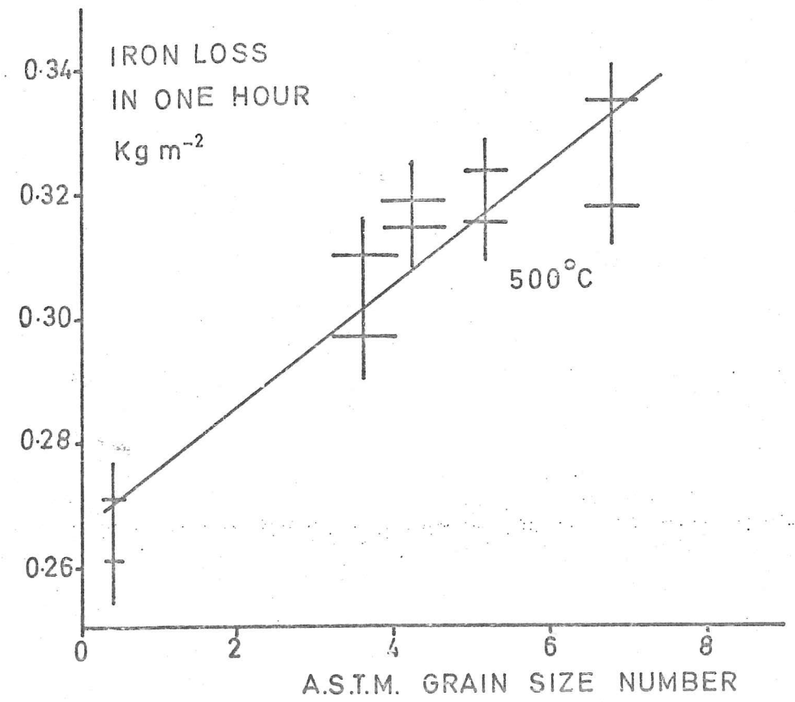

FIG. 60

A.S.T.M. grain size number. (Figs. 57, 58, 59, 60) Only the grain boundary length per unit area would seem to have any practical significance, but this gave the worst correlation.

However, at the largest grain sizes the attack may be influenced by the small number of grain orientations at the surface, i.e. the development of a texture. The attack rate is not necessarily the same on all orientations. As with the microstructure results, the trend is clearer at 500° C. The range of grain sizes was wide but even though the grain boundary energy of α iron is quite high (~700 ergs/cm^2), the range of energies per unit volume could not approach that of fine pearlite. Thus although it can be assumed that in the absence of other factors the grain size is of significance, it is in the wrong sense to explain the effect of pearlite spacings.

Evidence for the mechanism by which grain size influences attack rate is hard to find. There is very little evidence of grain boundary penetration (7, 72), and when it is observed (Fig. 61) it may be the spurious result of polishing or etching. Being covered by a thicker alloy layer attack at such penetration should be restricted.

6:3:2 Investigations of electrolytic effects

Conventional corrosion phenomena require both ionic and electronic processes to make a complete corrosion circuit. Electronic conduction is obviously possible in molten zinc, all the components being good electronic conductors, but it is difficult to envisage any suitable

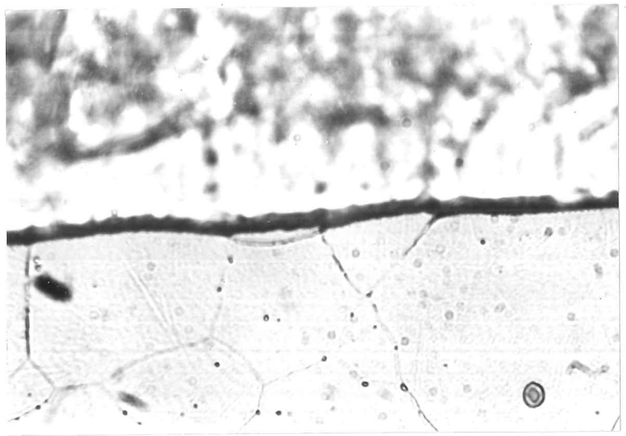

(a)

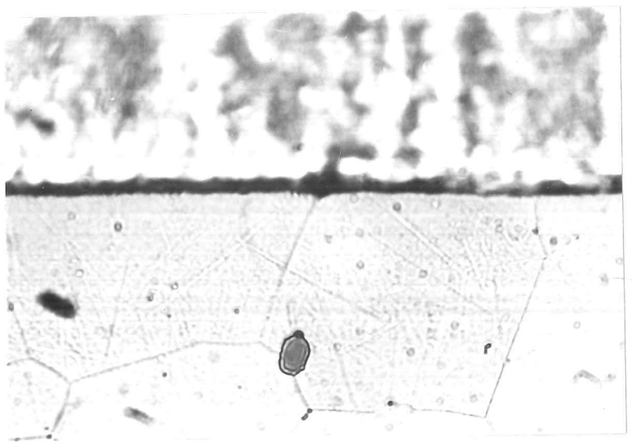

(b)

Fig. 61 (a) and (b). Possible slight grain boundary attack on armco iron after 1 hour at 500° C. Picral etch, x 860.

ionic reactions. Nevertheless many of the features regarding the effect of carbon on the attack rate could be explained using concepts from aqueous corrosion. Thus the increase in carbon increases attack if it is in the form of cementite, the cathodic surface of an attack system under cathodic control, but small such regions polarise easily, so that fine pearlite is less effective in increasing the attack than is coarse pearlite or a spherodized structure.

To investigate this it was hoped to be able to prepare massive lumps of cementite by the intensive carburization of armco iron, and to this end 3 specimens were heated in a carburizing mixture for 10 days at 950° C, being removed every 12 hours, surface ground to remove any oxide, and repacked with a fresh mixture. Unfortunately this was quite unsuccessful, the result being some 40% cementite in the form of coarse pearlite and grain boundary cementite. This is presumably because of the slow diffusion rate of carbon in cementite, so that once a layer of cementite forms at the surface the reaction becomes much slower.

To try to increase cementite content by another route carbon was added to a molten cast iron containing 4.1% carbon, and after a time of superheat to allow for dissolution, cast into water. It may be that the carbon never dissolved, or else precipitated out on cooling, but the structure contained mainly graphite. The attempt was abandoned.

Table 6

Attack for one hour ($Kg\ m^{-2} \times 10^3$) on plain armco iron and heavily carburized armco iron either separately or when in contact.

(a) At 450° C

	Armco	Carburized armco
Separately	82	108
In contact	125	123
Separately	125	118
In contact	94	110

(b) At 500° C

Separately	282	1090
In contact	353	1040
Separately	303	1140
In contact	284	1120

To attempt to measure any electrical potential directly a sample of the carburized armco iron was spot welded to a thick tungsten wire, and the potential between this and a piece of plain armco iron similarly spot welded was measured as they were lowered into the molten zinc at 450° C. A difference of 0.2 mV was detected, the carburized specimen being +ve. A similar value was recorded however when the experiment was repeated with the specimens now in contact and immersed in the zinc inside a silica tube. Use of plain iron wires gave a similar result again. It was felt that this potential was a thermo-electric effect generated at the specimen's interfaces, together with effects due to the use of "compensating cables" at heated junctions. True corrosion or thermo-electric potentials could not be measured without bringing the "cold junctions" out to a cooler region, i.e. rods or wires of cementite were needed. Since these were not available direct measurements were abandoned.

An alternative experiment was then tried, measuring the attack on plain armco iron and carburized iron separately, at different times, and then while spot-welded together at one edge. If some form of electolytic reaction was occuring the attack rate should differ when the two specimens were in contact. The results are displayed in Table 6.

Errors arise particularly from the measurement of areas when the two specimens were welded together, and

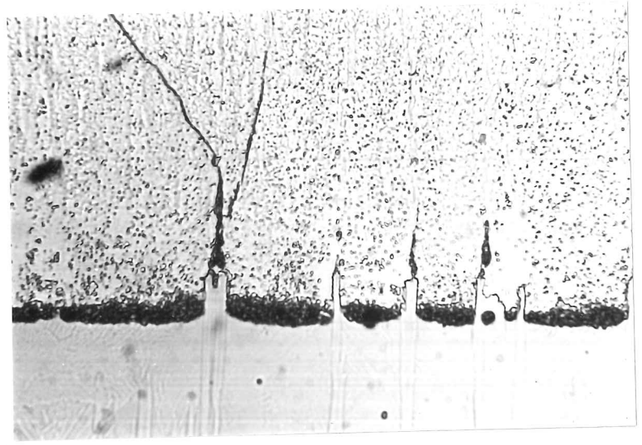

(a).

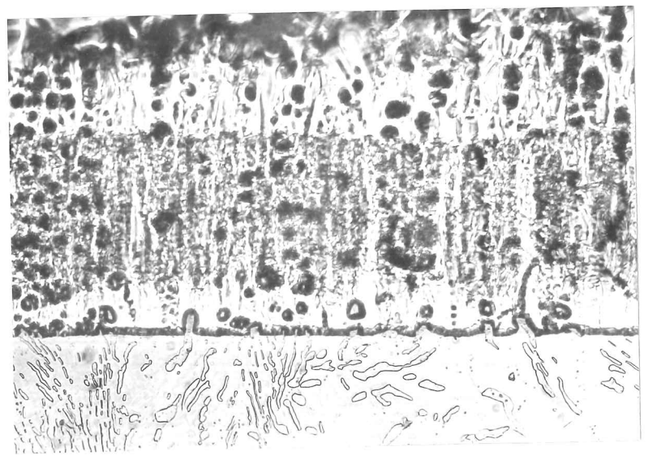

(b)

Fig. 62 (a) Attack on carburized armco iron, with protruding cementite, after 1 hour in zinc at 450° C. Picral etch, x 540.
(b) As (a) but on a "spherodised" eutectoid steel, x 270.

in the potential loss or gain of iron when the weld was broken for subsequent weighing. However, from these results there is no reason to suggest that the attack on ferrite is speeded up by contact with cementite. It would be more convincing if the carburized specimen was in fact free of ferrite itself. It may be that any effect is very localized and is not apparent over the whole of the plain armco specimen.

6:4 Conclusions

The evidence supporting the hypotheses of an electrochemical effect or a surface energy effect is either weak or non-existant. Direct support for the alternative, i.e. a modification of the alloy layers, is however difficult to find. Attempts to use the electron micro-probe to investigate the alloy layers formed over large pearlite colonies (Fig. 51) proved unsuccessful. The carbon-containing regions were obviously very small, producing perhaps the smoky effect, and the soft and weak X-rays excited within these regions were probably absorbed by the surrounding metal.

Optical examination of alloy layers on some of the coarser microstructures was more informative. The heavy etching and high magnifications required generally left the alloy structure out of focus, but it was clear that the cementite resisted attack to a greater degree than the ferrite, but eventually broke off and was left as isolated particles in the alloy layer. (Fig 62) These

particles were probably slowly reacting to form a mixed carbide of the form Fe_3ZnC (73). This might then become richer in zinc, with possible elimination of elemental carbon.

The effect of carbon could thus be by one of two mechanisms. Particles of cementite or perhaps Fe_3ZnC might physically break up the iron-zinc alloy layers, creating cracks and voids, and also phase boundaries, all of which might be expected to aid diffusion. This effect might be concentrated in the gamma and coherent delta layers, where diffusion is perhaps normally restricted. Alternatively the carbon could become more intimately associated with the intermetallic compounds, altering the crystal structures in such a way as to influence diffusion rates.

If this latter possibility were the case then it might be expected that the more homogeneous microstructures such as martensite or bainite should suffer the greatest attack because the carbon from these would be liberated more easily, being combined in very small particles. Coarser structures, such as globular cementite would affect the intermetallics more slowly as the particles of cementite were broken up.

It must therefore be concluded that the effect of carbon is by means of the disruption of the intermetallic layers by particles of cementite. Small such particles are less effective and are more rapidly consumed, so that attack is greatest on structures containing large particles of cementite.

CHAPTER 7

SOME MISCELLANEOUS RESULTS

In this chapter are collected some experimental results which do not conveniently fall under a previous title. They arise from experiments which it was hoped would throw further light on the iron-zinc reactions, but generally failed to do so. This was either because the aspect they were to investigate did not in fact exist, or because the experimental techniques required were too difficult and effort spent on developing them was felt to be misdirected.

7:1 Twisting of thin specimens

If molten zinc is allowed to react with one side of a thin specimen while the other is protected by some inert layer, the formation of the alloy layers is accompanied by stresses which tend to twist the specimen with the alloyed side outward. On a large thin sheet this tends to produce a spherical shape, which is constrained by the elastic properties of the metal, but a thin strip will tend to curl up into a spiral. It was hoped that this twisting process could be monitored and would give a rapid indication of the rate of attack.

Pieces of shim steel, 3 thou. thick, were taken and cut to give specimens about 40 mm. long and 5 mm. wide. To confine the distortion to one plane only

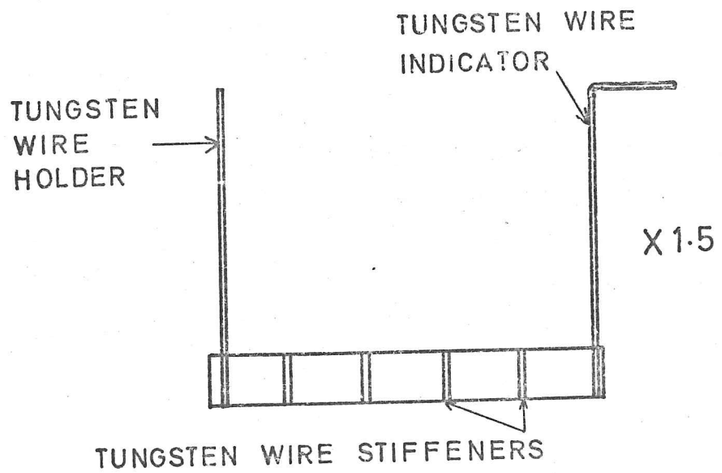

FIG.63 SPECIMENS USED TO MEASURE RATE OF TWISTING

stiffeners in the form of tungsten wire were spot-welded on at intervals. At one end a longer piece of tungsten wire was used as a holder, and at the other end a similar length of wire, bent over at the top, was used as an indicator (Fig. 63).

After annealing two coats of a milk-of-lime wash were applied to one side of the strip, that with the stiffening wires on. Onto the other side was brushed a thin coating of a melted resin flux.

The specimen was now lowered into the zinc, being held by the protruding wire. The angle made by the indicator was noted at intervals. It was found that this angle altered irregularly from specimen to specimen at a given time, and that the curvature on a given specimen was generally not uniform along its length. Considerable distortion could occur as the specimen penetrated the surface of the zinc on immersion, and again on removal.

The angle swept through by the free end of the specimen during one hour's immersion at 450° varied from 40° to 720°. Similar wide variations were found during shorter runs at 500°C, or at 450°C in zinc + 5% aluminium. Some of this variation may have been due to zinc attacked on the back of the specimen, where the flux had wetted the milk-of-lime wash. Specimens evenly attacked on both sides did not twist. Further variations may have been produced by uneven annealing, or by convection currents within the zinc. It was felt that these results demonstrated the unreliability of

Table 7

Effect of applied electric potentials on attack.

Weight loss in one hour (Kg m^{-2})x10^3

Active area of specimens ~ 660 mm^2

Steel En 1a

at 500° C		at 495° C	
No current	563 610 507	No current	325
steel -ve, 1.5v, 16A	503	steel -ve 0.8v, 15A	333
steel +ve, 1.6v, 16A	530	steel +ve 0.8v, 15A	324

Steel "BB" at 450° C in zinc +0.5% aluminium

No current	97
Steel -ve 2.2v, 16A	185
Steel +ve 2.2v, 16A	236
Steel +ve 2.1v, 16A	271

the method, and did not warrant further development.

7:2 Effect of an applied electrical potential

There had been some indications (74) that an applied electrical potential between a steel or aluminium specimen and the molten zinc would influence the attack rate. This might have been by a mechanism similar to cathodic protection in aqueous corrosion, i.e. bringing the steel to a lower potential where the reaction $Fe \rightarrow Fe^{2+}$ no longer occurs. Alternatively the effect might have been due to an influence by the potential gradient on diffusion rates in the alloy layer. With aluminium in zinc the effect might have been by the attraction of oxygen ions within the zinc to the aluminium surface to form or heal an alumina film.

To investigate this method of protection specimens in the form of discs with a suitable central hole were bolted between two tungsten washers with tungsten nuts on the tungsten rod previously used for the rotating disc work. The tungsten was insulated by coats of "Gum-Gum" and was connected to a power supply; electrical contact with the molten zinc was made by means of another tungsten rod. Because of the very low resistance of the circuit very high currents were needed to maintain potentials likely to be effective; these currents were provided by a heavy duty low voltage power supply, giving up to 16 amps. The results are displayed in Table 7.

Some degree of scatter is due to zinc penetration under the tungsten washers, but it is clear that there is little or no effect at 500° C or 495° C, and at

450° C the effect is to increase the attack for both senses of potential. In fact only about half of the measured voltage drop occurred across the specimen-zinc boundary, the rest occurring at the zinc-tungsten electrode. It may be that the potentials produced were inadequate for the purpose. Not knowing the mechanism by which the potential might act it is impossible to estimate its necessary magnitude. There is obviously some effect taking place at 450° C, but since it is the same for both senses of current it was assumed to be a heating effect at the interface, bringing the local temperature into the linear region.

Because of the very high currents required to maintain a sizeable potential, and with no evidence that this potential had any effect in reducing the rate of attack, this method was dismissed as impracticable. It was likely that the previous evidence pointing towards some effect (74) was due to the poor temperature control in the furnace used for this work, resulting in considerable differences in attack rate on different specimens.

As a final possibility it was thought that alumina films might be protected or healed within molten zinc by an applied potential, i.e. by a sort of "in situ" anodising. This would require the presence of some oxygen ions in the zinc, and the concentration of these would be low. Nevertheless it was felt that the alumina film should have a high electrical resistance and so need only some low current to maintain a

Table 8

Effect of applied electric potential on alumina films in molten zinc at 500° C. Current densities of about 1 KA m^{-2}

Pure aluminium

0.9v +ve, rising to 0.95v after 15 mins

current initially 2A, dropping to 1.9A

Previously anodised aluminium

0.65v +ve 2A No change during 15 mins

0.8 v -ve 2A No change during 15 mins

Steel carburized at 900° C for ½ hr.	Steel carburized at 900° C for , hr, then ½ hr 900° C in air.
0.3v -ve, 1.5 A dropping to 1.4 A after 15 mins.	0.25v -ve, 1.4 A, no change in 15 mins.
0.4v +ve, 1.5 A. No change in 15 mins	0.45v +ve 1.5 A, no change in 15 mins.

significant potential. Some tests were therefore carried out on pure anodised aluminium and two calorized steel specimens, making electrical contact through a crocodile clip, and dipping the other half of the specimen into the zinc, with current returning again via a tungsten electrode.

As can be seen from Table 8 the conductivity of the alumina films was very high and no anodising type of behaviour was detected. It was felt that the applied potential was unlikely to produce any protection. Weight loss measurements were not attempted because of the long inhibition period before attack would start.

7:3 Effect of gases in the molten zinc

It was thought just possible that dissolved gases within the zinc might have some influence on the nature of the attack. Oxygen, or perhaps dissolved zinc oxide might have some effect on the attack on carbon steels. To investigate this possibility gases were artificially introduced into the zinc.

Specimens of steel "BB" in the form of discs were suspended in a vertical plane, and a pyrex glass probe introduced below them, so that gases passed through the probe bubbled up on either side of the specimen. Hydrogen or oxygen-free nitrogen were used, and tests run for one hour at nominal temperatures of 500° C and 450° C. The results are displayed in Table 9.

The gas flow rate was some three bubbles per second, and the hydrogen was ignited at the zinc surface by a gas torch. The extra heat input from this

Table 9

Effect of gases on attack rate

A. At 500° C

Gas	Actual Temperature	Weight loss unit area ($Kg\ m^{-2}$)x10^3
Hydrogen	500°	217
No Gas	500°	270
Hydrogen	500°	208
Nitrogen	480°	200
No Gas	495°	256

B. At 450° C

Hydrogen	470°	206
Nitrogen	470°	214
No Gas	480°	333

system caused the bulk zinc temperature to rise, particularly at 450° C. To balance this the torch was also used over the zinc for the other runs at 450° C. There was also a cooling effect due to the flow of cool gas, particularly in the vicinity of the specimen, so that the final run, at "450° C" without any gas flow, somewhat overheated.

Bearing in mind these temperature fluctuations and the agitation produced by the rising bubbles, it would seem that both gases reduced the rate of attack. This was probably due to local cooling around the specimen. To detect any further effect would require more pre-heating of the gas.

7:4 Effect of inclusions

The behaviour of inclusions was not specifically studied, but iron-manganese oxides were present in the armco iron, and manganese sulphides in steel En 1a. The presence of such inclusions seemed to have no effect on the attack rate on the steel around them. As attack around them progressed they would at first project into the iron-zinc alloy layer, then later be pulled out of the steel, leaving a hole (Fig. 64). As they moved outward they became increasingly broken up, either by chemical action or more likely by compressive stresses. It may reasonably be concluded that these, and probably other smaller inclusions, have no affect on the iron-zinc reactions in the concentrations normally encountered.

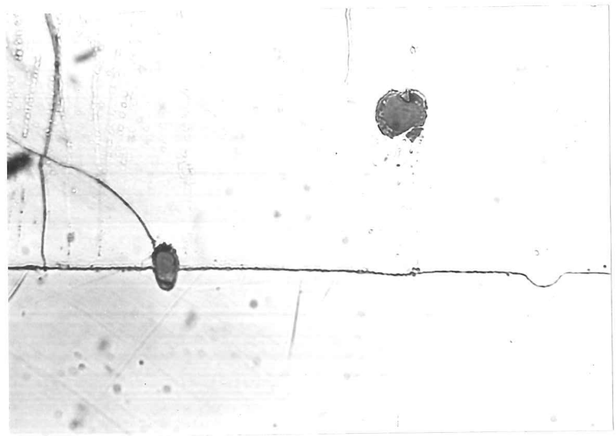

(a)

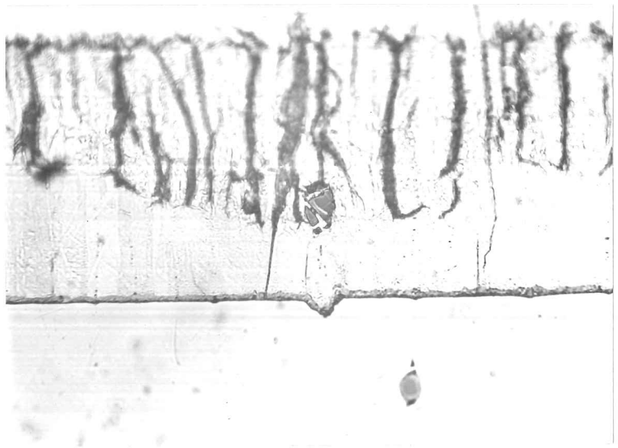

(b)

Fig. 64 Inclusions in armco iron after 12 hours in zinc at 450° C. Unetched. (a) x 680 (b) x 430.

7:5 Selective dissolution of alloy layers

Selective removal of solder from the surface of soldered plates, revealing the intermetallic compounds underneath, has been useful in resolving certain problems (75), and it was hoped to do the same for zinc. It was reported (76) that mixtures of chromium trioxide, orthophosphoric acid, sulphuric acid and water at 75-95° C would remove zinc without affecting the iron-zinc alloys.

This was investigated using a mixture of 20 g. Cr_2O_3, 5 ml. H_3PO_4, 11 ml. H_2SO_4 and 50 ml. water. Specimens of pure zinc, iron-zinc alloy and a galvanized specimen were immersed in this for 4 hours at 80° C with occasional inspections. The dissolution rate was slow, but eventually all the zinc and zinc alloy was removed. Only by stopping at some arbitrary intermediate point could the intermetallic layer be examined, and this was certainly being attacked by the solution.

It should be possible to selectively attack the layers by electrolytic dissolution. Attempts to do this by anodic dissolution in saturated potassium chloride solution, N/5 sodium benzoate, and boric acid, sodium borate and potassium chloride, all proved unsuccessful. With the low current densities used the dissolution rate was slow but not selective. There were no distinct changes in the potential-time curves which would indicate the end of the dissolution of a particular alloy composition. Better results might be obtained by a proper potentiostatic analysis of the coating

since the intermetallic alloys have distinct potentials with respect to a calomel electrode (77).

7:6 Dilatometry

Dilatometry experiments with small iron-zinc couples or pieces of alloy on iron were not very satisfactory. All showed a distinct contraction on heating. The first specimen was heated to 500° C in a vacuum and most of the zinc was found to have sublimed and condensed in a cooler part of the system. Future runs were in air, and there was some trouble with oxidation, and also the temperature control of the system. It was difficult to explain the degree of contraction, most of which was recovered on cooling. Some of this effect might have been due to the formation of intermetallic compounds, but might have been due to some experimental error.

7:7 Effect of crystal structure

It was thought that the various other alloying elements might act by means of a stimulation of the growth of a particular intermetallic compound because of a similar crystal structure, similar to the effect of certain alloying elements in steel on the stability of austenite. An attempt was therefore made to correlate the crystal structure of the different intermetallic compounds, the structure of alloying elements and their effect on attack. This was based on Horstmann's data, using either widening of the range of the linear

region or the increase in the attack rate constants. It was impossible to arrive at any conclusions because of the widely different concentrations of the alloying elements, and because most of these elements had a cubic or hexagonal structure, with none monoclinic or even tetragonal.

CHAPTER 8

CONCLUSIONS AND SUGGESTIONS FOR FURTHER WORK

It has become clear that relative to the attack on pure iron at 450° C, most factors increase the attack rate. However, by knowing the importance of each factor it may be possible to avoid its consequences, i.e. by means such as keeping the temperature in a safer region. It is clearly impossible to reduce the attack to zero except on inherently resistant materials such as tungsten. The best that can be hoped for is to isolate the vulnerable material from the zinc by means of some protective layer, but the physical conditions and changes that such a layer must withstand are severe.

One of the best barrier layers has been a special chemical-resistant enamel, but thermal shock causes this to crack and eventually fail. It is possible that the oxide layers described in Chapter 5 would prove more satisfactory in service, but further improvements might be needed, perhaps by modification with silicon, nickel etc.

Some further tests are to be carried out by spinning sprayed and calorized specimens in molten zinc. This may indicate whether such specimens would resist erosion by flowing zinc but it is felt that this small scale test may not be a good way of predicting the life of industrial equipment. Being rather small the laboratory specimen has a large amount of

edge and corner regions compared with the flat surfaces. Such regions are weak because of the difficulties involved in calorizing or spraying, and are liable to be damaged during subsequent heat treatment or handling. Erosion during spinning may also be particularly severe, at the edges of the specimens. Failure of the specimens at the edges would thus not prove that larger items, such as thermocouple sheaths, which could be treated more evenly and held without damage during heat treatment, would also fail in this manner. The only reliable test would be on full scale items. A further problem with the rotating disc system might be that the "Gun-Gum" protection on the magnet would fail before the specimen, resulting in dissolution of the magnet.

The effect of aluminium in the zinc also needs further work, to clarify the sequence of formation of alloy layers and the rates of attack. It is clear that a wide range of phenomena are involved, and the present lack of knowledge of important data such as diffusion rates means that no predictions of behaviour can be made.

The effect of carbon in the steel is also interesting, and further work could be done to investigate more fully the attack on high carbon steels or cast irons. White cast iron might be quite resistant if consisting mainly of cementite.

Appendix 1

Calculation of effusion rate for zinc vapour.

For Knudsen effusion of a vapour through a small orifice we have (60):

$$G = K(P_1 - P_2)\sqrt{\frac{M}{2\pi RT}}$$

where G = number of grams of vapour crossing 1 cm^2 in 1 sec.

P_1 ; P_2 = vapour pressures on either side of the orifice (dynes per cm^2)

M = molecular weight.

R = Gas constant

T = Temperature, ^oK

K = Clausing's correction to allow for the finite thickness of the orifice. If thickness is 1, and radius r, for $1/r > 1.5$

$$K = \frac{1 + 0.4\ (\ 1/r\ )}{1 + 0.95\ (\ 1/r\ ) + 0.15\ (\ 1/r\ )^2}$$

Thus taking $l = 1$ cm, $r = 10^{-2}$ cm

$K = \simeq 0.026$

Then if $\Delta p = 0.1$ cm Hg.

$T = 800^oK$

$M = 65$

$R = 8.3 \times 10^7$ erg $^oK^{-1}$ mol^{-1}

$G \simeq 5.2 \times 10^{-5}$ $gm/cm^2/sec.$

If the area of such pores per unit area of the porous medium is 10^{-2}, i.e. ~ 30 such pores/cm^2

Then $G_1 \simeq 5.2 \times 10^{-7}$ gm/cm^2 of nominal area/sec

$\simeq 2 \times 10^{-3}$ gm/cm^2 nominal area/hr.

This calculation assumes:

1. That Knudsen flow is applicable, i.e. mean free path of vapour is at least an order of magnitude greater than the dimensions involved; this means in practice $\Delta P < 0.1$ mm Hg., i.e. probably not applicable.
2. That Clausing's factor K can be evaluated by the formula quoted even with $1/r$ so large.
3. That the pores are straight continuous tubes, with no condensation occurring within them.

Appendix 2

Details of surface treatments applied to discs of armco iron.

(1) Oxidation

A blue oxide film was developed on the iron by hanging it above the molten zinc bath for 3 hours.

(2) Phosphating

The specimen was treated for 15 mins. at 60° C in a mixture of 200 cc. Orthophosphoric acid + 200 cc. water + 5 g. ferric nitrate.

(3) Chromating

The specimen was electrolysed for about 1 min. at 5 volts and 5 amps (over $\sim 2 \times 10^{-3}$ m^2) in a mixture of 35 g. chromium trioxide +25 g. sodium chlorate per litre, at 45° C. This gave a pale brown coating which was washed well with hot water and dried with acetone.

(4) Siliconising

Two specimens were heated in a crucible packed with a mixture of 20 g. powdered silicon (50 - 200 μm mesh) + 80 g. alumina powder + 2 g. sodium fluoride, with charcoal on the surface of the crucible. After 19 hours at 1000° C a very thick coating was produced, blue-grey in colour. This was quite adherent but very hard and brittle and fractured around the hole when drilling was attempted.

(5) Borax

(a) Orthoboric acid was dissolved in methanol and cleaned specimens were dipped in and slowly withdrawn. Subsequent heat treatment at 200° C for 2 hours or 400° C for 1 hour produced a glaze which was clear at the lower temperature or brown at the higher.

(b) Heated specimens were rolled in orthoboric acid powder, which was fused on at 400° C for 1 hour.

The glaze produced was brittle and soluble in water. Best coatings were produced by method (b).

References

1. E.J. Daniels: J.Inst.Metals 1931 46 p.81

2. D. Horstmann and F.K. Peters: Proc.Ninth Intern.Conf. on Hot Dip Galvanising, Dusseldorf 1970, London, Z.D.A. 1971.

3. A.A. Hershman: Proc.Seventh Intern.Conf. on Hot Dip Galvanising, 1964. Oxford, Pergamon P. 1967.

4. A.A. Hershman: Proc. Eighth Intern.Conf. on Hot Dip Galvanising, 1967. London, Z.D.A. 1967.

5. M. Hansen and K. Anderko: Constitution of binary alloys. New York, McGraw-Hill, 1958.

6. I.L.Z.R.O. Research Digest No. 25, Spring 1970, International Lead Zinc Research Organisation, Inc. New York.

7. C. Allen and J. Mackowiak; J.Inst.Metals 1963 91 p.369.

8. R.H. Palmer, R.H. Thresh and J.J. Sebisty: Proc. Ninth Intern.Conf. on Hot Dip Galvanising, Dusseldorf 1970. London, Z.D.A., 1971.

9. D. Horstmann and F.K. Peters: Arch.f. Eisenhüttenw., 1969 40 p. 621.

10. C. Allen and J. Mackowiak: Corr.Sci 1963, 3 p. 87.

11. H. Bablik: "Galvanising" London, E. and F. Spon, 1950.

12. C.J. Smithells: Metals Reference Book. London, Butterworths, 1967.

13. C. Allen and J. Mackowiak; Corr.Sci. 1963, 3, p. 89.

14. D.H. Rowland: Trans.Amer.Soc.Metals. 1948 40 p. 983.

15. E. Scheil and H. Wurst. Z. Metallkde., 1938, 30, p.4.

16. D. Horstmann: Proc. Fourth Intern.Conf. on Hot Dip Galvanising, Milan 1956. London, Z.D.A. 1957.

17. D. Horstmann. Arch.Eisenhüttenw., 1954, 25, p. 215.

18. E. Scheil and H. Wurst. Z. Metallkunde, 1937, 29 224.

19. E. Scheil: Z.Metallkunde. 1935, 27, p.76.

20. D.F. Cook: Effect of pressure on attack by zinc-aluminium alloys on Iron. B.Sc. Thesis, Surrey University, 1968.

21. Influence of steel surface roughness on the structure of the zinc coating: Anon. Bull. Thermisch Verzinken, 1968, No. 683.

22. D.I. Cameron and M.K. Ormay. Proc.Sixth Intern. Conf. on Hot Dip Galvanising, Interlaken, 1961. London, Z.D.A. 1962, p.276.

23. D. Horstmann. Stahl u.Eisen 1960, 80(2), p.1531.

24. K. Ruttewit. Metall, 1960, 14. o. 769.

25. J. Sedzimir and H. Szymanska, Neue Huette 1969, 14(3), p.176.

26. W. Rüdeker, A. Hankel and W. Friehe. Bänder Bleche Rohre 1969, 10(5), p.294.

27. W. Hummitzsch. Schweissen u. Schneiden 1968, 20(3), p.97

28. Imperial Smelting Corporation Ltd., Metallurgical Research Department, Statement No. 9, 1964.

29. W. Hodge, R.M. Evans, A.F. Haskins, J.Metals 1955, 7, p.824.

30. K.Ruttewit, Metall. 1959, 13, p.735.

31. M.A. Haughton: Proc. Second Intern.Conf. on Hot Dip Galvanising, Düsseldorf 1952. London, Z.D.A. 1953.

32. D.C. Pearce. Paper: Meeting Am.Hot Dip Galv. Assoc., Sept. 1970.

33. A.R. Borzillo and C.W. Hahn; Trans.Amer.Soc. Metals 1969 62(3) p.729.

34. W. Köster and T. Gödecke. Proc.Ninth Intern. Conf. on Hot Dip Galvanising, Düsseldorf 1970. London, Z.D.A. 1971.

35. D. Horstmann. Arch.Eisenhüttenw. 1956, 27(5) p. 297.

36. L.M. Bernick and W.C. Sievert: Processing of Galvannealed Steel. Mechanical Working and Steel Processing IV. A.I.M.E. Met.Soc.Conferences Vol. 44. Pittsburgh 1965. New York, Gordon and Breach, 1969.

37. A.G. Ward and J.W. Taylor. J.Inst.Metals 1957, 86, p.36.

38. D.A. Stevenson and J. Wulff. Trans.Met.Soc.Amer. Inst.Min.Met.Eng., 1961, 221 p.279.

39. Eisenberg. Tobias and Wilke. Amer.Inst.Chem. Eng. Progress Symposium No. 16, 1955, 51, p.1

40. V.G. Levich. Physicochemical Hydrodynamics Prentice-Hall, Englewood Cliffs, 1962.

41. D.P. Gregory and A.C. Riddiford: J.Chem.Soc., 1956, 731, p.3756.

42. Prate and Adams. Anal.Chem. 1966, 38 p.153.

43. N. Gregory, J.J. Stewart and W.S. Walker. Phil. Trans. Roy.Soc.A. 1955, 248 p.155.

44. V.N. Eremenko, Ya.V.Natanzon, Sov.Met.Sci 1966, 2(5) p.411.

45. V.N. Eremenko, Ya.V.Natanzon and O.F. Galadzhii Sov.Met.Sci 1967, 3(2) p.134.

46. V.N. Eremenko, Ya.V.Natanzon and V.R. Ryabov. Sov.Met.Sci 1968, 4(3) p. 209.

47. V.N. Eremenko, Ya.V.Natanzon and O.F. Galadzhii Fhig-Khim.Mekh.Mat. 1968 4(6) p.665.

48. M. Kosaka, M. Kato, M. Mizuta and S. Minowa. Rep. Gov.Ind.Research Inst., Nagoya. 1965, 14, p.171.

49. M. Kosaka and S. Minowa. Rep.Gov.Ind. Research Inst., Nagoya, 1967, 16(8), p.250.

50. M. Kosaka, M. Kato and S. Minowa, Rep.Gov.Ind. Research Inst. Nagoya 1967, 16(9), p.273.

51. Carnet, Lewis and Kappesser; Trans.Inst.Chem.Eng. 1969, 47, p.222.

52. T.R. Russell, W.E. Goodrich, W. Cross and N.P. Allen. J.Inst.Metals. 1928, 40(2), p.250.

53. The Calorizing Corporation of Great Britain Ltd. Private communication, November 1970.

54. R.L. Cairns, Banded and Fibrous Structures in Steels. Ph.D. Thesis, Cambridge, 1965.

55. C. Sykes and J.W. Bampfylde: J.Iron Steel Inst. 1934, 130, p.389.

56. S.L. Case and K.R. Vanltorn: Aluminium in Iron and Steel: John Wiley, New York, 1953.

57. E.R. Petty. J.Inst.Metals 1960-61, 89 p.343.

58. Imperial Smelting Corporation Ltd. Private Communication.

59. O. Kubaschewski and B.E. Hopkins; Oxidation of metals and alloys. Butterworths, London, 1962.

60. An.N. Nesmeyanov. Vapour Pressure of the Elements. Infosearch, London, 1963.

61. L.L. Shreir: Corrosion. Newnes, London, 1963.

62. R. Drewett. Corr.Sci. 1969 9 p.823.

63. A.A. Gusev. Protective coatings on metals. Vol 2 p. 136. Edited: G.V. Samsonov. Consultants Bureau, New York, 1970

64. W. Jost, Diffusion. Academic Press, New York, 1960.

65. S. Jayaram and S.V. Visvanathan. Tisco, 1966 13, p.25.

66. R.H. Tharby. Effect of the carbon content on the attack of molten zinc on steel. Diploma in Technol. Thesis. Battersea College of Technol. 1961.

67. H. Fletcher. Effect of carbon content of steels on their dissolution in liquid zinc, Diploma in Technol. Thesis, Battersea College of Technol. 1962.

68. B.S. Connor. Study of the effect of carbon content of steels on their dissolution in zinc-aluminium alloys. B.Sc. Thesis, University of Surrey, 1968.

69. Hondros: Energetics of solid-solid interfaces Interfaces Conference, Melbourne, August 1969. Butterworths, London, 1969.

70. Isothermal Transformation Diagrams, United States Steel, Pittsburgh, 1966.

71. G.E. Pellissier, M.F. Hawkes, W.A. Johnson and R.F. Mehl. Amer.Soc.Metals 1942 30 p.1049.

72. V.I. Nikitin, J.App.Chemistry of U.S.S.R. 1969, 42(2) p.282.

73. G. Jackel, H.E. Bühler and L. Meyer. Proc.Ninth Intern.Conf. on Hot Dip Galvanising, Düsseldorf, 1970, London, Z.D.A. 1971.

74. Dr. T.R. Shelley, Cambridge University, Private communication. 1968.

75. C.J. Thwaites and C.A. Mackay, Metal Finishing Journal, 1968. Tin Research Institute Publication No. 386.

76. G.A. Kokorin. Sb.Tr. Tsent. Nauch. Issled. Inst. Chem.Met. (U.S.S.R.) 1969, No. 66, p.87.

77. E. Büchel and H. Bosch. Stahl u.Eisen 1970, 90 (11) p.557.